

REVIEWS OF TOPICAL PROBLEMS PACS numbers: **12.10.–g**, 12.60.Fr, 12.60.Jv

Phenomenological aspects of supersymmetric extensions of the Standard Model

R B Nevzorov

DOI: https://doi.org/10.3367/UFNe.2022.07.039223

Contents

Abstract. The breakdown of gauge symmetry within Grand Unified Theories (GUTs) can result in supersymmetric (SUSY) extensions of the Standard Model (SM) at low energies, which allows the electroweak scale to be almost stabilized. The gauge coupling unification, Higgs sector, and restrictions on the sparticle spectrum are considered in the framework of several SUSY extensions of the SM. Possible manifestations of these SUSY models and existing experimental limits are also discussed.

Keywords: Grand Unified Theories and models, extensions of the Standard Model, supersymmetry, dark matter, non-standard Higgs bosons, supersymmetric partners of known particles, leptoquarks, exotic particles

1. Introduction

The discovery of the Higgs boson by the Large Hadron Collider (LHC) experiments [1, 2] is an important step forward towards our understanding of the mechanism of electroweak symmetry breaking. The present status and future prospects of investigations in this area of High Energy Physics are summarized in Ref. [3]. The discovery of the Higgs state is consistent with the Standard Model (SM), which involves all known fundamental particles and describes rather precisely most experimental data measured in earth-based experiments. On the other hand, there are several problems that stimulate the exploration of different extensions of the SM. One of them is the weakness of gravitational interaction as compared with the strong and electroweak forces.

R B Nevzorov
Lebedev Physical Institute, Russian Academy of Sciences, Leninskii prosp. 53, 119991 Moscow, Russian Federation
E-mail: nevzorovrb@lebedev.ru

Received 30 August 2021, revised 25 July 2022
Uspekhi Fizicheskikh Nauk **193** (6) 577 – 613 (2023)
Translated by the author

The Lagrangian of the SM is invariant under the Poincaré group and $SU(3)_C \times SU(2)_W \times U(1)_Y$ gauge symmetry transformations. The Poincaré group is an extension of the Lorentz group that includes time and space translations. In the 1970s, S Coleman and J Mandula proved a theorem regarding the symmetry of the S-matrix [4]. According to this theorem, the most general symmetry which quantum field theory can have is a tensor product of the Poincaré group and an internal group. Thus, it is rather problematic to combine the Poincaré and internal symmetries, which prevents the unification of gauge interactions with gravity. The Coleman–Mandula theorem can be overcome within graded Lie algebras that have the following structure:

$$[\hat{B}, \hat{B}] = \hat{B}\,, \qquad [\hat{B}, \hat{F}] = \hat{F}\,, \qquad \{\hat{F}, \hat{F}\} = \hat{B}\,,$$

where $\hat{B}$ and $\hat{F}$ are bosonic and fermionic generators. Graded Lie algebras that contain the Poincaré algebra are called supersymmetries. The simplest $N = 1$ supersymmetry (SUSY) involves a single Weyl spinor operator Q_α and its complex conjugate $Q_\alpha^\dagger = \overline{Q}_{\dot\alpha}$. These operators change the spin of the state, i.e.,

$$Q_\alpha|\text{fermion}\rangle = |\text{boson}\rangle\,, \qquad \overline{Q}_{\dot\alpha}|\text{boson}\rangle = |\text{fermion}\rangle\,.$$

The renormalization group (RG) flow of the $SU(3)_C$, $SU(2)_W$, and $U(1)_Y$ gauge couplings in the framework of the simplest SUSY extension of the SM — the minimal supersymmetric Standard Model (MSSM) — indicates that at very high energies $E \sim M_X \gtrsim 10^{16}$ GeV the SM can be embedded into Grand Unified Theories (GUTs) [5] based on gauge groups such as SU(5), SO(10), or E_6. In the case of minimal SU(5) GUTs, each SM family of quarks and leptons forms one antifundamental and one antisymmetric second-rank tensor representation of SU(5), i.e., $\overline{5}+10$. Within SO(10) GUTs, each family of SM fermions may belong to a single 16-dimensional spinor representation of SO(10). Such models predict the existence of right-handed neutrinos, which may be used for the see-saw mechanism [6, 7].

SUSY algebra implies that each supermultiplet has the same number of bosonic and fermionic degrees of freedom. As a consequence, in $N=1$ SUSY GUTs with the E_6 gauge group, the fundamental 27 representation of E_6 can contain one family of SM fermions, as well as the Higgs doublet. The simplest representation of E_6 decomposes under the $SO(10)\times U(1)_\psi$ subgroup as

$$27 \to \left(16, \frac{1}{\sqrt{24}}\right) \oplus \left(10, -\frac{2}{\sqrt{24}}\right) \oplus \left(1, \frac{4}{\sqrt{24}}\right). \qquad (1)$$

The first and second quantities in parentheses are the SO(10) representation and extra $U(1)_\psi$ charges, respectively. As before, the supermultiplet $(16, 1/\sqrt{24})$ can include one family of quarks and leptons. The doublet of the Higgs bosons may form components of the supermultiplet $(10, -2/\sqrt{24})$. The SM gauge bosons are assigned to the adjoint representation of E_6, i.e., a 78-plet. In $N=2$ SUSY GUTs with the E_8 gauge symmetry, all SM bosons and SM fermions may belong to a single 248 representation of E_8. This representation decomposes under the E_6 subgroup of E_8 as follows:

$$248 \to 78 \oplus 3\times 27 \oplus 3\times\overline{27} \oplus 8\times 1. \qquad (2)$$

In Eqn (2), three generations of SM fermions can be associated with three 27-plets which may also contain the doublet of the Higgs bosons, while some components of the 78-plet may form multiplets of SM gauge bosons.

Near the GUT scale, the E_6 gauge group may be broken down into its $SU(3)_C\times SU(2)_W\times U(1)_Y\times U(1)_\psi\times U(1)_\chi$ subgroup. For instance, E_6 can be broken into its maximal subgroup $SO(10)\times U(1)_\psi$ with a sequential breakdown of SO(10) into $SU(5)\times U(1)_\chi$ and SU(5) into the SM gauge group $SU(3)_C\times SU(2)_W\times U(1)_Y$ (for reviews, see, for example, Refs [8, 9]). If the $U(1)_\chi\times U(1)_\psi$ symmetry is broken down into its discrete subgroup $P_M=(-1)^{3(B-L)}$, where B and L are baryon and lepton numbers, then such a breakdown of E_6 may result in a variety of SUSY models at low energies, including the MSSM and its extensions. The U(1) extensions of the MSSM with extra $U(1)'$ gauge symmetry may arise when the rank-6 model with additional $U(1)_\chi\times U(1)_\psi$ symmetry is reduced further to an effective rank-5 model with only one extra gauge symmetry $U(1)'$, which is a linear superposition of $U(1)_\chi$ and $U(1)_\psi$:

$$U(1)' = U(1)_\chi \cos\theta_{E_6} + U(1)_\psi \sin\theta_{E_6}. \qquad (3)$$

The first reviews in which the phenomenological implications of SUSY extensions of the SM were discussed were published in the 1980s [10–13]. The MSSM and its different extensions have been intensively studied for the last forty years. Since there are many models of this type, their detailed consideration in one review is not possible. Therefore, in this article, we consider only three models: MSSM, the simplest extension of the MSSM — the Next-to-minimal supersymmetric Standard Model (NMSSM), and the $U(1)_N$ extension of the MSSM (E_6SSM), which corresponds to the value of $\theta_{E_6}=\arctan\sqrt{15}$.

So far, no indication of the presence of the superpartners of SM particles has been detected. Nevertheless, there are many possible manifestations of the SUSY extensions of the SM which have been searched for in various experiments. These manifestations have been analyzed in hundreds of papers. Because this area of high energy physics is so wide, here we focus on a few selected aspects of the SUSY phenomenology that seem to be the most important ones. In Section 2, the hierarchy problem in GUTs and string theory is briefly discussed. In Section 3, we specify the MSSM, NMSSM, and E_6SSM. In the framework of these models, the renormalization group flow of the SM gauge couplings and their unification at very high energies $E\sim M_X \gtrsim 10^{16}$ GeV are examined in Section 4. The SUSY extensions of the SM predict that an upper bound exists on the lightest Higgs boson mass. This is one of the most important predictions of these models. The detection of a new scalar with a mass of around 125 GeV by the LHC experiments, which manifests itself in interactions with gauge bosons and fermions as an SM-like Higgs boson, set some constraints on the parameter space of SUSY models. In this context, in Section 5, the breakdown of gauge symmetry and the spectrum of the Higgs states within the MSSM, NMSSM, and E_6SSM are considered.

Astrophysical and cosmological observations indicate that about 20–25% of the energy density of the Universe exists in the form of dark matter [14]. Thus, nonluminous matter constitutes most of the matter in our Universe. In SUSY extensions of the SM, the lightest supersymmetric particle (LSP) tends to be the lightest neutralino which is neutral and can be stable. This makes it one of the most suitable candidates for cold dark matter. Direct detection searches for dark matter and the Higgs mass measurement strongly constrain the allowed region of the parameter space in the simplest SUSY models. In Section 6, the corresponding restrictions are considered in the framework of the constrained MSSM and constrained E_6SSM. They lead to stringent bounds on the sparticle spectrum in the simplest scenarios. LHC experimental limits on the masses of new states, which are predicted by the SUSY models under consideration, as well as some possible manifestations of these states, are discussed in the second to last section of this review. Section 8 is reserved for our conclusions.

2. Hierarchy problem and landscape of string theory vacua

The breakdown of gauge symmetry within GUTs near some high energy scale M_X can result in the gauge group and field content of the SM with the Higgs scalar potential

$$V(H) = m_H^2\, H^\dagger H + \lambda\,(H^\dagger H)^2 + \ldots. \qquad (4)$$

In order to ensure that the doublet of the Higgs fields H acquires the vacuum expectation value (VEV) $\langle H\rangle = v/\sqrt{2}\simeq 174$ GeV breaking the electroweak (EW) symmetry, $|m_H^2|$ is required to be of the order of $(100\ \text{GeV})^2$. Although in some GUTs the parameter m_H^2 may vanish at the tree level (see, for example, [15, 16]), most commonly $|m_H^2|$ tends to be about M_X^2. Moreover, even if m_H^2 is equal to zero there are radiative corrections to the mass squared of the $SU(2)_W$

doublet of the Higgs scalars that are quadratic in the masses of the heavy states which interact with H [17–19]. In GUTs, these heavy states have masses of the order of M_X, which means that, if the SM is to be embedded in GUTs, these high scale theories generally require an extreme form of fine tuning to prevent $|m_H|$ (or the EW scale) from becoming of the same order as M_X, known as the hierarchy problem.

Within the SM, such destabilization of the EW scale can be identified with the radiative corrections that lead to the quadratic divergences of loop integrals. These loop integrals can be truncated at some high energy cutoff scale Λ. Taking Λ as high as the GUT scale M_X would require a tuning of m_H^2 in Eqn (4) to 26 decimal places to maintain its phenomenologically acceptable value.

The situation is rather different in SUSY extensions of the SM. Soon after supersymmetry was proposed [20–23], it was also realized that the local version of SUSY (supergravity) leads to a partial unification of gauge interactions with gravity [24–26]. Because supergravity (SUGRA) is a nonrenormalizable theory, it should be regarded as a low energy limit of some renormalizable or finite theory. The best candidate for such a theory is a ten-dimensional superstring theory with $E_8 \times E_8'$ gauge symmetry [27]. Compactification of the extra dimensions in this theory gives rise to the breakdown of E_8 to E_6 or its subgroups in the observable sector [28]. The remaining E_8' gauge group plays the role of a hidden sector. This sector contains superfields that interact with the observable ones only by means of gravity. It is assumed that the hidden sector fields acquire VEVs generating the spontaneous breakdown of local supersymmetry. The breakdown of local SUSY results in the appearance of a massless fermion with spin $1/2$ — the goldstino, which is swallowed up by the superpartner of a graviton with spin $3/2$ — the gravitino, which becomes massive. This phenomenon is called the super-Higgs effect [29–31].

At low energies, such a breakdown of local supersymmetry induces a set of soft SUSY breaking terms in the observable sector [32–35] that define the masses and couplings of the superpartners of SM bosons and fermions. Here, we restrict our consideration to the simplest SUGRA models, in which the soft SUSY breaking parameters and the sparticle mass scale are determined by the gravitino mass ($m_{3/2}$). Nevertheless, there is also a large class of models in which the gravitino can be much lighter than the superpartners of other particles [36–39].

The gauge symmetry breaking within SUSY GUTs at the scale M_X can give rise to a variety of extensions of the SM with softly broken supersymmetry at low energies if $m_{3/2} \ll M_X$. In supersymmetric theories, the quadratic divergences get cancelled identically because of the SUSY relationships between the dimensionless couplings of boson–fermion and boson–boson interactions [40–43]. The soft breakdown of SUSY implies that these relationships remain intact, so that the quadratic divergences from boson loops cancel those from the fermion ones. In this case, the effective cut-off scale Λ is replaced by the SUSY breaking scale, which is of the order of the masses of sparticles, i.e., $\sim m_{3/2}$. Because of this, for the last thirty years, the SUSY extensions of the SM with sparticle masses that lie well below the TeV scale were considered natural SUSY models. To date, there has not been any evidence of the existence of such light sparticles. If gravitinos and other sparticles have masses in the range of a few TeV, then the fine tuning, which is required to stabilize the EW scale, is of the order of $10^{-3}-10^{-2}$ [44, 45]. The generation of a large mass hierarchy between the GUT scale M_X and $m_{3/2}$ is a nontrivial problem. It can be induced within the nonperturbative scenario of SUSY breaking, which is caused by gaugino condensation in the hidden sector [46].

The fine tuning associated with the stabilization of the EW scale, which is caused by the emergence of the mass gap between the sparticle mass scale and the measured Higgs mass, has engendered some doubts as to whether low energy supersymmetry is nature's solution to the hierarchy problem. On the other hand, an incredible amount of fine-tuning of the vacuum energy is needed to keep the cosmological constant as small as observed. Indeed, a fit to the recent data shows that there is a tiny energy density (cosmological constant) spread all over the Universe, $\rho_\Lambda \sim 10^{-55} M_Z^4$ [14], where M_Z is the Z-boson mass. It is responsible for the accelerated expansion of the Universe and constitutes 70–73% of its total energy density [14]. At first glance, this dark energy density should be much larger than its measured value. The presence of a gluon condensate is expected to contribute an energy density of the order of $\sim \Lambda_{QCD}^4 \simeq 10^{-12} M_Z^4$. Even much larger contributions must come from breakdown of SUSY and the EW symmetry breaking. Because of the enormous cancellation among the contributions of different condensates to ρ_Λ, the smallness of the cosmological constant should be regarded as a fine-tuning problem.

It is not obvious if the two problems mentioned above can be considered separately. In this context, it is worth discussing important developments in string theory that have emerged in the 21st century. Starting in 2001, it was realized that the multitude of string theory vacua [47–49] provided a setting for Weinberg's anthropic solution to the cosmological constant problem [50]. The space of such string theory vacua is called the 'landscape.' In the string theory landscape, of the order of 10^{500} different vacuum states might exist [51]. Each of these states may have different matter content, different gauge groups, and different values of physical constants, including ρ_Λ. Our Universe is then just one of a vast ensemble of universes contained within a multiverse. In any anthropically allowed (livable) universe, the vacuum energy density can not be too large. Otherwise, this universe would expand too quickly to allow galaxy and star formation, and consequently no observers would be present to measure ρ_Λ. Similar arguments can be used to explain the magnitude of other mass scales within the SM. In particular, if the Higgs VEV was considerably larger than our universe's measured value, then there would not be any stable nuclei and nuclear physics would not be as we know it [52, 53]. In other words, the solution to both the hierarchy and cosmological constant problems might not involve natural cancellations, but follow from a completely different reasoning, such as the idea that galaxy and star formation, chemistry and biology, are simply impossible without these scales having the values found in our Universe [50, 52–55]. In this case, SUSY is still a necessary ingredient in a fundamental theory of nature such as string theory.

Recent developments in string theory have applied a statistical approach to the large multitude of universes, corresponding to the landscape of vacua present in the theory [51, 56–60]. For the case of the string theory landscape, the concept of *stringy naturalness* was introduced [60]. It implies that the value of the observable O_2 is more natural than a value O_1 if more phenomenologically viable vacua lead to O_2 than to O_1. The performed analysis indicates that, among the vast number of vacua, there can be a small subset exhibiting low scale SUSY breaking with a sparticle mass scale below 1 TeV. However, the fine tuning required to achieve a small cosmological constant implies the need for a much larger number of such vacua.

Remarkably, the total number of vacua in string theory can be large enough to fine-tune both the cosmological constant and the Higgs mass, favoring the highest soft SUSY breaking terms [59–61], which are consistent with generating the EW scale. In this case, the Higgs mass $m_{\mathrm{h}} \sim 125$ GeV is statistically favored, while most sparticles have masses beyond LHC search limits [62, 63]. It is thus statistically feasible in string theory for us to live in a universe fine-tuned in the way we find it, thereby having both a small cosmological constant and the EW scale stabilized in the 100-GeV range. This idea motivated the introduction of the Split SUSY scenario [64–74]. Within the corresponding SUSY models, the TeV-scale lightest neutralino can be an appropriate cold dark matter candidate [65–68], while all sfermions have masses which are substantially larger than 10 TeV. Several string motivated constructions result in this type of sparticle spectrum [75–87]. Supersymmetry in the Split SUSY scenario is not used to stabilize the weak scale. In the vast landscape of possible string theory vacua, we may find ourselves in the observed ground state simply because of a cosmic selection rule, i.e., the anthropic principle [50].

3. Supersymmetric extensions of the Standard Model

The Lagrangian of SUSY models based on the softly broken supersymmetry can be written as the sum

$$\mathcal{L} = \mathcal{L}_{\mathrm{SUSY}} + \mathcal{L}_{\mathrm{soft}}\,, \tag{5}$$

where $\mathcal{L}_{\mathrm{SUSY}}$ is invariant under SUSY transformations, whereas $\mathcal{L}_{\mathrm{soft}}$ includes a set of terms which break supersymmetry. $\mathcal{L}_{\mathrm{SUSY}}$ is determined by a set of chiral (Φ_i) and vector (V_m) superfields, as well as by a superpotential $W(\Phi_k)$ of the model under consideration. The chiral superfields can be presented in the following form:

$$\Phi_i(x^\mu, \theta, \bar\theta) = \phi_i(y^\mu) + \sqrt{2}\,\theta\psi_i(y^\mu) + \theta\theta F_i(y^\mu)\,, \tag{6}$$

where $y^\mu = x^\mu + \mathrm{i}\theta\sigma^\mu\bar\theta$, $\sigma^\mu = (1, \sigma^i)$, σ^i are 2×2 Pauli matrices, θ_α and $\bar\theta_{\dot\alpha}$ (α, $\dot\alpha = 1, 2$) are fermionic anticommuting Grassmann coordinates. Here, ϕ_i is a complex scalar field, F_i is an auxiliary complex scalar field, and ψ_i is a left-handed Weyl spinor field. In Lagrangian (5), there are no kinetic terms for the fields F_i, so F_i can be eliminated. The coefficients in expansion (6), i.e., ϕ_i, F_i, and ψ_i, are called components of a superfield Φ_i. In the Wess–Zumino gauge [88], the vector superfield takes the form

$$\begin{aligned} V_m = V_m^a(x^\mu, \theta, \bar\theta)t^a = \Big(&-\theta\sigma^\nu\bar\theta V_{m\nu}^a(x^\mu) + \mathrm{i}\theta\theta\bar\theta\bar\lambda_m^a(x^\mu) \\ &- \mathrm{i}\bar\theta\bar\theta\theta\lambda_m^a(x^\mu) + \frac{1}{2}\,\theta\theta\bar\theta\bar\theta D_m^a(x^\mu)\Big)t^a\,, \end{aligned} \tag{7}$$

where t^a are the generators of the non-Abelian group, $V_{m\nu}^a(x)$ are the corresponding gauge fields, while the spinor fields $\lambda_m^a(x)$ are associated with the superpartners of the gauge fields, which are usually referred to as gauginos. $D_m^a(x)$ are another type of auxiliary field which do not have any kinetic terms, so they can also be eliminated.

The superpotential $W(\Phi_k)$ is a holomorphic (analytic) function of Φ_k which may involve the products of chiral superfields only and must not contain any terms like $\Phi_i\Phi_j^\dagger$ or $\Phi_i\Phi_j\Phi_k^\dagger$. Moreover, $W(\Phi_k)$ is required to be invariant under the gauge group transformations. The function $W(\Phi_k)$ has to involve only up to the third power of the superfields Φ_i to obtain a renormalizable Lagrangian, i.e.,

$$W(\Phi_k) = a_i\Phi_i + \frac{1}{2}\,\mu_{ij}\Phi_i\Phi_j + \frac{1}{6}\,y_{ijk}\Phi_i\Phi_j\Phi_k\,. \tag{8}$$

In Eqn (8) the sum over all possible combinations of chiral superfields is understood while a_i, μ_{ij}, and y_{ijk} are constants. The linear terms in the superpotential (8) are normally forbidden by the gauge symmetry.

Since the set of terms which results in the soft breaking of SUSY is known [89], $\mathcal{L}_{\mathrm{soft}}$ is given by

$$\begin{aligned} -\mathcal{L}_{\mathrm{soft}} &= \left(\frac{1}{2}\sum_{a,m} M_m\lambda_m^a\lambda_m^a + \mathrm{h.c.}\right) + V_{\mathrm{soft}}\,, \\ V_{\mathrm{soft}} &= \sum_{i,j} m_{ij}^2\phi_i^\dagger\phi_j + \sum_{i,j,k}\Big(\frac{1}{6}\,A_{ijk}y_{ijk}\phi_i\phi_j\phi_k \\ &\quad + \frac{1}{2}\,B_{ij}\,\mu_{ij}\phi_i\phi_j + t_i a_i\phi_i + \mathrm{h.c.}\Big)\,, \end{aligned} \tag{9}$$

where λ_m^a are gauginos of the gauge group associated with index m. The terms in $\mathcal{L}_{\mathrm{soft}}$ clearly break SUSY, because they involve only scalars and gauginos and not their respective superpartners. A set of soft SUSY breaking parameters includes gaugino masses M_{A}, soft scalar masses m_{ij}^2, tadpole couplings t_i, and trilinear and bilinear scalar couplings (A_{ijk} and B_{ij}). The soft terms in $\mathcal{L}_{\mathrm{soft}}$ are capable of giving masses to all of the scalars and gauginos.

3.1 MSSM and NMSSM

Since from the $N = 1$ SUSY algebra it follows that each SUSY multiplet must have an equal number of bosonic and fermionic degrees of freedom, the simplest supersymmetric extensions of the SM should contain scalar degrees of freedom associated with left-handed and right-handed SM fermions. In other words, these models have to include scalar particles, i.e., left-handed and right-handed squarks and sleptons, in addition to the ordinary quarks and leptons. These SUSY extensions of the SM should also involve the fermionic partners of SM gauge bosons (gauginos) and Higgs bosons (higgsinos).

In the SM, one Higgs doublet H is used to generate the masses for up- and down-type quarks and charged leptons. These masses are induced by means of the Yukawa interactions of quarks and leptons with the Higgs fields. More precisely, the masses of the down-type quarks and charged leptons are generated by the Higgs doublet itself, whereas the conjugated Higgs doublet $\mathrm{i}\sigma_2 H^\dagger$ gives rise to the masses of up-type quarks. In SUSY models, the Higgs-fermion Yukawa interactions can originate from the superpotential $W(\Phi_k)$ only. Since $W(\Phi_k)$ is an analytic function of the chiral superfields, it can not involve any conjugate superfield like $\mathrm{i}\sigma_2 H^\dagger$. Thus, we have no other choice than to introduce a second Higgs doublet H_2 with the opposite hypercharge, which gives masses to the up-type quarks. The presence of the second Higgs doublet also ensures the cancellation of anomalies.

Thus, the simplest SUSY extension of the SM, i.e., MSSM, includes the following set of chiral superfields:

$$\begin{aligned} &Q_a = (u_a,\, d_a) \sim \left(3,\, 2,\, \frac{1}{6}\right), \qquad && u_a^c \sim \left(\bar{3},\, 1,\, -\frac{2}{3}\right), \\ &L_a = (\nu_a,\, e_a) \sim \left(1,\, 2,\, -\frac{1}{2}\right), \qquad && d_a^c \sim \left(\bar{3},\, 1,\, \frac{1}{3}\right), \\ &H_1 = (H_1^0,\, H_1^-) \sim \left(1,\, 2,\, -\frac{1}{2}\right), \qquad && e_a^c \sim (1,\, 1,\, 1), \\ &H_2 = (H_2^+,\, H_2^0) \sim \left(1,\, 2,\, \frac{1}{2}\right), \end{aligned} \tag{10}$$

where the first and second quantities in the parentheses are the $SU(3)_C$ and $SU(2)_W$ representations of the corresponding supermultiplet, the third quantity in the parentheses is the $U(1)_Y$ hypercharge, while a is a family index that runs from 1 to 3. Here, Q_a and L_a contain the doublets of the left-handed quark and lepton superfields, e_a^c, u_a^c, and d_a^c are associated with the right-handed lepton, up- and down-type quark superfields, respectively. H_1 and H_2 involve the doublets of Higgs superfields that induce the masses of all quarks and leptons. In Eqns (10) and further, we omit all isospin and color indexes related to $SU(2)_W$ and $SU(3)_C$ gauge interactions.

In addition to Higgs, quark, and lepton chiral superfields, the MSSM includes three vector supermultiplets,

$$\begin{aligned} &\hat{V}_1 \sim (1,\, 1,\, 0)\,, \quad \hat{V}_2 = V_2^a \tau^a \sim (1,\, 3,\, 0)\,, \\ &\hat{V}_3 = V_3^a T^a \sim (8,\, 1,\, 0)\,, \end{aligned} \tag{11}$$

which are associated with $U(1)_Y$, $SU(3)_C$, and $SU(2)_W$ interactions, respectively. $\hat{V}_1$ is an abelian vector superfield that contains the $U(1)_Y$ gauge field and its superpartner, which is called a bino. $\hat{V}_2$ involves a triplet of $SU(2)_W$ gauge bosons and their superpartners (winos). $\hat{V}_3$ includes an octet of gluons and an octet of their superpartners (gluinos). As a result of the mixing between a bino, neutral wino, and neutral higgsino, a set of neutral fermionic states (neutralino) is formed. The mixing of a charged wino and charged higgsino gives rise to charged fermionic states, which are called charginos.

In order to reproduce the Higgs-fermion Yukawa interactions that induce the masses of all quarks and charged leptons in the SM, we need to include the following sum of the products of chiral superfields in the MSSM superpotential:

$$W_{\rm MSSM} = y_{ab}^U Q_a u_b^c H_2 + y_{ab}^D Q_a d_b^c H_1 + y_{ab}^L L_a e_b^c H_1 + \mu H_1 H_2\,, \tag{12}$$

where a and b are family indices. In Eqn (12), the Yukawa couplings y_{ab}^U, y_{ab}^D, and y_{ab}^L are dimensionless 3×3 matrices in family space that determine the masses of quarks and charged leptons as well as the phase of the Cabibbo–Kobayashi–Maskawa (CKM) matrix. Here, we also include a term $\mu H_1 H_2$ which is not present in the Lagrangian of the SM. It gives rise to the masses of the superpartners of Higgs bosons (higgsinos). The μ term, as it is traditionally called, can be written as $\mu (H_1)_\alpha (H_2)_\beta \varepsilon^{\alpha\beta}$, where $\varepsilon^{\alpha\beta}$ is used to tie together $SU(2)_W$ weak isospin indices $\alpha, \beta = 1, 2$ in a gauge invariant way.

Although Eqn (12) defines the MSSM superpotential, there are extra terms that one can write which are gauge invariant and analytic in the chiral superfields. These additional terms are given by

$$W_{\rm NR} = \lambda_{abd}^L L_a L_b e_d^c + \lambda_{abd}^{L\prime} L_a Q_b d_d^c + \mu_a' L_a H_2 + \lambda_{abd}^B u_a^c d_b^c d_d^c\,. \tag{13}$$

The terms in $W_{\rm NR}$ violate either lepton or baryon number, resulting in rapid proton decay. The most general renormalizable gauge invariant superpotential of the simplest SUSY extension of the SM is a sum of Eqns (12) and (13), i.e., $W = W_{\rm MSSM} + W_{\rm NR}$. The terms given by Eqn (13) are absent in the SM. The inclusion of such terms in the Lagrangian of the SM would violate Lorentz invariance. Since B- and L-violating processes have not been observed in nature, the terms in $W_{\rm NR}$ must be very strongly suppressed.

The baryon and lepton number violating processes in the MSSM can be suppressed by postulating the invariance of the Lagrangian under R-parity transformations (P_R) or, equivalently, matter parity transformations (P_M)

$$P_R = (-1)^{3(B-L)+2s}\,, \qquad P_M = (-1)^{3(B-L)}\,, \tag{14}$$

where s is the spin of the particle. It is easy to check that the quark and lepton supermultiplets have $P_M = -1$, while the Higgs and vector supermultiplets have $P_M = +1$. Matter parity forbids all terms in $W_{\rm NR}$. This symmetry commutes with SUSY, as all component fields of a given supermultiplet have the same matter parity. The advantage of matter parity is that it can in principle be an exact and fundamental symmetry, whereas B and L themselves cannot, since they are known to be violated by nonperturbative electroweak effects. Indeed, matter parity can originate from the continuous $U(1)_{B-L}$ gauge symmetry that satisfies anomaly cancellation conditions. Thus, P_M can survive as an exactly conserved discrete remnant subgroup of $U(1)_{B-L}$. Although matter parity forbids all renormalizable interactions which violate B and L in the MSSM, one may expect that baryon and/or lepton number violation can occur in tiny amounts due to the nonrenormalizable terms in the Lagrangian.

Matter parity conservation and R-parity conservation are equivalent, since the product of $(-1)^{2s}$ for the particles involved in any interaction vertex in a theory, which conserves angular momentum, is always equal to $+1$. At the same time, particles within the same supermultiplet do not have the same R-parity, and there is no physical principle behind it. Due to matter parity conservation, it secretly does commute with SUSY. Nevertheless, the R-parity assignment is very useful for phenomenology, because all of the SM particles and the Higgs bosons have even R-parity, while all of the squarks, sleptons, gauginos, and higgsinos have odd R-parity. The R-parity odd particles are known as 'SUSY particles' or 'sparticles.' Since in the conventional MSSM R-parity is conserved, there can not be any mixing between states with $P_R = +1$ and $P_R = -1$. Furthermore, every interaction vertex in the MSSM contains an even number of $P_R = -1$ states. This has three important phenomenological consequences:

• the lightest supersymmetric particle (LSP) must be absolutely stable and can play the role of nonbaryonic dark matter. In most supersymmetric scenarios, the LSP is the lightest neutralino which is a mixture of higgsinos and gauginos. Since the lightest neutralino is a heavy weakly interacting particle, it explains well the large scale structure of the Universe and can provide the correct relic abundance of dark matter if its mass $m_{\chi_1^0}$ is of the order of the TeV scale;

• in collider experiments sparticles can only be created in pairs;

• each sparticle must eventually decay into a final state that contains an odd number of LSPs (usually just one). Since the stable lightest neutralinos can not be detected directly, their signature would be missing energy and transverse momentum in the final state.

SUSY predicts that bosons and fermions from one SUSY multiplet have to be degenerate. Because superpartners of quarks and leptons have not been observed yet, supersymmetry must be broken, i.e., all sparticles have to be heavy. In general, $\mathcal{L}_{\text{soft}}$ is given by Eqn (9). The inclusion of the soft SUSY breaking terms in the MSSM introduces many new parameters that were not present in the SM. A careful count reveals that there are more than one hundred masses, phases, and mixing angles in the MSSM Lagrangian that cannot be rotated away. On the other hand, new parameters may lead to flavor mixing and/or *CP* violating effects which are severely constrained by different experiments. In order to avoid potentially dangerous processes, one can assume that all soft SUSY breaking parameters are real and $m_{ij}^2 \simeq m_i^2 \delta_{ij}$. As a result, we get

$$-\mathcal{L}_{\text{soft}}^{\text{MSSM}} = \sum_i m_i^2 |\phi_i|^2 + \bigg(\frac{1}{2}\sum_{a,m} M_m \lambda_m^a \lambda_m^a + \sum_{a,b}\big[A_{ab}^U y_{ab}^U Q_a u_b^c H_2 + A_{ab}^D y_{ab}^D Q_a d_b^c H_1 + A_{ab}^L y_{ab}^L L_a e_b^c H_1\big] + B\mu H_1 H_2 + \text{h.c.}\bigg)\,. \qquad (15)$$

In Eqn (15), λ_3^a, λ_2^a, and λ_1^1 are gluinos, winos, and bino, respectively, while Q_a, u_a^c, d_a^c, L_a, e_a^c, H_1, and H_2 are scalar components of the corresponding chiral superfields.

The MSSM suffers from the μ problem: the superpotential of the MSSM contains only one bilinear term $\mu H_1 H_2$ which can be present before SUSY is broken. One would naturally expect it to be of the order of either the GUT scale M_X or the Planck scale M_{Pl}. If $\mu \sim M_X (\sim M_{\text{Pl}})$, then the Higgs scalars get a huge positive contribution $\sim \mu^2$ to their squared masses and EW Symmetry breaking (EWSB) does not occur. On the other hand, the parameter μ cannot simply be omitted. If $\mu = 0$ at some scale Q, the mixing between Higgs doublets is not generated at any scale below Q due to the nonrenormalization theorems [90, 91]. In this case, the minimum of the Higgs boson potential is attained for $\langle H_1 \rangle = 0$. Because of this, down-type quarks and charged leptons remain massless. In order to get the correct pattern of EWSB, μ is required to be of the order of the sparticle mass scale.

In the NMSSM [92–105] (for reviews see [106–108]), which contains an additional SM singlet superfield S, the superpotential is invariant under the transformations of a discrete Z_3 symmetry, i.e., $\Phi_i \to \exp(2i\pi/3)\Phi_i$. This symmetry forbids any bilinear terms in the superpotential allowing the interaction of S with the Higgs doublets $\hat{H}_1$ and $\hat{H}_2$:

$$W_{\text{NMSSM}} = \lambda S(H_1 H_2) + \frac{\kappa}{3} S^3 + W_{\text{MSSM}}(\mu = 0)\,. \qquad (16)$$

On the EW scale, the superfield S gets a nonzero vacuum expectation value ($\langle S \rangle = s/\sqrt{2}$) generating automatically an effective μ-term ($\mu = \lambda \langle S \rangle$) of the required size. The cubic term of the new singlet superfield $\hat{S}$ in the superpotential breaks the Peccei–Quinn symmetry [109, 110], i.e., an additional U(1) global symmetry. When $\kappa = 0$, this extra U(1) global symmetry gets spontaneously broken by the VEV of the singlet field S, giving rise to a massless Goldstone boson, the Peccei–Quinn (PQ) axion [111]. In the PQ-symmetric NMSSM, astrophysical observations exclude any choice of the parameters unless one allows s to be enormously large ($> 10^9 - 10^{11}$ GeV) [112–118], which leads to the hierarchy problem. The nonzero values of κ allow us to avoid the appearance of an axion in the particle spectrum.

Although the explicit breakdown of the extra global U(1) symmetry into its discrete Z_3 subgroup in the NMSSM seems to be well justified, the NMSSM itself is not without problems. The vacuum expectation values of the Higgs fields break the Z_3 symmetry. This leads to the formation of domain walls in the early Universe [119]. Such a domain structure of the vacuum creates unacceptably large anisotropies in the cosmic microwave background radiation [120]. In an attempt to break the Z_3 symmetry, operators suppressed by powers of the Planck scale could be introduced, but it has been shown that these operators give rise to quadratically divergent tadpole contributions, which destabilize the mass hierarchy [121]. Dangerous operators can be eliminated if an invariance under Z_2^R or Z_5^R symmetries is imposed [122, 123]. The linear term $\Lambda\hat{S}$ in the superpotential which is induced in this case by high order operators is too small to upset the mass hierarchy but large enough to prevent the appearance of domain walls. The superpotential of the corresponding modification of the NMSSM (MNSSM) can be written as [123–127]

$$W_{\text{MNSSM}} = \lambda S(H_1 H_2) + \xi S + W_{\text{MSSM}}(\mu = 0)\,. \qquad (17)$$

Other modifications of the NMSSM were also discussed [128–133].

3.2 $U(1)_N$ extensions of MSSM and E_6

In the $U(1)'$ extensions of the MSSM inspired by E_6, the extra $U(1)'$ gauge symmetry forbids the μ term $\mu(H_1 H_2)$ in the superpotential if $\theta_{E_6} \neq 0$ and $\theta_{E_6} \neq \pi$. Nevertheless, these extensions of the SM allow the interaction of the Higgs doublets H_1 and H_2 with the new SM singlet superfield S, which carries the $U(1)'$ charge only. This interaction is described by the term $\lambda S(H_1 H_2)$ in the superpotential. At the same time, the S^3 term is forbidden by the $U(1)'$ gauge symmetry. It is expected that, in the SUSY models under consideration, the superfield S develops a large VEV, breaking the $U(1)'$ gauge symmetry and inducing an effective μ term of the required size. There are no problems associated with the appearance of the PQ axion in the particle spectrum or domain walls in such models.

In the E_6 inspired $U(1)'$ extensions of the MSSM, the anomalies are automatically cancelled if the low energy particle spectrum consists of a complete representations of E_6. Consequently, in these models, one is forced to augment the minimal particle spectrum by a number of exotics which, together with ordinary quarks and leptons, form complete fundamental 27 representations of E_6. Thus, we will assume that the particle content of these models includes at least three fundamental representations of E_6 at low energies. These multiplets decompose under the $SU(5) \times U(1)_\psi \times U(1)_\chi$

subgroup of E_6 as follows:

$$
\begin{aligned}
27_i \to & \left(10, \frac{1}{\sqrt{24}}, -\frac{1}{\sqrt{40}}\right)_i + \left(5^*, \frac{1}{\sqrt{24}}, \frac{3}{\sqrt{40}}\right)_i \\
& + \left(5^*, -\frac{2}{\sqrt{24}}, -\frac{2}{\sqrt{40}}\right)_i + \left(5, -\frac{2}{\sqrt{24}}, \frac{2}{\sqrt{40}}\right)_i \\
& + \left(1, \frac{4}{\sqrt{24}}, 0\right)_i + \left(1, \frac{1}{\sqrt{24}}, -\frac{5}{\sqrt{40}}\right)_i . \qquad (18)
\end{aligned}
$$

The first, second, and third quantities in parentheses are the SU(5) representation and extra $U(1)_\psi$ and $U(1)_\chi$ charges, respectively, while i is a family index that runs from 1 to 3. An ordinary SM family, which contains the doublets of left-handed quarks Q_i and leptons L_i, right-handed up- and down-quarks (u_i^c and d_i^c), as well as right-handed charged leptons (e_i^c), is assigned to

$$
\left(10, \frac{1}{\sqrt{24}}, -\frac{1}{\sqrt{40}}\right)_i + \left(5^*, \frac{1}{\sqrt{24}}, \frac{3}{\sqrt{40}}\right)_i .
$$

Right-handed neutrinos N_i^c are associated with the last term in Eqn (18), $(1, 1/\sqrt{24}, -5/\sqrt{40})_i$. The next-to-last term, $(1, 4/\sqrt{24}, 0)_i$, represents new SM-singlet fields S_i with nonzero $U(1)_\psi$ charges that therefore survive down to the EW scale. The pair of $SU(2)_W$-doublets (H_i^d and H_i^u) that are contained in

$$
\left(5^*, -\frac{2}{\sqrt{24}}, -\frac{2}{\sqrt{40}}\right)_i \quad \text{and} \quad \left(5, -\frac{2}{\sqrt{24}}, \frac{2}{\sqrt{40}}\right)_i
$$

have the quantum numbers of Higgs doublets. They form either Higgs or Inert Higgs $SU(2)_W$ multiplets.[1] Other components of these SU(5) multiplets form color triplets of exotic quarks $\overline{D}_i$ and D_i with electric charges $+1/3$ and $-1/3$, respectively. These exotic quark states carry a $B-L$ charge ($\pm 2/3$) twice as large as that of ordinary ones. In phenomenologically viable E_6 inspired models, they can be either diquarks or leptoquarks.

The presence of the Z' boson associated with extra U(1) gauge symmetry and exotic matter in the low-energy spectrum stimulated extensive studies of such models over the years [8, 134–144]. In Ref. [145], the Tevatron and LHC Z' mass limits in these models are discussed, while different aspects of the phenomenology of exotic quarks and squarks are considered in [146]. Also, the implications of E_6 inspired SUSY models have been studied for EW symmetry breaking [147–153], neutrino physics [154, 155], and models explaining the fermion mass hierarchy and mixing [156], leptogenesis [157, 158] and EW baryogenesis [159, 160], the muon anomalous magnetic moment [161, 162], the electric dipole moment of the electron [163] and tau lepton [164], lepton flavor violating processes like $\mu \to e\gamma$ [165], and CP-violation in the Higgs sector [166]. The neutralino sector in E_6 inspired SUSY models was analyzed previously in [152, 163–165, 167–174]. The Higgs sector and the upper bound on the mass of the lightest Higgs boson in these models were examined in Refs [153, 174–180].

Within the class of rank-5 E_6 inspired SUSY models, there is a unique linear superposition of $U(1)_\chi$ and $U(1)_\psi$ that allows zero charges for the right-handed neutrinos and thus a high scale see-saw mechanism. The corresponding Abelian $U(1)_N$ gauge symmetry is associated with $\theta_{E_6} = \arctan\sqrt{15}$ in Eqn (3). Only in this Exceptional Supersymmetric Standard Model (E_6SSM) [176, 177, 181–183] may right-handed neutrinos be superheavy, shedding light on the origin of the mass hierarchy in the lepton sector and providing a mechanism for the generation of the baryon asymmetry in the Universe via leptogenesis [157, 158]. The $U(1)_Y$ and $U(1)_N$ charges of different components of the 27-plet are given in Table 1.

Table 1. $U(1)_Y$ and $U(1)_N$ charges of different components of 27-plet.

	Q_i	u_i^c	d_i^c	L_i	e_i^c	N_i^c	S_i	H_i^u	H_i^d	D_i	$\overline{D}_i$
$\sqrt{\frac{5}{3}}Q_i^Y$	$\frac{1}{6}$	$-\frac{2}{3}$	$\frac{1}{3}$	$-\frac{1}{2}$	1	0	0	$\frac{1}{2}$	$-\frac{1}{2}$	$-\frac{1}{3}$	$\frac{1}{3}$
$\sqrt{40}\,Q_i^N$	1	1	2	2	1	0	5	-2	-3	-2	-3

Supersymmetric models with an additional $U(1)_N$ gauge symmetry were studied in [155] in the context of nonstandard neutrino models with extra singlets, in [167] from the point of view of $Z-Z'$ mixing, in [152, 184, 185], where the renormalization group (RG) flow of couplings was examined, and in [151–153], where EWSB was studied. The neutralino sector in these models was explored in [152, 167, 168]. The presence of a Z' boson and of exotic quarks predicted by the Exceptional SUSY model provided spectacular new physics signals at the LHC, which were analyzed in [176–180, 186, 187]. The particle spectrum and collider signatures associated with it were studied within the constrained version of the E_6SSM in [188–192].

Although the presence of TeV scale exotic matter in E_6 inspired SUSY models gives rise to spectacular collider signatures, it also causes some serious problems. To demonstrate this, let us consider the rank-6 E_6 inspired SUSY models with two extra U(1) gauge symmetries — $U(1)_\chi$ and $U(1)_\psi$. In these models, the most general renormalizable superpotential which is allowed by the $SU(3)\times SU(2)\times U(1)_Y\times U(1)_\chi\times U(1)_\psi$ gauge symmetry can be written in the following form:

$$
\begin{aligned}
W_{E_6} &= W_0 + W_1 + W_2 , \\
W_0 &= \lambda_{ijk} S_i (H_j^d H_k^u) + \kappa_{ijk} S_i (D_j \overline{D}_k) + h_{ijk}^N N_i^c (H_j^u L_k) \\
&\quad + h_{ijk}^U u_i^c (H_j^u Q_k) + h_{ijk}^D d_i^c (H_j^d Q_k) + h_{ijk}^E e_i^c (H_j^d L_k) , \\
W_1 &= g_{ijk}^Q D_i (Q_j Q_k) + g_{ijk}^q \overline{D}_i d_j^c u_k^c , \qquad (19) \\
W_2 &= g_{ijk}^N N_i^c D_j d_k^c + g_{ijk}^E e_i^c D_j u_k^c + g_{ijk}^D (Q_i L_j) \overline{D}_k .
\end{aligned}
$$

In Eqn (19), summation over repeated family indexes ($i, j, k = 1, 2, 3$) is implied. In such models, $B-L$ number is conserved automatically, since the corresponding global symmetry $U(1)_{B-L}$ is a linear superposition of $U(1)_Y$ and $U(1)_\chi$. At the same time, if terms in W_1 and W_2 are simultaneously present in the superpotential, then baryon and lepton numbers are violated. In other words, one cannot define the baryon and lepton numbers of the exotic quarks D_i and $\overline{D}_i$ so that the complete Lagrangian is invariant separately under $U(1)_B$ and $U(1)_L$ global symmetries. In this case, Yukawa interactions in W_1 and W_2 give rise to rapid proton decay.

Another problem is associated with the presence of three families of H_i^u and H_i^d. All these Higgs-like doublets can couple to ordinary quarks and charged leptons of different

[1] We use the terminology 'Inert Higgs' to denote Higgs-like doublets that do not develop VEVs.

generations, resulting in phenomenologically unwanted flavor changing transitions. For example, nondiagonal flavor interactions contribute to the amplitude of $K^0 - \overline{K}^0$ oscillations and give rise to new channels of muon decay like $\mu \to e^- e^+ e^-$. To suppress flavor changing processes, one can impose an approximate Z_2^H symmetry, under which all superfields except one pair of H_i^d and H_i^u (say $H_d \equiv H_3^d$ and $H_u \equiv H_3^u$) and one SM-type singlet field ($S \equiv S_3$) are odd [176, 177]. When all Z_2^H symmetry violating couplings are small, this discrete symmetry allows suppressing the most dangerous baryon and lepton number violating operators as well, since it forbids all terms in W_1 and W_2.

However, if the Z_2^H symmetry were exact, the lightest exotic quarks would be extremely long-lived particles. Indeed, since the Z_2^H symmetry forbids all Yukawa interactions in W_1 and W_2, superpotential (19) does not contain any operator that allows the lightest exotic quarks to decay. Moreover, the Lagrangian of such a model is invariant not only with respect to $U(1)_L$ and $U(1)_B$ but also under $U(1)_D$ symmetry transformations:

$$D_j \to \exp(i\alpha) D_j \,, \qquad \overline{D}_k \to \exp(-i\alpha) \overline{D}_k \,. \tag{20}$$

The $U(1)_D$ invariance ensures that the lightest exotic quark is very long-lived. The $U(1)_L$, $U(1)_B$, and $U(1)_D$ global symmetries are expected to be broken by a set of nonrenormalizable operators which are suppressed by the inverse power of the GUT scale M_X. These operators give rise to decays of the exotic quarks but do not lead to rapid proton decay. Since the extended gauge symmetry in the considered rank-6 E_6 inspired SUSY models forbids any dimension five operators that break $U(1)_D$ global symmetry, the lifetime of the lightest exotic quarks is expected to be of the order of

$$\tau_D \gtrsim \frac{M_X^4}{\mu_D^5} \,, \tag{21}$$

where μ_D is the mass of the lightest exotic quark. When $\mu_D \simeq 1$ TeV, the lifetime of the lightest exotic quarks $\tau_D \gtrsim 10^{49}$ GeV^{-1} $\sim 10^{17}$ yr, i.e., considerably larger than the age of the Universe.

Long-lived exotic quarks would have been copiously produced during the very early epochs of the Big Bang. Those lightest exotic quarks which survived annihilation would subsequently have been confined in heavy hadrons, which would annihilate further. The remaining heavy hadrons originating from the Big Bang should be present in terrestrial matter. There are very strong upper limits on the abundances of nuclear isotopes which contain such stable relics in the mass range from 1 GeV to 10 TeV. Different experiments indicate that their relative concentrations should not exceed 10^{-15} per nucleon [193–195]. At the same time, various theoretical estimations [196, 197] show that, if remnant particles existed in nature today, their concentration would be expected to be at the level of 10^{-10} per nucleon. Therefore, E_6 inspired models with very long-lived exotic quarks are ruled out.

Thus, the Z_2^H symmetry defined above can only be an approximate one. When all Z_2^H symmetry violating couplings are small ($\lesssim 10^{-4}$), this discrete symmetry allows flavor changing processes to be suppressed. Nevertheless, the breakdown of the Z_2^H symmetry should not give rise to operators leading to rapid proton decay. The appropriate suppression of the proton decay rate can be achieved if one imposes either a Z_2^L or a Z_2^B discrete symmetry [176]. When the Lagrangian is invariant with respect to a Z_2^L symmetry, under which all superfields except lepton ones (L_i, e_i^c, N_i^c) are even (Model I), then the baryon number conservation requires exotic quarks to be diquarks, i.e., $B_D = -2/3$ and $B_{\overline{D}} = 2/3$. The invariance of the Lagrangian with respect to Z_2^B symmetry (Model II), under which only the exotic quark (D_i and $\overline{D}_i$) and lepton superfields (L_i, e_i^c, N_i^c) are odd, implies that $\overline{D}_i$ and D_i manifest themselves in the Yukawa interactions as leptoquarks, i.e., $B_D = 1/3$, $B_{\overline{D}} = -1/3$, $L_D = 1$, and $L_{\overline{D}} = -1$. The transformation properties of different components of 27-plets under the Z_2^H, Z_2^L, and Z_2^B discrete symmetries are presented in Table 2 (for a recent review, see [198]).

Table 2. Transformation properties of different components of 27-plets under the Z_2^H, Z_2^L, and Z_2^B discrete symmetries.

	Q_i	u_i^c	d_i^c	L_i	e_i^c	N_i^c	S_α	H_α^u	H_α^d	D_i	$\overline{D}_i$	H_u	H_d	S
Z_2^H	−	−	−	−	−	−	−	−	−	−	−	+	+	+
Z_2^L	+	+	+	−	−	−	+	+	+	+	+	+	+	+
Z_2^B	+	+	+	−	−	−	+	+	+	−	−	+	+	+

It is worth noting that, in the E_6 inspired SUSY models under consideration, different supermultiplets that are expected to stem from the same E_6 supermultiplet transform differently under the transformations of the Z_2^H, Z_2^L, and Z_2^B discrete symmetries. As a consequence, these symmetries obviously do not commute with E_6, and one can naively think that this may be inconsistent with GUTs based on the E_6 gauge group. Moreover, the necessity of introducing multiple discrete symmetries to ameliorate phenomenological problems that generically arise due to the presence of low mass exotics is an undesirable feature of these models. In this context, we now specify the SUSY model with additional $U(1)_N$ gauge symmetry that can originate from E_6 GUTs.

3.3 E_6SSM

Again, let us assume that, near the GUT scale, E_6 or its subgroup is broken down into the $SU(3)_C \times SU(2)_W \times U(1)_Y \times U(1)_\psi \times U(1)_\chi$ gauge symmetry, while the particle spectrum of SUSY model involves three 27-plets of E_6, ensuring anomaly cancellation. In our model building strategy, we use the SU(5) SUSY GUT as a guideline. Indeed, the low-energy spectrum of the MSSM, in addition to the complete SU(5) multiplets, contains an extra pair of doublets from 5 and $\overline{5}$ fundamental representations, that plays the role of Higgs fields which break EW symmetry. In the MSSM, potentially dangerous operators that lead to rapid proton decay are forbidden by the matter parity Z_2^M under which Higgs doublets are even, while all matter superfields that fill in complete SU(5) representations are odd. Following this inspirational example, we augment three 27-plets of E_6 by a number of components M_l and $\overline{M}_l$ from extra $27'_l$ and $\overline{27'}_l$ below the GUT scale. Because additional pairs of multiplets M_l and $\overline{M}_l$ have opposite $U(1)_Y$, $U(1)_\psi$, and $U(1)_\chi$ charges, their contributions to the anomalies get cancelled identically. As in the case of the MSSM, we allow the set of multiplets M_l to be used for the breakdown of gauge symmetry. If the corresponding set includes $H^u \equiv H_u$, $H^d \equiv H_d$, S, and $N^c \equiv N_H^c$, then the $SU(2)_W \times U(1)_Y \times U(1)_\psi \times U(1)_\chi$ symmetry can be broken down into $U(1)_{em}$, associated with electromagnetism. The VEVs of S and N^c break $U(1)_\psi$ and $U(1)_\chi$ entirely, while the $SU(2)_W \times U(1)_Y$

symmetry remains intact. When the neutral components of H_{u} and H_{d} acquire nonzero VEVs, the $\mathrm{SU}(2)_W \times \mathrm{U}(1)_Y$ symmetry gets broken into $\mathrm{U}(1)_{\mathrm{em}}$ and the masses of all fermions and bosons are generated.

It is assumed that all multiplets M_l are even under some $\tilde{\mathrm{Z}}_2^H$ symmetry, while three copies of the complete fundamental representations of E_6 are odd. This forbids couplings in the superpotential that come from $27_i \times 27_j \times 27_k$. On the other hand, the $\tilde{\mathrm{Z}}_2^H$ symmetry allows the Yukawa interactions that stem from $27'_l \times 27'_m \times 27'_n$ and $27'_l \times 27_i \times 27_k$. In contrast to the Z_2^H symmetry, it is expected that the discrete $\tilde{\mathrm{Z}}_2^H$ symmetry remains intact. The multiplets M_l have to be even under the $\tilde{\mathrm{Z}}_2^H$ symmetry, because they get large VEVs. Otherwise, the VEVs of the corresponding fields lead to the breakdown of the discrete $\tilde{\mathrm{Z}}_2^H$ symmetry, giving rise to baryon and lepton number violating operators in general. To ensure the correct breakdown of the $\mathrm{U}(1)_N$ gauge symmetry, the set of $\tilde{\mathrm{Z}}_2^H$ even supermultiplets in the E_6SSM also involves a pure singlet superfield ϕ, which is uncharged under all of the gauge symmetries [199, 200]. If the set of multiplets M_l includes only one pair of doublets H_{d} and H_{u}, the $\tilde{\mathrm{Z}}_2^H$ symmetry defined above permits suppressing unwanted FCNC processes at the tree level, since down-type quarks and charged leptons couple to just one Higgs doublet H_{d}, whereas the up-type quarks couple to H_{u} only.

The superfields $\overline{M}_l$ can be either odd or even under this $\tilde{\mathrm{Z}}_2^H$ symmetry. Depending on whether these fields are even or odd under $\tilde{\mathrm{Z}}_2^H$, a subset of terms in the most general renormalizable superpotential can be written as

$$W_{\mathrm{total}} = Y'_{lmn} 27'_l 27'_m 27'_n + Y_{lij} 27'_l 27_i 27_j + \tilde{Y}_{lmn} \overline{27'}_l \overline{27'}_m \overline{27'}_n + \frac{\kappa}{3}\,\phi^3 + \frac{\mu_\phi}{2}\,\phi^2 + \Lambda_F \phi + Y'_{mn} \phi\, 27'_m \overline{27'}_n + \mu'_{il}\, 27_i\, \overline{27'}_l + \tilde{\mu}'_{ml}\, 27'_m \overline{27'}_l + \ldots, \tag{22}$$

where Y'_{lmn}, Y_{lij}, $\tilde{Y}_{lmn}$, Y'_{mn}, and κ are Yukawa couplings, while μ'_{il}, $\tilde{\mu}'_{ml}$, μ_ϕ, and Λ_F are mass parameters. One should keep in mind that only M_l and $\overline{M}_l$ components of $27'_l$ and $\overline{27'}_l$ appear below the GUT scale. All other components of these $27'_l$ and $\overline{27'}_l$ gain masses of the order of M_{X}. The form of the mass terms associated with $\overline{M}_l$ in Eqn (22) depend on the transformation properties of these superfields. Indeed, if $\overline{M}_l$ is odd under $\tilde{\mathrm{Z}}_2^H$ symmetry, then the term $\tilde{\mu}'_{ml} 27'_m \overline{27'}_l$ is forbidden, while μ'_{il} can have nonzero values. When $\overline{M}_l$ is even, μ'_{il} vanish, whereas $\tilde{\mu}'_{ml} 27'_m \overline{27'}_l$ is allowed by $\tilde{\mathrm{Z}}_2^H$ symmetry. In general mass parameters, μ'_{il} and $\tilde{\mu}'_{ml}$ are expected to be of the order of the GUT scale. In order to allow some of the $\overline{M}_l$ multiplets to survive to low energies, we assume that the corresponding mass terms are forbidden at high energies and get induced at some intermediate scale which is much lower than M_{X}.

The VEVs of the superfields N_H^{c} and $\overline{N}_H^{\mathrm{c}}$ (that originate from $27'_N$ and $\overline{27'}_N$) can be used not only for the breakdown of $\mathrm{U}(1)_\psi$ and $\mathrm{U}(1)_\chi$ gauge symmetries but also to generate Majorana masses for right-handed neutrinos N_i^{c}. The corresponding mass terms can be induced through interactions [181]

$$\Delta W_N = \frac{\varkappa_{ij}}{M_{\mathrm{Pl}}}\,(27_i\,\overline{27'}_N)(27_j\,\overline{27'}_N)\,. \tag{23}$$

The nonrenormalizable operators (23) give rise to right-handed neutrino masses which are substantially lower than the VEVs of $\langle \overline{N}_H^{\mathrm{c}} \rangle$ and $\langle N_H^{\mathrm{c}} \rangle$. In this case, the right-handed neutrinos can be superheavy only if $\mathrm{U}(1)_\psi \times \mathrm{U}(1)_\chi$ symmetry is broken down into

$$\mathrm{U}(1)_N = \frac{1}{4}\,\mathrm{U}(1)_\chi + \frac{\sqrt{15}}{4}\,\mathrm{U}(1)_\psi \tag{24}$$

somewhere near the GUT scale. Since N_H^{c} and $\overline{N}_H^{\mathrm{c}}$ acquire very large VEVs, both supermultiplets must be even under the $\tilde{\mathrm{Z}}_2^H$ symmetry.

The VEVs of N_H^{c} and $\overline{N}_H^{\mathrm{c}}$ may also break the $\mathrm{U}(1)_{B-L}$ symmetry. In particular, the VEV of N_H^{c} can induce the bilinear terms $M_{ij}^L (H_i^{\mathrm{u}} L_j)$ and $M_{ij}^B (D_i d_j^{\mathrm{c}})$ in the superpotential. Although such a breakdown of gauge symmetry might be possible, the extra exotic particles tend to be rather heavy in this case and thus irrelevant for collider phenomenology. Therefore, we shall assume further that the couplings of N_H^{c} to 27_i are forbidden. This, for example, can be achieved by imposing an extra discrete Z_2 symmetry, which implies $N_H^{\mathrm{c}} \to -N_H^{\mathrm{c}}$ and $\overline{N}_H^{\mathrm{c}} \to -\overline{N}_H^{\mathrm{c}}$. Although this symmetry forbids the interactions $27'_N 27_i 27_j$ in the superpotential, it allows nonrenormalizable interactions (23) that induce large Majorana masses for right-handed neutrinos.

The mechanism of the $\mathrm{U}(1)_\psi$ and $\mathrm{U}(1)_\chi$ symmetry breaking discussed above ensures that the VEVs of N_H^{c} and $\overline{N}_H^{\mathrm{c}}$ break $\mathrm{U}(1)_\psi \times \mathrm{U}(1)_\chi$ gauge symmetry down into $\mathrm{U}(1)_N \times \mathrm{P}_M$. Such a spontaneous breakdown of the $\mathrm{U}(1)_\psi$ and $\mathrm{U}(1)_\chi$ symmetries can occur, because P_M is a discrete subgroup of $\mathrm{U}(1)_\psi$ and $\mathrm{U}(1)_\chi$. Moreover, the $\tilde{\mathrm{Z}}_2^H$ symmetry is a product of

$$\tilde{\mathrm{Z}}_2^H = \mathrm{P}_M \times \mathrm{Z}_2^E\,, \tag{25}$$

where Z_2^E is a discrete symmetry associated with the exotic states [181]. The transformation properties of different components of 27_i, $27'_l$, and $\overline{27'}_l$ supermultiplets under the $\tilde{\mathrm{Z}}_2^H$, Z_2^M, and Z_2^E symmetries are summarized in Table 3. As follows from Table 3, all components of 27-plets that contain exotic states, i.e., $\overline{D}_i$, D_i, H_i^{d}, H_i^{u}, and S_i, are odd under the $\tilde{\mathrm{Z}}_2^E$ symmetry. Because the low-energy effective Lagrangian of the models under consideration is invariant under the $\tilde{\mathrm{Z}}_2^H$ and

Table 3. Transformation properties of different components of E_6 supermultiplets and superfield ϕ under $\tilde{\mathrm{Z}}_2^H$, P_M, and Z_2^E discrete symmetries.

	27_i	27_i	$27'_{H_{\mathrm{u}}}$ $(27'_{H_{\mathrm{d}}})$	$27'_S$	$\overline{27'}_{H_{\mathrm{u}}}$ $(\overline{27'}_{H_{\mathrm{d}}})$	$\overline{27'}_S$	$27'_N$ $(\overline{27'}_N)$	$27'_L$ $(\overline{27'}_L)$	1
	$Q_i, u_i^{\mathrm{c}}, d_i^{\mathrm{c}}, L_i, e_i^{\mathrm{c}}, N_i^{\mathrm{c}}$	$\overline{D}_i, D_i, H_i^{\mathrm{d}}, H_i^{\mathrm{u}}, S_i$	H_{u} (H_{d})	S	$\overline{H}_{\mathrm{u}}$ $(\overline{H}_{\mathrm{d}})$	$\overline{S}$	N_H^{c} $(\overline{N}_H^{\mathrm{c}})$	L_4 $(\overline{L}_4)$	ϕ
$\tilde{\mathrm{Z}}_2^H$	−	−	+	+	−	+	+	+	+
P_M	−	+	+	+	+	+	−	−	+
Z_2^E	+	−	+	+	−	+	−	−	+

P_M symmetries, it is also invariant under the transformations of the Z_2^E symmetry. Z_2^E symmetry conservation implies that the lightest exotic state, which is odd under this symmetry, is absolutely stable and contributes to the relic density of dark matter.

As was mentioned before, in SUSY models, the lightest supersymmetric particle (LSP), i.e., the lightest R-parity odd state, must be stable. If in the models under consideration the lightest exotic state (i.e., state with $Z_2^E = -1$) has even R-parity, then the conservation of the Z_2^E symmetry and R-parity forbids the decay of this exotic particle, as well as the decay of the lightest R-parity odd state. When the lightest exotic state is also the lightest R-parity odd particle, either the lightest R-parity even exotic state or the next-to-lightest R-parity odd state with $Z_2^E = +1$ must be absolutely stable. Thus, these E_6 inspired SUSY models contain at least two dark-matter candidates.

Within the E_6SSM, the $U(1)_N$ gauge symmetry gets broken by the VEVs of S and $\overline{S}$. Their VEVs should be sufficiently large ($\gtrsim 10$ TeV), because they induce the mass of the Z' as well as the masses of all exotic quarks and inert higgsinos. Because of this, $\overline{S}$ should be even under the $\tilde{Z}_2^H$ symmetry and all components of the superfields S and $\overline{S}$ are required to gain TeV scale masses.

If the set of $\tilde{Z}_2^H$ even supermultiplets M_l involve only H_u, H_d, S, and N_H^c, then the Lagrangian of this model is invariant under $U(1)_D$ symmetry transformations, and the lightest exotic quarks are extremely long-lived particles. Indeed, in this case, the $\tilde{Z}_2^H$ symmetry forbids all Yukawa interactions in W_1 and W_2 that allow the lightest exotic quarks to decay. Such models are basically ruled out. To ensure that the lightest exotic quarks decay within a reasonable time, the set of $\tilde{Z}_2^H$ even supermultiplets M_l needs to be supplemented by the $SU(2)_W$ doublet of lepton superfields L_4 that survives to low energies. In this case, $\overline{D}_i$ and D_i can interact with leptons and quarks only while the couplings of these exotic quarks to a pair of quarks are forbidden by the postulated $\tilde{Z}_2^H$ symmetry. The baryon number is then conserved and exotic quarks are leptoquarks.

The relatively light components of the supermultiplets L_4 and $\overline{L}_4$ can significantly facilitate the process of the generation of the baryon asymmetry of the Universe, which is caused by out–of-equilibrium decays of the lightest right-handed neutrino and sneutrino. In the E_6SSM, these states contribute to the CP asymmetries that control the corresponding process. Moreover, the components of the supermultiplets L_4 and $\overline{L}_4$ give rise to extra CP asymmetries associated with the new channels of the decays of the lightest right-handed neutrino and its superpartner [157]. The appropriate value of the baryon asymmetry can be induced within the E_6SSM even when the lightest right-handed neutrinos/sneutrinos have masses which are less than $10^6 - 10^7$ GeV, so successful thermal leptogenesis may be achieved without encountering a gravitino problem [201, 202].

The simplest scenario implies that $\overline{H}_u$ and $\overline{H}_d$ are odd under the $\tilde{Z}_2^H$ symmetry, while L_4 and $\overline{L}_4$ are $\tilde{Z}_2^H$ even. Then, $\overline{H}_u$ and $\overline{H}_d$ get combined with the superposition of the corresponding components from 27_i so that the resulting vectorlike states gain masses of the order of M_X. The supermultiplets L_4 and $\overline{L}_4$ are also expected to form vectorlike states. However, these states are required to be light enough to ensure that the lightest exotic quarks decay sufficiently fast. The appropriate mass term $\mu_L L_4 \overline{L}_4$ in the superpotential can be induced within SUGRA models just after the breakdown of local SUSY if the Kähler potential contains an extra term $(Z_L(L_4\overline{L}_4) + \text{h.c.})$ [203, 204]. Thus, E_6SSM implies that the low energy matter content of this models involves

$$\left[(Q_i,\, u_i^c,\, d_i^c,\, L_i,\, e_i^c,\, N_i^c)\right] + (D_i,\, \overline{D}_i) + S_i + H_\alpha^u + H_\alpha^d + L_4 + \overline{L}_4 + N_H^c + \overline{N}_H^c + S + \overline{S} + H_u + H_d + \phi\,, \qquad (26)$$

where the components of the superfields N_i^c, N_H^c, and $\overline{N}_H^c$ are expected to gain masses which are much larger than 100 TeV, while the remaining matter survives down to the TeV scale. In Eqn (26), $\alpha = 1, 2$ and $i = 1, 2, 3$. Integrating out N_i^c, N_H^c, and $\overline{N}_H^c$ and ignoring all suppressed nonrenormalizable interactions, one gets an explicit expression for the superpotential in this case [199]:

$$\begin{aligned} W_{E_6\mathrm{SSM}} &= \lambda S(H_u H_d) - \sigma\phi S\overline{S} + \frac{\kappa}{3}\,\phi^3 + \frac{\mu_\phi}{2}\,\phi^2 + \Lambda_F\phi \\ &+ \lambda_{\alpha\beta} S(H_\alpha^d H_\beta^u) + \kappa_{ij} S(D_i\overline{D}_j) + \tilde{f}_{i\alpha} S_i(H_\alpha^d H_u) \\ &+ f_{i\alpha} S_i(H_d H_\alpha^u) + g_{ij}^D (Q_i L_4)\overline{D}_j + h_{i\alpha}^E e_i^c (H_\alpha^d L_4) \\ &+ \mu_L L_4\overline{L}_4 + \tilde{\sigma}\phi L_4\overline{L}_4 + W_{\mathrm{MSSM}}(\mu = 0)\,. \end{aligned} \qquad (27)$$

The $U(1)_N$ extensions of the MSSM with exact $\tilde{Z}_2^H$ symmetry discussed in this section have at least one drawback. These models imply that a number of incomplete E_6 multiplets survive below the scale M_X. In fact, the number of incomplete E_6 multiplets tends to be larger than the number of generations. The appropriate splitting of 27-plets can be naturally achieved in the framework of E_6 GUTs with an extra compact dimension (orbifold GUTs) [181]. In orbifold GUT models, the dimension five operators, which are caused by an exchange of the color triplet higgsino multiplets and give rise to proton decay in ordinary GUTs, do not get induced [205]. Proton stability was discussed in the context of orbifold GUT models in [205–215]. In these models, the proton decay is mediated by dimension six operators generated by the leptoquark gauge bosons [216].

4. Gauge coupling unification

The approximate unification of the SM gauge couplings remains one of the most attractive features of SUSY extensions of the SM based on experimental data. In the MSSM and NMSSM, the running of the SM gauge couplings is described by a system of the renormalization group (RG) equations (RGEs), which can be written in the following form:

$$\frac{d\alpha_i}{dt} = \frac{\beta_i \alpha_i^2}{2\pi}\,, \qquad \beta_i = b_i + \frac{\tilde{b}_i}{4\pi}\,, \qquad (28)$$

where b_i and $\tilde{b}_i$ are one-loop and two-loop contributions to the β functions [217–224], $t = \log(q/M_Z)$, and q is a renormalization scale, with the index i running from 1 to 3 corresponding to $U(1)_Y$, $SU(2)_W$, and $SU(3)_C$ interactions, respectively. One can obtain an approximate solution of the RG equations (28) that at high energies can be written as [225]

$$\frac{1}{\alpha_i(t)} = \frac{1}{\alpha_i(M_Z)} - \frac{b_i}{2\pi}\,t - \frac{C_i}{12\pi} - \Theta_i(t) + \frac{b_i - b_i^{\mathrm{SM}}}{2\pi}\ln\frac{T_i}{M_Z}\,. \qquad (29)$$

The second term in Eqn (29) is the contribution of the one-loop β function in the RG flow of the SM gauge couplings.

The third term on the right-hand side of Eqn (29) is the $\overline{\mathrm{MS}} \to \overline{\mathrm{DR}}$ conversion factor with $C_1 = 0$, $C_2 = 2$, $C_3 = 3$ [226, 227]. Although the contributions of the third terms are quite small, they should be included when the contributions of two-loop corrections to the β functions are taken into account

$$\Theta_i(t) = \frac{1}{8\pi^2} \int_0^t \tilde{b}_i \, \mathrm{d}\tau \,. \tag{30}$$

The threshold corrections are associated with the last terms in Eqn (29), which are determined by

$$T_i = \prod_{k=1}^{N} (m_k)^{\Delta b_i^k / (b_i - b_i^{\mathrm{SM}})} \,, \tag{31}$$

where b_i^{SM} are the coefficients of the one-loop β functions in the SM, while m_k and Δb_i^k are masses and contributions to the one-loop β functions due to new particles appearing in the SUSY models under consideration. Because the two-loop corrections to the running of the gauge couplings $\Theta_i(t)$ are considerably smaller than the leading terms, the gauge and Yukawa couplings in $\tilde{b}_i$ are usually replaced by the corresponding solutions of the RG equations obtained in the one-loop approximation. The threshold corrections associated with the last terms in Eqn (29) are of the same order as or even less than $\Theta_i(t)$. Therefore, in Eqn (31), only leading one-loop threshold effects are taken into account.

Relying on the approximate solution of the RG equations (29), one can establish the relationships between the values of the gauge couplings on the EW and GUT scales for any SUSY model. Then, by using the expressions describing the RG flow of $\alpha_1(t)$ and $\alpha_2(t)$, it is rather easy to find the scale M_{X} where $\alpha_1(M_{\mathrm{X}}) = \alpha_2(M_{\mathrm{X}}) = \alpha_0$ and the value of the overall gauge coupling α_0 on this scale. Substituting M_{X} and α_0 into the solution of the RG equations for the strong gauge coupling, one finds the value of $\alpha_3(M_{\mathrm{Z}})$ for which exact gauge coupling unification takes place [228]:

$$\begin{gathered}\frac{1}{\alpha_3(M_{\mathrm{Z}})} = \frac{1}{b_1 - b_2}\left[\frac{b_1 - b_3}{\alpha_2(M_{\mathrm{Z}})} - \frac{b_2 - b_3}{\alpha_1(M_{\mathrm{Z}})}\right] - \frac{1}{28\pi} + \Theta_s - \Delta_s \,, \\ \Theta_s = \frac{b_2 - b_3}{b_1 - b_2}\,\Theta_1 - \frac{b_1 - b_3}{b_1 - b_2}\,\Theta_2 + \Theta_3 \,, \qquad \Theta_i = \Theta_i(M_{\mathrm{X}}) \,,\end{gathered} \tag{32}$$

where Δ_s are combined threshold corrections whose precise form depends on the model under consideration.

In the MSSM and NMSSM, the one-loop contributions to the β functions b_i are given by

$$b_i = \begin{pmatrix} 0 \\ -6 \\ -9 \end{pmatrix} + N_{\mathrm{H}} \begin{pmatrix} 3/10 \\ 1/2 \\ 0 \end{pmatrix} + 2N_{\mathrm{G}} \,, \tag{33}$$

where N_{H} is the number of the Higgs doublets ($N_{\mathrm{H}} = 2$ in the case of the MSSM and NMSSM), whereas N_{G} is the number of fermion generations. From Eqn (33), it follows that, in the one–loop approximation, the scale M_{X}, where the unification of the gauge couplings takes place, is almost insensitive to N_{G}. Indeed, all quarks, leptons, and their superpartners form complete SU(5) multiplets and, as a consequence, make the same contribution to the one-loop β functions. Thus, the differences among the corresponding β functions do not depend on N_{G} or the number of complete SU(5) multiplets. At the same time, the value of the overall gauge coupling α_0 grows with the increasing number of complete SU(5) matter multiplets. The requirement of the validity of perturbation theory up to the scale M_{X} sets a stringent constraint on the number of complete SU(5) matter supermultiplets that can survive to low energies in addition to three generations of fermions and sfermions [229].

In the MSSM, the contribution of the threshold corrections Δ_s in Eqn (32) takes the form [225, 228, 230, 231]

$$\begin{aligned} &\Delta_s = -\frac{19}{28\pi} \ln \frac{\tilde{M}_{\mathrm{S}}}{M_{\mathrm{Z}}} \,, \qquad \tilde{M}_{\mathrm{S}} = \frac{T_2^{100/19}}{T_1^{25/19} T_3^{56/19}} \,, \\ &T_1 = \mu^{4/25} m_{\mathrm{A}}^{1/25} \left(\prod_{i=1,2,3} m_{\tilde{\mathrm{Q}}_i}^{1/75} m_{\tilde{\mathrm{d}}_i}^{2/75} m_{\tilde{\mathrm{u}}_i}^{8/75} m_{\tilde{\mathrm{L}}_i}^{1/25} m_{\tilde{\mathrm{e}}_i}^{2/25} \right) , \\ &T_2 = M_{\tilde{\mathrm{W}}}^{8/25} \mu^{4/25} m_{\mathrm{A}}^{1/25} \left(\prod_{i=1,2,3} m_{\tilde{\mathrm{Q}}_i}^{3/25} m_{\tilde{\mathrm{L}}_i}^{1/25} \right) , \\ &T_3 = M_{\tilde{\mathrm{g}}}^{1/2} \left(\prod_{i=1,2,3} m_{\tilde{\mathrm{Q}}_i}^{1/12} m_{\tilde{\mathrm{u}}_i}^{1/24} m_{\tilde{\mathrm{d}}_i}^{1/24} \right) , \end{aligned} \tag{34}$$

where m_{A}, $M_{\tilde{\mathrm{g}}}$, and $M_{\tilde{\mathrm{W}}}$ are the masses of the heavy Higgs states and superpartners of the $\mathrm{SU}(3)_C$ and $\mathrm{SU}(2)_W$ gauge bosons; $m_{\tilde{\mathrm{u}}_i}$, $m_{\tilde{\mathrm{d}}_i}$, and $m_{\tilde{\mathrm{Q}}_i}$ are the masses of the right-handed and left-handed squarks; and $m_{\tilde{\mathrm{L}}_i}$ and $m_{\tilde{\mathrm{e}}_i}$ are the masses of the left-handed and right-handed sleptons. Assuming for simplicity that superpartners of all quarks are degenerate, i.e., their masses are equal to $m_{\tilde{\mathrm{q}}}$, and all sleptons have a common mass $m_{\tilde{l}}$, we find

$$\tilde{M}_{\mathrm{S}} \simeq \mu \left(\frac{m_{\mathrm{A}}}{\mu}\right)^{3/19} \left(\frac{M_{\tilde{\mathrm{W}}}}{\mu}\right)^{4/19} \left(\frac{M_{\tilde{\mathrm{W}}}}{M_{\tilde{\mathrm{g}}}}\right)^{28/19} \left(\frac{m_{\tilde{l}}}{m_{\tilde{\mathrm{q}}}}\right)^{3/19} . \tag{35}$$

For $\mu \simeq 1-2$ TeV, the scale $\tilde{M}_{\mathrm{S}}$ varies in the mass range of 200–300 GeV [225, 228, 230–234]. From Eqns (32) and (35) as well as Table 4, it follows that, for such small values of the scale $\tilde{M}_{\mathrm{S}}$, exact gauge coupling unification can be attained only for large values of $\alpha_3(M_{\mathrm{Z}}) \gtrsim 0.123$ [235, 236]. For $\tilde{M}_{\mathrm{S}} \simeq M_{\mathrm{Z}}$, the exact unification of the SM gauge couplings is achieved if $\alpha_3(M_{\mathrm{Z}}) \geqslant 0.126$ [230, 237]. Such large values of $\alpha_3(M_{\mathrm{Z}})$ are disfavored by the recent fit to experimental data.

To simplify the analysis of the RG flow of the SM gauge couplings, one can set $T_1 = T_2 = T_3 = \tilde{M}_{\mathrm{S}}$. In Fig. 1, the evolution of the SM gauge couplings from the EW (M_{Z}) scale to the GUT scale ($M_{\mathrm{X}} \simeq 2 \times 10^{16}$ GeV) is plotted as a function of $\log(q/M_{\mathrm{X}})$ for $T_1 = T_2 = T_3 = \tilde{M}_{\mathrm{S}} = 2$ TeV. Dotted lines show the uncertainty in $\alpha_i(t)$ caused by variations in $\alpha_3(M_{\mathrm{Z}})$ from 0.116 to 0.120. The results presented in Fig. 1 indicate that it is rather problematic to

Table 4. Corrections to $1/\alpha_i(M_{\mathrm{X}})$ and $1/\alpha_3(M_{\mathrm{Z}})$ induced by two-loop contributions to beta functions in the MSSM and E$_6$SSM* for $\alpha(M_{\mathrm{Z}}) = 1/127.9$, $\sin^2\theta_{\mathrm{W}} = 0.231$, $\alpha_3(M_{\mathrm{Z}}) = 0.118$, and $\tan\beta = 10$.

	Θ_1	Θ_2	Θ_3	Θ_s
MSSM	0.556	0.953	0.473	−0.764
E$_6$SSM I	1.558	2.322	2.618	−0.250
E$_6$SSM II	1.604	2.385	2.638	−0.305

* In the case of the E$_6$SSM, we consider two cases: the scenario E$_6$SSM I corresponds to $\kappa(M_{Z'}) = \kappa_1(M_{Z'}) = \kappa_2(M_{Z'}) = \lambda(M_{Z'}) = \lambda_1(M_{Z'}) = \lambda_2(M_{Z'}) = g_1'(M_{Z'})$, $g_1'^2(M_{Z'}) = 0.227$, $g_{11}(M_{Z'}) = 0.0202$; in the scenario E$_6$SSM II, we fix $\kappa_i = \lambda_i = 0$, $g_1'^2(M_{Z'}) = 0.227$, $g_{11}(M_{Z'}) = 0.0202$.

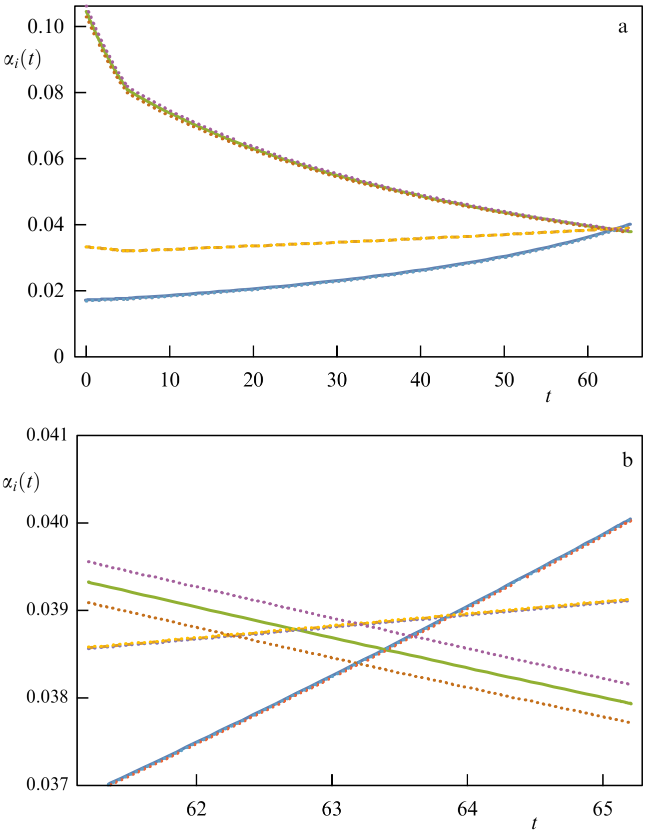

Figure 1. (a) Two-loop RG flow of $\alpha_1(t)$, $\alpha_2(t)$, and $\alpha_3(t)$ as a function of $t = \log(q/M_Z)$ and (b) the running of SM gauge couplings near the scale M_X calculated within the MSSM in the two-loop approximation for $\tan\beta = 10$, $T_1 = T_2 = T_3 = \tilde{M}_S = 2$ TeV, $\alpha_s(M_Z) = 0.118$, $\alpha(M_Z) = 1/127.9$, and $\sin^2\theta_W = 0.231$. Solid, dashed, and bold lines correspond to the running of $\alpha_1(t)$, $\alpha_2(t)$, and $\alpha_3(t)$. Dotted lines represent the uncertainty in $\alpha_i(t)$ caused by the variation in $\alpha_3(M_Z)$ from 0.116 to 0.120.

attain the exact gauge coupling unification in the framework of the MSSM when $\alpha_3(M_Z) = 0.116-0.120$.

Now, let us consider the RG flow of gauge couplings within the E$_6$SSM. To simplify our analysis, we assume that $U(1)_\psi \times U(1)_\chi$ gauge symmetry is broken down into $U(1)_N \times P_M$ near the scale M_X. Nevertheless, even in this simplest scenario, the running of the gauge couplings in the E$_6$SSM is affected by kinetic term mixing between the gauge fields associated with the $U(1)_Y$ and $U(1)_N$ interactions. Such mixing basically arises in all extensions of the SM with extra $U(1)'$ gauge symmetry [238]. In the basis in which the interactions between gauge and matter fields have the canonical form, i.e., a covariant derivative D_μ which acts on the doublet of the left-handed quarks is given by

$$D_\mu = \partial_\mu - \mathrm{i} g_3 A^a_\mu T^a - \mathrm{i} g_2 W^b_\mu \tau^b - \mathrm{i} g_Y Q^Y_i B^Y_\mu - \mathrm{i} g_N Q^N_i B^N_\mu \,, \tag{36}$$

the gauge kinetic part of the Lagrangian can be written as

$$\mathcal{L}_{\mathrm{kin}} = -\frac{1}{4}\left(F^Y_{\mu\nu}\right)^2 - \frac{1}{4}\left(F^N_{\mu\nu}\right)^2 - \frac{\sin\chi}{2}\, F^Y_{\mu\nu}F^N_{\mu\nu} - \frac{1}{4}\left(G^a_{\mu\nu}\right)^2 - \frac{1}{4}\left(W^b_{\mu\nu}\right)^2 . \tag{37}$$

In Eqns (36), (37), A^a_μ, W^b_μ, B^Y_μ, and B^N_μ represent $SU(3)_C$, $SU(2)_W$, $U(1)_Y$, and $U(1)_N$ gauge fields, $G^a_{\mu\nu}$, $W^b_{\mu\nu}$, $F^Y_{\mu\nu}$, and $F^N_{\mu\nu}$ are field strengths for the corresponding gauge interactions, while g_3, g_2, g_Y, and g_N are $SU(3)_C$, $SU(2)_W$, $U(1)_Y$, and $U(1)_N$ gauge couplings, respectively.

Although one can expect that, near the GUT scale M_X the parameter $\sin\chi$ is equal to zero at the tree-level, it arises from loop effects since

$$\mathrm{Tr}\,(Q^Y Q^N) = \sum_{i=\text{chiral fields}} (Q^Y_i Q^N_i) \neq 0 \,. \tag{38}$$

The complete E$_6$ multiplets do not contribute to this trace. Its nonzero value is due to the incomplete $27'_L + \overline{27'}_L$ supermultiplets of the original E$_6$ symmetry from which only L_4 and $\overline{L}_4$ survive to low energy. This leads to the mixing between the gauge fields. The mixing in the gauge kinetic part of Lagrangian (37) can be easily eliminated by means of a nonunitary transformation of the two $U(1)$ gauge fields [239–242]:

$$B^Y_\mu = B_{1\mu} - B_{2\mu}\tan\chi \,, \qquad B^N_\mu = \frac{B_{2\mu}}{\cos\chi} \,. \tag{39}$$

In terms of the new gauge variables $B_{1\mu}$ and $B_{2\mu}$, the covariant derivative (36) becomes [238]

$$D_\mu = \partial_\mu - \mathrm{i} g_3 A^a_\mu T^a - \mathrm{i} g_2 W^b_\mu \tau^b - \mathrm{i} g_1 Q^Y_i B_{1\mu} - \mathrm{i}(g'_1 Q^N_i + g_{11} Q^Y_i) B_{2\mu} \,, \tag{40}$$

where

$$g_1 = g_Y \,, \qquad g'_1 = \frac{g_N}{\cos\chi} \,, \qquad g_{11} = -g_Y \tan\chi \,. \tag{41}$$

In the new Lagrangian, written in terms of the new gauge variables $B_{1\mu}$ and $B_{2\mu}$, the mixing effect is concealed in the interaction between the $U(1)_N$ gauge field and matter fields and is characterized by a new off-diagonal gauge coupling g_{11}. The covariant derivative (40) can be rewritten in a more compact form,

$$D_\mu = \partial_\mu - \mathrm{i} g_3 A^a_\mu T^a - \mathrm{i} g_2 W^b_\mu \tau^b - \mathrm{i} Q^{\mathrm{T}} G B_\mu \,, \tag{42}$$

where $Q^{\mathrm{T}} = (Q^Y_i, Q^N_i)$, $B^{\mathrm{T}}_\mu = (B_{1\mu}, B_{2\mu})$, and G is a 2×2 matrix of new gauge couplings,

$$G = \begin{pmatrix} g_1 & g_{11} \\ 0 & g'_1 \end{pmatrix} . \tag{43}$$

In this approximation, the gauge kinetic mixing changes effectively the $U(1)_N$ charges of the fields to

$$\tilde{Q}_i \equiv Q^N_i + Q^Y_i \delta \,, \tag{44}$$

where $\delta = g_{11}/g'_1$, while the $U(1)_Y$ charges remain the same. As the gauge coupling constants g_{11} and g'_1 are scale dependent, the effective $U(1)_N$ charges (44) are scale dependent as well. The particle spectrum now depends on the effective $U(1)_N$ charges $\tilde{Q}_i$.

The exploration of the RG flow of the gauge couplings within the E$_6$SSM should include an analysis of the evolution of four diagonal gauge couplings, $g_3(t)$, $g_2(t)$, $g_1(t)$, and $g'_1(t)$, which correspond to the $SU(3)_C$, $SU(2)_W$, $U(1)_Y$, and $U(1)_N$ gauge interactions, respectively, as well as an investigation of the running of one off-diagonal gauge coupling, $g_{11}(t)$. Using the matrix notation for the structure of $U(1)$ interactions (42), (43), the RG equations can be written in a compact form [239–242]:

$$\frac{\mathrm{d}G}{\mathrm{d}t} = G \times B\,, \qquad \frac{\mathrm{d}g_2}{\mathrm{d}t} = \frac{\beta_2 g_2^3}{(4\pi)^2}\,, \qquad \frac{\mathrm{d}g_3}{\mathrm{d}t} = \frac{\beta_3 g_3^3}{(4\pi)^2}\,, \tag{45}$$

where B is a 2×2 matrix of β functions given by

$$B = \frac{1}{(4\pi)^2}\begin{pmatrix} \beta_1 g_1^2 & 2g_1 g_1' \beta_{11} + 2 g_1 g_{11}\beta_1 \\ 0 & g_1'^2 \beta_1' + 2 g_1' g_{11}\beta_{11} + g_{11}^2 \beta_1 \end{pmatrix}, \tag{46}$$

while β_i and β_{11} are β functions. In the one-loop approximation, the β functions associated with the U(1) interactions are given by

$$\beta_1 = \sum_i (Q_i^Y)^2 = \frac{48}{5}\,, \qquad \beta_1' = \sum_i (Q_i^N)^2 = \frac{213}{20}\,,$$
$$\beta_{11} = \sum_i Q_i^Y Q_i^N = -\frac{\sqrt{6}}{5}\,, \tag{47}$$

where the index i is summed over all possible chiral superfields. From Eqns (47), one can see that, in the E_6SSM, $\beta_1 \approx \beta_1' \gg \beta_{11}$ [181, 184]. Since near the GUT scale it is expected that $g_1(M_\mathrm{X}) \simeq g_1'(M_\mathrm{X})$ and $g_{11}(M_\mathrm{X}) \simeq 0$, the values of $g_1(t)$ and $g_1'(t)$ are almost the same at any scale $q \lesssim M_\mathrm{X}$, whereas the off-diagonal gauge coupling $g_{11}(t)$ is much smaller than the diagonal gauge couplings $g_1(t)$ and $g_1'(t)$. Because of this, one can disregard two-loop corrections to the off-diagonal β function β_{11}.

In the framework of the E_6SSM, in the one-loop approximation, $\beta_2 = 4$ and $\beta_3 = 0$. Since the one-loop β function of strong interactions vanishes, any reliable analysis of the RG flow of the gauge coupling requires the inclusion of two-loop corrections to the β functions of gauge couplings. In the E_6SSM, the two-loop β functions of the diagonal gauge couplings were calculated in Refs [181, 184].

As in the case of the MSSM, one can use the approximate solution of the RG equations (29) to analyze the evolution of the SM gauge couplings within the E_6SSM. In this case, one should substitute into Eqn (29) the expressions for b_i and $\tilde b_i$ calculated in the framework of the E_6SSM, whereas T_1, T_2, T_3, and $\tilde M_S$ in Eqns (29), (31), and (34) have to be replaced by $\tilde T_1$, $\tilde T_2$, $\tilde T_3$, and $\tilde T_S$:

$$\begin{aligned}
\tilde T_S &= \frac{\tilde T_2^{172/19}}{\tilde T_1^{55/19}\,\tilde T_3^{98/19}}\,,\\
\tilde T_1 &= T_1^{5/11}\mu_\mathrm{L}^{4/55} m_\mathrm{L}^{2/55}\Bigg(\prod_{i=1,2,3} m_{\tilde \mathrm{D}_i}^{4/165}\mu_{\mathrm{D}_i}^{8/165}\Bigg)\\
&\quad\times\Bigg(\prod_{\alpha=1,2} m_{\mathrm{H}_\alpha}^{2/55}\mu_{\tilde \mathrm{H}_\alpha}^{4/55}\Bigg),\\
\tilde T_2 &= T_2^{25/43}\mu_\mathrm{L}^{4/43} m_\mathrm{L}^{2/43}\Bigg(\prod_{\alpha=1,2} m_{\mathrm{H}_\alpha}^{2/43}\mu_{\tilde \mathrm{H}_\alpha}^{4/43}\Bigg),\\
\tilde T_3 &= T_3^{4/7}\Bigg(\prod_{i=1,2,3} m_{\tilde \mathrm{D}_i}^{1/21}\mu_{\mathrm{D}_i}^{2/21}\Bigg).
\end{aligned} \tag{48}$$

Here, μ_{D_i} and $m_{\tilde \mathrm{D}_i}$ are the masses of exotic quarks and their superpartners; m_{H_α} and $\mu_{\tilde \mathrm{H}_\alpha}$ are the masses of inert Higgs and inert higgsino fields; m_L and μ_L are the masses of the scalar and fermion components of L_4 and $\overline{L}_4$, while T_1, T_2, and T_3 are the effective threshold scales in the MSSM (34).

As before, to simplify our numerical studies of the running of diagonal gauge couplings in the E_6SSM, we fix the effective SUSY threshold scales to be equal, i.e., $\tilde T_1 = \tilde T_2 = \tilde T_3 = \tilde T_S$. The results of our numerical analysis are summarized in Fig. 2. We apply the two-loop SM β functions to describe the running of gauge couplings between M_Z and $\tilde T_S$. Then, the two-loop RG equations of the E_6SSM are used to compute the flow of $g_i(t)$ for $q \gtrsim \tilde T_S$. In order to calculate the evolution of the Yukawa couplings, the sets of one-loop RG equations of the SM and E_6SSM are used. Low energy values of g_1' and g_{11} are chosen so that all four diagonal gauge couplings are approximately equal near the GUT scale M_X and $g_{11}(M_\mathrm{X}) \simeq 0$.

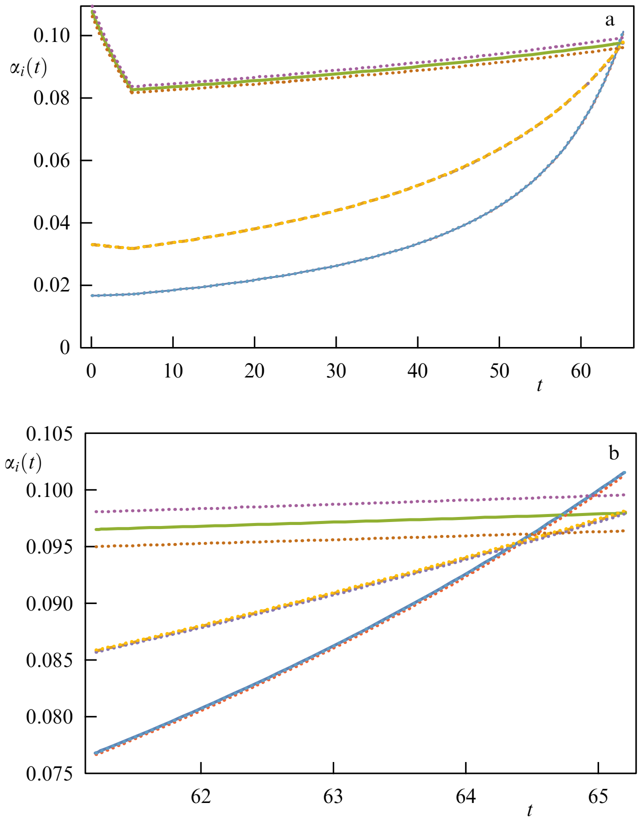

Figure 2. (a) Two-loop RG flow of $\alpha_1(t)$, $\alpha_2(t)$, and $\alpha_3(t)$ as a function of $t = \log(q/M_Z)$ and (b) running of the gauge couplings near scale M_X, calculated within the E_6SSM in the two-loop approximation for $\tan\beta = 10$, $\tilde T_1 = \tilde T_2 = \tilde T_3 = \tilde T_S = 2$ TeV, $\alpha_\mathrm{s}(M_Z) = 0.118$, $\alpha(M_Z) = 1/127.9$, $\sin^2\theta_\mathrm{W} = 0.231$, $\kappa_1(T_S) = \kappa_2(T_S) = \kappa_3(T_S) = \lambda_1(T_S) = \lambda_2(T_S) = \lambda(T_S) = g_1'(T_S)$, and $\tilde f_{\alpha\beta} = f_{\alpha\beta} = g_{ij}^D = h_{i\alpha}^E = 0$. Solid, dashed, and bold lines correspond to the running of $\alpha_1(t)$, $\alpha_2(t)$, and $\alpha_3(t)$. Dotted lines represent the uncertainty in $\alpha_i(t)$ caused by the variation in $\alpha_3(M_Z)$ from 0.116 to 0.120.

The results of the numerical analysis presented in Fig. 2 demonstrate that an almost exact unification of the SM gauge couplings can be achieved in the E_6SSM for $\alpha_3(M_Z) \approx 0.116$ and $\tilde T_S = 2$ TeV. With increasing (decreasing) effective threshold scale $\tilde T_S$, the value of $\alpha_3(M_Z)$, at which the exact gauge coupling unification takes place near the scale $M_\mathrm{X} \simeq 3\times 10^{16}$ GeV, becomes lower (greater). The threshold scale $\tilde T_S$, which can be parameterized in terms of the effective threshold scale $\tilde M_S$,

$$\tilde T_S = \tilde M_S \left(\frac{\mu_\mathrm{L}^{12/19} m_\mathrm{L}^{6/19}}{\mu_{\mathrm{D}_3}^{12/19} m_{\tilde \mathrm{D}_3}^{6/19}}\right)\left(\prod_{\alpha=1,2}\frac{m_{\mathrm{H}_\alpha}^{6/19}\mu_{\tilde \mathrm{H}_\alpha}^{12/19}}{m_{\tilde \mathrm{D}_\alpha}^{6/19}\mu_{\mathrm{D}_\alpha}^{12/19}}\right), \tag{49}$$

can be substantially larger (or smaller) than in the MSSM. From Eqn (49), it is obvious that $\tilde T_S$ is determined by the masses of the scalar and fermion components of L_4 and $\overline{L}_4$. The mass term $\mu_L L_4 \overline{L}_4$ in the superpotential is not involved in the process of EW symmetry breaking. As a consequence, the parameters μ_L and $\tilde{T}_S$ remain arbitrary. The large range of variation in $\tilde{T}_S$ allows the exact unification of gauge couplings to be achieved for any value of $\alpha_3(M_Z)$ which is in agreement with current data.

It is worth noting here that, in principle, one could naively expect that large two-loop corrections to the diagonal β functions would spoil the unification of the SM gauge couplings entirely in the E_6SSM. Indeed, as follows from Table 4 the two-loop corrections to $\alpha_i(M_X)$ are considerably bigger in the E_6SSM than in the MSSM. This is not as surprising as it may first appear, because at any intermediate scale the values of the gauge couplings in the E_6SSM are substantially larger than the ones in the MSSM. Nevertheless due to the remarkable cancellation of different two-loop corrections in Eqn (32) the absolute value of Θ_s in the E_6SSM is less than a third of what it is in the MSSM (see Table 4). This cancellation is caused by the structure of the two-loop corrections to the diagonal β functions in the model under consideration. As a result, the prediction of the value of $\alpha_3(M_Z)$ at which the exact gauge coupling unification takes place is considerably lower in the E_6SSM than in the MSSM [184, 185].

It is also worthwhile to point out that, at high energies, the uncertainty in $\alpha_3(t)$ caused by the variations in $\alpha_3(M_Z)$ is much bigger in the E_6SSM than in the MSSM. This is because in the E_6SSM the strong gauge coupling grows slightly with an increase in the renormalization scale, whereas in the MSSM it decreases at high energies. This implies that the uncertainty in the high energy value of $\alpha_3(t)$ in the E_6SSM is approximately equal to the low energy uncertainty in $\alpha_3(t)$, while in the MSSM the interval of variations of $\alpha_3(t)$ near the scale M_X shrinks drastically. The relatively large uncertainty in $\alpha_3(M_X)$ in the E_6SSM, compared to the MSSM, allows us to achieve exact unification of gauge couplings for values of $\alpha_3(M_Z)$ which are within one standard deviation of its measured central value.

5. Higgs bosons in supersymmetric models

5.1 Higgs sector of the MSSM

Including soft SUSY breaking terms and radiative corrections, the resulting Higgs effective potential in the MSSM can be written as

$$V(H_1, H_2) = m_1^2 |H_1|^2 + m_2^2 |H_2|^2 - m_3^2 (H_1 H_2 + \text{h.c.}) + \sum_{a=1}^{3} \frac{g_2^2}{8} (H_1^+ \sigma_a H_1 + H_2^+ \sigma_a H_2)^2 + \frac{g'^2}{8} \left(|H_1|^2 - |H_2|^2\right)^2 + \Delta V , \tag{50}$$

where $g' = \sqrt{3/5} g_1$, g_2 and g_1 are the low energy (GUT normalized) $\mathrm{SU}(2)_W$ and $\mathrm{U}(1)_Y$ gauge couplings, $m_1^2 = m_{H_1}^2 + \mu^2$, $m_2^2 = m_{H_2}^2 + \mu^2$, and $m_3^2 = -B\mu$. The parameters B, $m_{H_1}^2$, and $m_{H_2}^2$ break global SUSY. In Eqn (50), ΔV represents the contribution of loop corrections to the Higgs effective potential. At the physical minimum of the scalar potential (50), the Higgs fields develop VEVs

$$\langle H_1 \rangle = \frac{1}{\sqrt{2}} \begin{pmatrix} v_1 \\ 0 \end{pmatrix}, \qquad \langle H_2 \rangle = \frac{1}{\sqrt{2}} \begin{pmatrix} 0 \\ v_2 \end{pmatrix}, \tag{51}$$

breaking the $\mathrm{SU}(2)_W \times \mathrm{U}(1)_Y$ gauge symmetry to $\mathrm{U}(1)_{\mathrm{em}}$ associated with electromagnetism. It is convenient to introduce $v = (v_1^2 + v_2^2)^{1/2} \simeq 246$ GeV and $\tan\beta = v_2/v_1$, which remains arbitrary.

At tree-level ($\Delta V = 0$), the Higgs potential is described by the sum of the first five terms in Eqn (50). It contains only three independent parameters: m_1^2, m_2^2, and m_3^2. The stable vacuum of the scalar potential (50) exists only if

$$m_1^2 + m_2^2 > 2|m_3|^2 . \tag{52}$$

Otherwise, the physical vacuum becomes unstable, i.e., $|v_1| = |v_2| \to \infty$. On the other hand, Higgs doublets acquire nonzero VEVs only when

$$m_1^2 m_2^2 < |m_3|^4 . \tag{53}$$

Indeed, if $m_1^2 m_2^2 > |m_3|^4$, then the scalar potential (50) is positive definite and its minimum corresponds to $|v_1| = |v_2| = 0$, i.e., the breakdown of EW symmetry does not take place. Using two equations for the extrema of the Higgs boson potential (50), i.e., $\partial V/\partial v_1 = 0$ and $\partial V/\partial v_2 = 0$, one finds

$$\sin(2\beta) = \frac{2m_3^2}{m_1^2 + m_2^2} , \tag{54}$$

$$\frac{\bar{g}^2}{4} v^2 = \frac{2(m_1^2 - m_2^2 \tan^2\beta)}{\tan^2\beta - 1} , \tag{55}$$

where $\bar{g} = (g_2^2 + g'^2)^{1/2}$. Requiring that $v^2 > 0$ and $|\sin(2\beta)| < 1$, we can reproduce conditions (52) and (53). The breakdown of the $\mathrm{SU}(2)_W \times \mathrm{U}(1)_Y$ symmetry induces the masses of the $W^{\pm}$ and Z bosons

$$M_W = \frac{g_2}{2} v , \qquad M_Z = \frac{\bar{g}}{2} v . \tag{56}$$

The inclusion of loop effects, which play an important role in the simplest SUSY extensions of the SM, makes the analysis of EW symmetry breaking much more complicated. In these models, the dominant contribution to ΔV comes from the loops involving the top-quark and its superpartners. Due to the EW symmetry breaking, two scalar superpartners ($\tilde{t}_L$ and $\tilde{t}_R$) of the left-handed and right-handed top quark states get mixed, resulting in the formation of two charged scalar fields with masses

$$m_{\tilde{t}_{1,2}} = \frac{1}{2} \left(m_Q^2 + m_U^2 + 2m_t^2 \pm \sqrt{(m_Q^2 - m_U^2)^2 + 4m_t^2 X_t^2} \right) , \tag{57}$$

where $X_t = A_t - \mu/\tan\beta$ is a stop mixing parameter, A_t is a trilinear scalar coupling associated with the top quark Yukawa coupling, and m_t is the running top quark mass which is defined as

$$m_t(M_t) = \frac{h_t(M_t)}{\sqrt{2}} v \sin\beta , \qquad m_t(M_t) = M_t \left[1 - 1.333 \frac{\alpha_3(M_t)}{\pi} - 9.125 \left(\frac{\alpha_s(M_t)}{\pi} \right)^2 \right] . \tag{58}$$

In the one-loop approximation, the contribution of the top-quark and its superpartners to ΔV is determined by the masses of the corresponding bosonic and fermionic states, i.e.,

$$\Delta V = \frac{3}{32\pi^2}\left[m_{\tilde{t}_1}^4\left(\ln\frac{m_{\tilde{t}_1}^2}{q^2}-\frac{3}{2}\right)+m_{\tilde{t}_2}^4\left(\ln\frac{m_{\tilde{t}_2}^2}{q^2}-\frac{3}{2}\right)\right.$$
$$\left. - 2m_t^4\left(\ln\frac{m_t^2}{q^2}-\frac{3}{2}\right)\right]. \qquad (59)$$

The inclusion of loop corrections modifies the equations for the extrema of the Higgs potential (54), (55). In particular, Eqn (55) can be written as

$$\frac{M_Z^2}{2} = \frac{m_{H_1}^2 + \Sigma_d^d - (m_{H_2}^2 + \Sigma_u^u)\tan^2\beta}{\tan^2\beta - 1} - \mu^2\,, \qquad (60)$$

where

$$\Sigma_d^d = \frac{1}{v_1}\frac{\partial\Delta V}{\partial v_1}\,, \qquad \Sigma_u^u = \frac{1}{v_2}\frac{\partial\Delta V}{\partial v_2}\,.$$

As was pointed out in Section 2, some degree of cancellation between the SUSY parameters appearing on the right-hand side of Eqn (60) is required to obtain the observed value of the Z boson mass $M_Z \simeq 91.2$ GeV. If the needed cancellation is large, then small changes in the SUSY parameters should result in a widely different value of M_Z, so that the considered spectrum is fine-tuned. The fine-tuning measures are used to quantify the sensitivity of M_Z to the SUSY parameters. In the literature, one can find two main SUSY fine-tuning measures. In this context, it is worth noting that the low energy values of μ, $m_{H_1}^2$, $m_{H_2}^2$, Σ_d^d, and Σ_u^u on the right-hand side of Eqn (60) depend on the set of fundamental parameters p_i of some high-scale theory. Therefore, the traditional measure, which was proposed in Refs [243, 244], does take underlying model assumptions into account. It is defined as

$$\varDelta_{BG} = \max_i\{c_i\}\,, \qquad c_i = \left|\frac{\partial\ln M_Z^2}{\partial\ln p_i}\right| = \left|\frac{p_i}{M_Z^2}\frac{\partial M_Z^2}{\partial p_i}\right|. \qquad (61)$$

On the other hand, Eqn (60) can be presented as a sum,

$$\frac{M_Z^2}{2} = \sum_i C_i + \sum_k \tilde{C}_k\,, \qquad (62)$$

where

$$C_{m_{H_1}} = \frac{m_{H_1}^2}{\tan^2\beta-1}\,, \quad C_{m_{H_2}} = -\frac{m_{H_2}^2\tan^2\beta}{\tan^2\beta-1}\,, \quad C_\mu = -\mu^2\,,$$
$$\tilde{C}_{\Sigma_d^d} = \frac{\Sigma_d^d}{\tan^2\beta-1}\,, \quad \tilde{C}_{\Sigma_u^u} = -\frac{\Sigma_u^u\tan^2\beta}{\tan^2\beta-1}\,.$$

The EW SUSY fine-tuning measure parameterizes how sensitive M_Z is to variations in each of the terms in Eqn (62). The coefficients $\tilde{C}_k$ are proportional to Σ_d^d and Σ_u^u that contain the sum of different contributions. The maximum of these contributions is used to compute $C_{\Sigma_d^d}$ and $C_{\Sigma_u^u}$, i.e.,

$$C_{\Sigma_d^d} = \max(\tilde{C}_{\Sigma_d^d})\,, \qquad C_{\Sigma_u^u} = \max(\tilde{C}_{\Sigma_u^u})\,.$$

The EW SUSY fine-tuning measure is defined as [245]

$$\varDelta_{EW} = \max_i\left\{\left|\frac{C_i}{M_Z^2/2}\right|\right\}. \qquad (63)$$

When CP is conserved, the MSSM Higgs sector involves two charged, one CP-odd, and two CP-even Higgs states. The masses of the charged and CP-odd Higgs bosons are

$$m_A^2 = m_1^2 + m_2^2 + \varDelta_A\,, \qquad M_{H^\pm}^2 = m_A^2 + M_W^2 + \varDelta_\pm\,, \quad (64)$$

where $\varDelta_\pm$ and $\varDelta_A$ are the loop corrections. In the leading approximation, the analytic expressions for the masses of the CP-odd and charged Higgs states were obtained in Refs [246–259] and [251–262], respectively.

The CP-even states are mixed and form a 2×2 mass matrix. It is convenient to introduce a new field space basis (H, h) rotated by the angle β with respect to the initial one:

$$\mathrm{Re}\,H_1^0 = \frac{h\cos\beta - H\sin\beta + v_1}{\sqrt{2}}\,,$$
$$\mathrm{Re}\,H_2^0 = \frac{h\sin\beta + H\cos\beta + v_2}{\sqrt{2}}\,. \qquad (65)$$

In this new basis, only one diagonal entry M_{11}^2 depends on m_1^2, m_2^2, and m_3^2 [263]:

$$M^2 = \begin{pmatrix} M_{11}^2 & M_{12}^2 \\ M_{21}^2 & M_{22}^2 \end{pmatrix} = \begin{pmatrix} \dfrac{1}{v^2}\dfrac{\partial^2 V}{\partial\beta^2} & \dfrac{1}{v}\dfrac{\partial^2 V}{\partial v\,\partial\beta} \\ \dfrac{1}{v}\dfrac{\partial^2 V}{\partial v\,\partial\beta} & \dfrac{\partial^2 V}{\partial v^2} \end{pmatrix}, \qquad (66)$$

$$M_{11}^2 = m_A^2 + M_Z^2\sin^2(2\beta) + \varDelta_{11}\,,$$
$$M_{22}^2 = M_Z^2\cos^2(2\beta) + \varDelta_{22}\,, \qquad (67)$$
$$M_{12}^2 = M_{21}^2 = -\frac{1}{2}M_Z^2\sin(4\beta) + \varDelta_{12}\,,$$

where

$$\varDelta_{22} = 4v^2\frac{\partial^2\Delta V}{\partial(v^2)^2}\,, \qquad \varDelta_{12} = 2\left(\frac{\partial^2\Delta V}{\partial\beta\,\partial(v^2)} - \frac{1}{v^2}\frac{\partial\Delta V}{\partial\beta}\right),$$
$$\varDelta_{11} = 4\frac{\partial\Delta V}{\partial(v^2)} + \frac{1}{v^2}\frac{\partial^2\Delta V}{\partial\beta^2} - \varDelta_A\,. \qquad (68)$$

In the leading approximation, the contributions from loop corrections $\varDelta_{ij}$ were analyzed in Refs [246–259, 264–282]. In Eqns (67), (68), the equations for the extrema of the Higgs boson effective potential are used to eliminate m_1^2, m_2^2, and m_3^2.

From Eqns (64) and (67), it can be seen that at tree-level the masses of the Higgs bosons in the MSSM can be parameterized in the terms m_A and $\tan\beta$ only. The masses of the two CP-even eigenstates obtained by diagonalizing the matrix (66)–(68) are given by

$$m_{h_1,h_2}^2 = \frac{1}{2}\left(M_{11}^2 + M_{22}^2 \mp \sqrt{(M_{22}^2 - M_{11}^2)^2 + 4M_{12}^4}\right). \quad (69)$$

With increasing m_A, which should be identified with the sparticle mass scale, the masses of all Higgs particles grow. At very large values of m_A ($m_A^2 \gg M_Z^2$), the masses of charged, CP-odd, and the heaviest CP-even states are almost degenerate, i.e., $M_{H^\pm} \simeq m_{h_2} \simeq m_A$, whereas the lightest Higgs boson mass approaches its theoretical upper limit $(M_{22}^2)^{1/2}$.

At tree-level, the lightest Higgs boson mass in the MSSM is always less than $M_Z|\cos(2\beta)|$. This theoretical upper bound was derived in Refs [283–285]. Although the inclusion of loop corrections does not change the qualitative pattern of the Higgs spectrum, the upper bound on the lightest Higgs mass in the MSSM increases:

$$m_{\mathrm{h}_1} \leqslant \sqrt{M_Z^2 \cos^2(2\beta) + \Delta_{22}}\,. \tag{70}$$

In Ref. [248], an approximate analytic expression for the sum of one-loop and two-loop corrections associated with Δ_{22} was obtained in the leading approximation (see also [286]):

$$\Delta_{22} \approx \frac{3}{2\pi^2}\frac{m_t^4}{v^2}\left[\frac{1}{2}U_t + L + \frac{1}{16\pi^2}\left(3\frac{m_t^2}{v^2} - 32\pi\alpha_3\right)\right.$$
$$\left.\times (U_t L + L^2)\right] - \frac{3}{4\pi^2}\frac{m_t^2}{v^2}\left[M_Z\cos(2\beta)\right]^2 L\,, \tag{71}$$

where

$$L = \ln\frac{M_S^2}{m_t^2}\,, \qquad U_t = \frac{2X_t^2}{M_S^2}\left(1 - \frac{X_t^2}{12M_S^2}\right),$$

and $M_S = \sqrt{m_{\tilde{t}_1} m_{\tilde{t}_2}}$. As follows from Eqns (71), the contribution of loop corrections Δ_{22} is proportional to m_t^4, where m_t is the running top quark mass, and depends rather weakly on M_S. The lightest Higgs boson mass reaches its maximal value for $\tan\beta \gg 1$ and $X_t = \pm\sqrt{6}M_S$ ($U_t = 6$).

For fixed values of $\tan\beta$, M_S, and X_t, the accuracy of the theoretical predictions for the lightest Higgs boson mass in the MSSM has improved very significantly over the last 10–15 years (for a recent review, see [287]). The inclusion of loop corrections allows reproducing the observed value of the Higgs mass. However, even for $m_A^2 \gg M_Z^2$ and $\tan\beta \gg 1$, a large loop contribution of $\Delta_{22} \approx (85\ \mathrm{GeV})^2$, which is nearly as large as M_Z^2, is required to raise the lightest Higgs boson mass to 125 GeV. The values of $\Delta_{22} \simeq M_Z^2$ can be obtained only if $M_S \gtrsim 1$ TeV [287]. Using Eqns (61) and (63), one can estimate that fine-tuning of the order of $10^{-3} - 10^{-2}$ is needed to stabilize the EW scale within the MSSM in this case [44, 45].

5.2 Spectrum of Higgs bosons in NMSSM

The fine-tuning of the MSSM can be partially ameliorated in the scale invariant NMSSM. Ignoring all possible Z_3 symmetry violating operators in the superpotential, the potential energy of the Higgs field interaction in this model can be presented as a sum:

$$V = V_F + V_D + V_{\mathrm{soft}} + \Delta V\,, \tag{72}$$

$$V_F = \lambda^2|S|^2\left(|H_1|^2 + |H_2|^2\right) + \lambda^2\left|(H_1 H_2)\right|^2$$
$$+ \lambda\kappa\left[S^{*2}(H_1 H_2) + \mathrm{h.c.}\right] + \kappa^2|S|^4\,, \tag{73}$$

$$V_D = \sum_{a=1}^{3}\frac{g_2^2}{8}\left(H_1^+\sigma_a H_1 + H_2^+\sigma_a H_2\right)^2 + \frac{g'^2}{8}\left(|H_1|^2 - |H_2|^2\right)^2, \tag{74}$$

$$V_{\mathrm{soft}} = m_1^2|H_1|^2 + m_2^2|H_2|^2 + m_S^2|S|^2$$
$$+ \left[\lambda A_\lambda S(H_1 H_2) + \frac{\kappa}{3}A_\kappa S^3 + \mathrm{h.c.}\right]. \tag{75}$$

At tree-level, the Higgs potential is described by the sum of the first three terms in Eqn (72). V_F and V_D are the F and D terms. Their structure is fixed by the superpotential (16) and the EW gauge interactions. The soft SUSY breaking terms are collected in V_{soft}. The set of the soft SUSY breaking parameters involves soft scalar masses m_1^2, m_2^2, m_S^2, as well as trilinear scalar couplings A_κ and A_λ. The last term in Eqn (72), ΔV, corresponds to the contribution of loop corrections. In the leading one-loop approximation, ΔV in the NMSSM is given by Eqn (59) in which μ has to be replaced by λS. Further, it is assumed that λ, κ, and all soft SUSY breaking parameters are real so that CP is conserved.

In a physical vacuum, the $\mathrm{SU}(2)_W$ doublets of the Higgs bosons develop VEVs (51). Singlet field S also acquires nonzero VEV $\langle S\rangle = s/\sqrt{2}$. The equations for the extrema of the full Higgs boson effective potential are given by

$$\frac{\partial V}{\partial s} = \left[m_S^2 + \frac{\lambda^2}{2}(v_1^2 + v_2^2) - \lambda\kappa v_1 v_2\right]s - \frac{\lambda A_\lambda}{\sqrt{2}}v_1 v_2$$
$$+ \frac{\kappa A_\kappa}{\sqrt{2}}s^2 + \kappa^2 s^3 + \frac{\partial\Delta V}{\partial s} = 0\,, \tag{76}$$

$$\frac{\partial V}{\partial v_1} = \left[m_1^2 + \frac{\lambda^2}{2}(v_2^2 + s^2) + \frac{\bar{g}^2}{8}(v_1^2 - v_2^2)\right]v_1$$
$$- \left(\frac{\lambda\kappa}{2}s^2 + \frac{\lambda A_\lambda}{\sqrt{2}}s\right)v_2 + \frac{\partial\Delta V}{\partial v_1} = 0\,, \tag{77}$$

$$\frac{\partial V}{\partial v_2} = \left[m_2^2 + \frac{\lambda^2}{2}(v_1^2 + s^2) + \frac{\bar{g}^2}{8}(v_2^2 - v_1^2)\right]v_2$$
$$- \left(\frac{\lambda\kappa}{2}s^2 + \frac{\lambda A_\lambda}{\sqrt{2}}s\right)v_1 + \frac{\partial\Delta V}{\partial v_2} = 0\,. \tag{78}$$

As in the MSSM, upon breakdown of the EW symmetry in the NMSSM, three goldstone modes ($G^\pm$ and G^0) emerge and are absorbed by the $W^\pm$ and Z bosons. In the field space basis rotated by an angle β with respect to the initial direction, i.e.,

$$\mathrm{Im}\,H_1^0 = \frac{P\sin\beta + G^0\cos\beta}{\sqrt{2}}\,, \qquad H_2^+ = H^+\cos\beta - G^+\sin\beta\,,$$
$$\mathrm{Im}\,H_2^0 = \frac{P\cos\beta - G^0\sin\beta}{\sqrt{2}}\,, \qquad H_1^- = G^-\cos\beta + H^-\sin\beta\,,$$
$$\mathrm{Re}\,H_1^0 = \frac{h\cos\beta - H\sin\beta + v_1}{\sqrt{2}}\,, \qquad \mathrm{Im}\,S = \frac{P_S}{\sqrt{2}}\,, \tag{79}$$
$$\mathrm{Re}\,H_2^0 = \frac{h\sin\beta + H\cos\beta + v_2}{\sqrt{2}}\,, \qquad \mathrm{Re}\,S = \frac{s+N}{\sqrt{2}}\,,$$

these unphysical degrees of freedom decouple, and the mass terms associated with physical states can be written as follows:

$$V_{\mathrm{mass}} = M_{\mathrm{H}^\pm}^2 H^+ H^- + \frac{1}{2}(P\ P_S)\,\tilde{M}^2\begin{pmatrix}P\\ P_S\end{pmatrix}$$
$$+ \frac{1}{2}(H\ h\ N)\,M^2\begin{pmatrix}H\\ h\\ N\end{pmatrix}. \tag{80}$$

Using the conditions for the extrema (76)–(78), one can express m_S^2, m_1^2, m_2^2 via other fundamental parameters, $\tan\beta$ and s. Substituting the obtained relations for the soft masses into the 2×2 CP-odd mass matrix $\tilde{M}_{ij}^2$, one finds:

$$\tilde{M}_{11}^2 = m_A^2 = \frac{4\mu^2}{\sin^2(2\beta)}\left(x - \frac{\kappa}{2\lambda}\sin(2\beta)\right) + \tilde{\Delta}_{11}\,, \tag{81}$$

$$\tilde{M}_{22}^2 = \frac{\lambda^2 v^2}{2}x + \frac{\lambda\kappa}{2}v^2\sin(2\beta) - 3\frac{\kappa}{\lambda}A_\kappa\mu + \tilde{\Delta}_{22}\,, \tag{82}$$

$$\tilde{M}_{12}^2 = \tilde{M}_{21}^2 = \sqrt{2}\lambda v\mu\left(\frac{x}{\sin(2\beta)} - 2\frac{\kappa}{\lambda}\right) + \tilde{\Delta}_{12}\,, \tag{83}$$

where $x = (1/2\mu)(A_\lambda + 2(\kappa/\lambda)\mu)\sin(2\beta)$, and $\mu = \lambda s/\sqrt{2}$ and $\tilde{\Delta}_{ij}$ are contributions of the loop corrections to the mass matrix elements. The *CP*-odd Higgs sector and the corresponding loop corrections were examined in Refs [288–293]. In the leading one-loop approximation, one finds

$$\tilde{\varDelta}_{22} = \frac{v\sin(2\beta)}{2s}\,\tilde{\varDelta}_{12} = \left[\frac{v\sin(2\beta)}{2s}\right]^2 \tilde{\varDelta}_{11}\,. \tag{84}$$

The mass matrix (81)–(83) can be easily diagonalized. Its eigenvalues are given by

$$m^2_{\mathrm{A_2,A_1}} = \frac{1}{2}\left(\tilde{M}^2_{11} + \tilde{M}^2_{22} \pm \sqrt{(\tilde{M}^2_{11} - \tilde{M}^2_{22})^2 + 4\tilde{M}^4_{12}}\right). \tag{85}$$

Since the charged components of the Higgs doublets are not mixed with the neutral Higgs states, the charged Higgs fields $H^{\pm}$ are already physical mass eigenstates with

$$M^2_{\mathrm{H^\pm}} = m^2_{\mathrm{A}} - \frac{\lambda^2 v^2}{2} + M^2_{\mathrm{W}} + \varDelta_{\pm}\,. \tag{86}$$

Here, $\varDelta_{\pm}$ includes loop corrections to the charged Higgs mass, which are basically the same as in the MSSM (accurate up to the substitution $\mu \to \lambda s/\sqrt{2}$).

In the rotated basis (H, h, N), the mass matrix of the NMSSM *CP*-even Higgs sector takes the form [128, 263]

$$M^2 = \begin{pmatrix} M^2_{11} & M^2_{12} & M^2_{13} \\ M^2_{21} & M^2_{22} & M^2_{23} \\ M^2_{31} & M^2_{32} & M^2_{33} \end{pmatrix} = \begin{pmatrix} \dfrac{1}{v^2}\dfrac{\partial^2 V}{\partial\beta^2} & \dfrac{1}{v}\dfrac{\partial^2 V}{\partial v\,\partial\beta} & \dfrac{1}{v}\dfrac{\partial^2 V}{\partial s\,\partial\beta} \\ \dfrac{1}{v}\dfrac{\partial^2 V}{\partial v\,\partial\beta} & \dfrac{\partial^2 V}{\partial v^2} & \dfrac{\partial^2 V}{\partial v\,\partial s} \\ \dfrac{1}{v}\dfrac{\partial^2 V}{\partial s\,\partial\beta} & \dfrac{\partial^2 V}{\partial v\,\partial s} & \dfrac{\partial^2 V}{\partial s^2} \end{pmatrix}, \tag{87}$$

$$M^2_{11} = m^2_{\mathrm{A}} + \left(\frac{\bar{g}^2}{4} - \frac{\lambda^2}{2}\right) v^2 \sin^2(2\beta) + \varDelta_{11}\,, \tag{88}$$

$$M^2_{22} = M^2_{\mathrm{Z}}\cos^2(2\beta) + \frac{\lambda^2}{2}\,v^2\sin^2(2\beta) + \varDelta_{22}\,, \tag{89}$$

$$M^2_{33} = 4\,\frac{\kappa^2}{\lambda^2}\,\mu^2 + \frac{\kappa}{\lambda}\,A_\kappa\mu + \frac{\lambda^2 v^2}{2}\,x - \frac{\kappa\lambda}{2}\,v^2\sin(2\beta) + \varDelta_{33}\,, \tag{90}$$

$$M^2_{12} = M^2_{21} = \left(\frac{\lambda^2}{4} - \frac{\bar{g}^2}{8}\right) v^2\sin(4\beta) + \varDelta_{12}\,, \tag{91}$$

$$M^2_{13} = M^2_{31} = -\frac{\sqrt{2}\lambda v\mu x\cos(2\beta)}{\sin(2\beta)} + \varDelta_{13}\,, \tag{92}$$

$$M^2_{23} = M^2_{32} = \sqrt{2}\lambda v\mu(1-x) + \varDelta_{23}\,, \tag{93}$$

where $\varDelta_{11}$, $\varDelta_{22}$, and $\varDelta_{12}$ are given by Eqns (68), in which $\varDelta_A$ and μ should be replaced by $\tilde{\varDelta}_{11}$ and $\lambda s/\sqrt{2}$, respectively, while

$$\varDelta_{13} = \frac{1}{v}\frac{\partial\Delta V}{\partial\beta\,\partial s}\,, \qquad \varDelta_{23} = 2v\,\frac{\partial^2\Delta V}{\partial(v^2)\partial s}\,, \qquad \varDelta_{33} = \frac{\partial^2\Delta V}{\partial s^2} - \frac{1}{s}\frac{\partial\Delta V}{\partial s}\,. \tag{94}$$

The *CP*-even Higgs sector and the corresponding loop corrections were explored in Refs [288–297]. As follows from Eqns (81)–(93) at tree-level, the spectrum of the Higgs bosons and their couplings depend on six parameters: λ, κ, $\mu = \lambda s/\sqrt{2}$, $\tan\beta$, A_κ, and m_{A} (or x).

Since the minimal eigenvalue of a Hermitian matrix does not exceed its smallest diagonal element, one Higgs scalar is always light. Its mass $m_{\mathrm{h_1}}$ remains smaller than $(M^2_{22})^{1/2} \sim M_{\mathrm{Z}}$ even when the sparticle mass scale M_{S} is much larger than the EW scale, i.e.,

$$m^2_{\mathrm{h_1}} \lesssim \frac{\partial^2 V(v^2)}{\partial v^2} = 4v^2\,\frac{\partial^2 V(v^2)}{\partial(v^2)^2} = M^2_{\mathrm{Z}}\cos^2(2\beta) + \frac{\lambda^2 v^2}{2}\sin^2(2\beta) + \varDelta_{22}\,. \tag{95}$$

At tree-level, the upper bound on the mass of the lightest Higgs scalar in the NMSSM was found in Refs [298, 299]. If $\lambda \gtrsim 0.6$, the theoretical bound (95) attains its maximal value for $\tan\beta \sim 1$. Taking $\lambda = 0.6$ and $\tan\beta = 2$, the tree-level contributions to $m_{\mathrm{h_1}}$ can reach 100 GeV, and $\varDelta_{22}$ is required to be about $(75\ \mathrm{GeV})^2$. As a consequence, M_{S} is allowed to be lower so that the NMSSM requires less fine-tuning than the MSSM [300, 301].

First, let us consider the MSSM limit of the NMSSM when the Yukawa couplings λ and κ are tiny. In this case, all terms which are proportional to λv_i and κv_i in the minimization conditions (76)–(78) can be ignored. On the other hand, Eqns (77), (78) imply that s should grow with decreasing λ to ensure the correct breakdown of EW symmetry. In the limit under consideration, Eqns (77), (78) reproduce two equations for the extrema of the MSSM Higgs potential with $\mu = \lambda s/\sqrt{2}$ and $m_3^2 = -(\lambda\kappa/2)s^2 - (\lambda/\sqrt{2})A_\lambda s$, while Eqn (76) takes the form

$$s\left(m_S^2 + \frac{\kappa A_\kappa}{\sqrt{2}}\,s + \kappa^2 s^2\right) \simeq 0\,. \tag{96}$$

Equation (96) always has at least one solution $s_0 = 0$. In addition, two nontrivial roots arise if $A_\kappa^2 > 8m_S^2$. They are given by

$$s_{1,2} \simeq \frac{-A_\kappa \pm \sqrt{A_\kappa^2 - 8m_S^2}}{2\sqrt{2}\kappa}\,. \tag{97}$$

When $m_S^2 > 0$, the root $s_0 = 0$ corresponds to the local minimum of the Higgs potential (72)–(75), which does not lead to an acceptable solution to the μ problem. The second nontrivial vacuum, which appears if $A_\kappa^2 > 8m_S^2$, remains unstable for $A_\kappa^2 < 9m_S^2$. Larger absolute values of A_κ ($A_\kappa^2 > 9m_S^2$) stabilize the second minimum, which is attained at $s = s_1(s_2)$ for negative (positive) A_κ. From Eqn (97), it becomes clear that increasing s can be achieved either by decreasing κ or by raising m_S^2 and A_κ. Since there is no natural reason why m_S^2 and A_κ should be very large while all other soft SUSY breaking terms are left in the TeV range, the values of λ and κ must go to zero simultaneously in the MSSM limit of the NMSSM.

Since in the MSSM limit of the NMSSM mixing between singlet states and neutral components of the Higgs doublets is small, the mass matrices (81)–(83) and (87)–(93) can be diagonalized using the perturbation theory [128]. In this case, the masses of the charged and one *CP*-odd Higgs states are determined by Eqns (64) and the masses of two *CP*-even Higgs bosons are the same as in the MSSM as well (see

Eqn (69)). The masses of the extra CP-even (H_s) and CP-odd (A_s) Higgs states, which are predominantly SM singlet fields, can be estimated as

$$m_{A_s}^2 \simeq -3\,\frac{\kappa}{\lambda}\,A_\kappa \mu\,, \tag{98}$$

$$m_{H_s}^2 \simeq 4\,\frac{\kappa^2}{\lambda^2}\,\mu^2 + \frac{\kappa}{\lambda}\,A_\kappa\mu + \frac{\lambda^2 v^2}{2}\,x\sin^2(2\beta) - \frac{2\lambda^2 v^2\mu^2}{M_Z^2\cos^2(2\beta)}\,(1-x)^2\,. \tag{99}$$

When $\kappa \sim \lambda$, the last two terms in Eqn (99) can be disregarded. The parameter A_κ occurs in the masses of extra scalar m_{H_s} and pseudoscalar $m_{A_s}^2$ with the opposite sign and is therefore responsible for their splitting. To ensure that the physical vacuum is a global minimum of the Higgs potential and the masses squared of all Higgs states are positive in this vacuum, the parameter A_κ must satisfy the following constraints:

$$-3\left(\frac{\kappa}{\lambda}\,\mu\right)^2 \lesssim A_\kappa\left(\frac{\kappa}{\lambda}\,\mu\right) \lesssim 0\,. \tag{100}$$

From Eqns (98)–(100), it follows that the masses of the SM singlet scalar and pseudoscalar are set by $(\kappa/\lambda)\mu$.

Decreasing κ reduces the masses of extra scalar and pseudoscalar states so that for $\kappa \ll \lambda$ they can be the lightest particles in the Higgs boson spectrum. For small but nonzero values of $\kappa^2 \ll \lambda^2 \ll 0.01$, the first and second terms can be comparable to the last ones in Eqn (99). Moreover, for large absolute values of $|\mu| \gtrsim M_Z$ and $\tan\beta \gg 1$, which are needed to get the SM-like Higgs boson with a mass of around 125 GeV in this case, $m_{H_s}^2$ tends to be negative if the auxiliary variable x differs too much from unity. As evident from Eqn (99), the positivity of $m_{H_s}^2$ implies that x has to be localized near unity, i.e.,

$$1 - \left|\frac{\sqrt{2}\kappa M_Z}{\lambda^2 v}\right| < x < 1 + \left|\frac{\sqrt{2}\kappa M_Z}{\lambda^2 v}\right|. \tag{101}$$

On the other hand, at tree-level for the parameter m_A^2, one finds

$$m_A^2 \simeq (\mu\tan\beta)^2\,x\,. \tag{102}$$

The restrictions (101) lead to the hierarchical structure of the Higgs spectrum [302–305]. Indeed, the charged, heaviest CP-odd and heaviest CP-even Higgs states are almost degenerate, with masses around m_A. All other Higgs bosons are considerably lighter. In particular, the masses of extra scalar and pseudoscalar states are set by $(2\kappa/\lambda)\mu \ll m_A$.

In the part of the NMSSM parameter space associated with $\kappa^2 \ll \lambda^2$, the main features of the NMSSM Higgs spectrum discussed above are retained, even when λ and κ are larger than 0.1. When $\lambda(M_X) \sim \kappa(M_X) \gtrsim 1$, the small ratio κ/λ at low energies can be due to the RG flow of these couplings from the GUT scale M_X to M_t. In the infrared region, the solutions of the NMSSM RG equations are focused near the intersection of the Hill-type effective surface and invariant line [129, 306–308]. As a result, at low energies, the ratio κ/λ tends to be less than unity even when $\kappa(M_X) > \lambda(M_X)$ initially. In Fig. 3, the dependence of the masses of the NMSSM Higgs bosons on m_A is explored. As a representative example, the Yukawa couplings are chosen so that $\lambda(M_X) = \kappa(M_X) = 2h_t(M_X) = 1.6$, which corresponds to $\tan\beta \approx 3$, $\lambda(M_t) \approx 0.6$ and $\kappa(M_t) \approx 0.36$. In order to obtain a realistic spectrum, the leading one-loop corrections from the top and stop loops are taken into account. From Fig. 3, it can be seen that the requirement of stability of the physical vacuum limits the range of variations of m_A from below and above, maintaining the mass hierarchy in the Higgs spectrum. Relying on this mass hierarchy, the approximate solutions for the Higgs masses and couplings can be obtained [302, 303]. The numerical results presented in Fig. 3 reveal that the masses of the heaviest CP-even, heaviest CP-odd, and charged Higgs states are approximately degenerate, while the other three neutral states are considerably lighter. This hierarchical structure of the Higgs spectrum ensures that the heaviest CP-even and CP-odd Higgs bosons are mainly composed of the components of the Higgs basis H and P, respectively. When the mass of the second lightest Higgs scalar is close to its minimal value in Fig. 3, this state manifests itself in interactions with other SM bosons and fermions as an SM-like Higgs boson. In this case, the lightest Higgs scalar and pseudoscalar are singlet dominated. These states have reduced couplings to SM bosons and fermions that could have allowed them to escape detection in earlier collider experiments at the LHC.

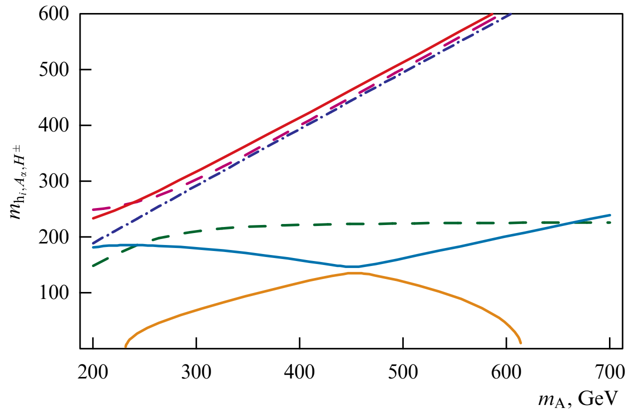

Figure 3. One-loop masses of NMSSM Higgs bosons versus m_A for $\lambda = 0.6$, $\kappa = 0.36$, $\mu = 150$ GeV, $\tan\beta = 3$, $A_\kappa = 135$ GeV, $m_Q^2 = m_U^2 = M_S^2$, $X_t = \sqrt{6}M_S$, and $M_S = 1.5$ TeV. Solid, dashed, and dashed–dotted lines correspond to the masses of CP-even, CP-odd, and charged Higgs bosons, respectively.

5.3 Upper bound on the mass of the lightest Higgs boson in the E$_6$SSM

As was mentioned in Section 3, the sector responsible for breaking the gauge symmetry in the E$_6$SSM includes two Higgs doublets, H_u and H_d, as well as the SM singlet fields S, $\overline{S}$, and ϕ. The resulting Higgs effective potential can be presented as four sums:

$$V = V_F + V_D + V_{\rm soft} + \Delta V\,, \tag{103}$$

$$V_F = \lambda^2|S|^2\left(|H_d|^2 + |H_u|^2\right) + \left|\lambda(H_d H_u) - \sigma\phi\overline{S}\right|^2 + \sigma^2|\phi|^2|S|^2 + \left|-\sigma(S\overline{S}) + \kappa\phi^2 + \mu_\phi\phi + \Lambda_F\right|^2, \tag{104}$$

$$V_D = \sum_{a=1}^{3}\frac{g_2^2}{8}\left(H_d^\dagger\sigma_a H_d + H_u^\dagger\sigma_a H_u\right)^2 + \frac{g'^2}{8}\left(|H_d|^2 - |H_u|^2\right)^2 + \frac{g_1'^2}{2}\left(\tilde{Q}_{H_d}|H_d|^2 + \tilde{Q}_{H_u}|H_u|^2 + \tilde{Q}_S|S|^2 - \tilde{Q}_S|\overline{S}|^2\right)^2, \tag{105}$$

$$
\begin{aligned}
V_{\text{soft}} &= m_S^2|S|^2 + m_{\overline{S}}^2|\overline{S}|^2 + m_{H_\text{d}}^2|H_\text{d}|^2 + m_{H_\text{u}}^2|H_\text{u}|^2 + m_\phi^2|\phi|^2 \\
&+ \Bigg[\lambda A_\lambda S(H_\text{u}H_\text{d}) - \sigma A_\sigma \phi(S\overline{S}) + \frac{\kappa}{3}\,A_\kappa\phi^3 + B\,\frac{\mu_\phi}{2}\,\phi^2 \\
&+ \xi A_F\phi + \text{h.c.}\Bigg]\,, \qquad (106)
\end{aligned}
$$

where g_1' is the $\mathrm{U}(1)_N$ gauge coupling, and $\tilde{Q}_{H_\text{d}}$, $\tilde{Q}_{H_\text{u}}$, and $\tilde{Q}_\text{S}$ are the effective $\mathrm{U}(1)_N$ charges of H_d, H_u, and S, respectively. As in the MSSM and NMSSM, the dominant contribution to ΔV, which comes from the loops containing the top-quark and its superpartners, is given by Eqn (59), in which μ has to be replaced by λS. At the same time, V_D contains new terms which are proportional to ${g_1'}^2$. These terms are not present in the MSSM or NMSSM. They represent D-term contributions due to the additional $\mathrm{U}(1)_N$ factor. At the physical minimum, H_u and H_d acquire VEVs (51), whereas

$$
\langle S\rangle = \frac{s_1}{\sqrt{2}}\,, \qquad \langle\overline{S}\rangle = \frac{s_2}{\sqrt{2}}\,, \qquad \langle\phi\rangle = \frac{\varphi}{\sqrt{2}}\,. \qquad (107)
$$

In the limit when $\sigma \to 0$, the $\mathrm{U}(1)_N$ D-term contribution to the scalar potential may force the minimum of this potential to be along the D-flat direction [309] so that $s_1 \simeq s_2 \sim \varphi \sim M_\text{S}/\sigma$, where M_S is the sparticle mass scale.

The masses of the vector bosons are induced via the interaction of the gauge fields with H_u, H_d, S, and $\overline{S}$. This results in $M_\text{W} = (g_2/2)v$. Meanwhile, the mechanism of the neutral gauge boson mass generation differs substantially. The $\mathrm{Z}-\mathrm{Z}'$ mass squared matrix is given by

$$
M_{ZZ'}^2 = \begin{pmatrix} \dfrac{\bar{g}^2}{4}\,v^2 & \varDelta^2 \\ \varDelta^2 & {g_1'}^2v^2\big(\tilde{Q}_{H_\text{d}}^2\cos^2\beta + \tilde{Q}_{H_\text{u}}^2\sin^2\beta\big) + {g_1'}^2\tilde{Q}_S^2 s^2 \end{pmatrix}, \qquad (108)
$$

where $s = \sqrt{s_1^2 + s_2^2}$ and

$$
\varDelta^2 = \frac{\bar{g}g_1'}{2}\,v^2\big(\tilde{Q}_{H_\text{d}}\cos^2\beta - \tilde{Q}_{H_\text{u}}\sin^2\beta\big)\,. \qquad (109)
$$

LHC constraints typically require the extra $\mathrm{U}(1)_N$ vector boson to be heavier than 4.5 TeV [310, 311]. To ensure that the Z' boson is sufficiently heavy, the SM singlet fields S must acquire large VEV, $s \geqslant 12$ TeV. In this case, the mass of the lightest neutral vector boson is very close to $M_\text{Z} = \bar{g}v/2$, the Z' mass is set by s, i.e., $M_{\text{Z}'} \approx g_1'\tilde{Q}_S\,s$, while the mixing between Z and Z' is very suppressed, i.e., the mixing angle $\alpha_{\text{ZZ}'} \lesssim 10^{-3}-10^{-4}$.

The spontaneous breakdown of the gauge symmetry within the E_6SSM gives rise to four massless Goldstone modes which are swallowed by the $\mathrm{W}^\pm$, Z, and Z' vector bosons. As a consequence, the Higgs spectrum involves two charged, three CP-odd, and five CP-even states. As in other SUSY models, one can compute the upper bound on the lightest Higgs scalar within the E_6SSM:

$$
\begin{aligned}
m_{\text{h}_1}^2 &\lesssim 4v^2\,\frac{\partial^2 V(v^2)}{\partial(v^2)^2} = \frac{\lambda^2}{2}\,v^2\sin^2(2\beta) + \frac{\bar{g}^2}{4}\,v^2\cos^2(2\beta) \\
&+ {g_1'}^2v^2\big(\tilde{Q}_{H_\text{d}}\cos^2\beta + \tilde{Q}_{H_\text{u}}\sin^2\beta\big)^2 + \varDelta_{22}\,. \qquad (110)
\end{aligned}
$$

The growth of the Yukawa couplings $\lambda(M_\text{t})$ and $h_\text{t}(M_\text{t})$ in the E_6SSM and NMSSM leads to the appearance of a Landau pole in the evolution of these Yukawa couplings. For each fixed value of $\tan\beta$, one can compute the maximal allowed value of $\lambda(M_\text{t}) = \lambda_{\max}$. The appearance of the Landau pole in

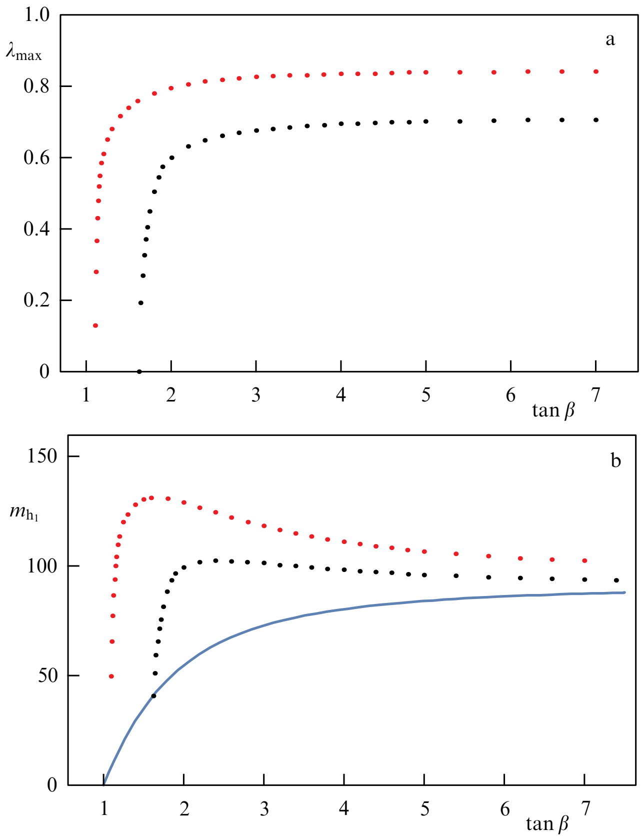

Figure 4. (a) Upper limit on $\lambda(M_\text{t})$ in the NMSSM (lower dotted line) and E_6SSM (upper dotted line) versus $\tan\beta$. (b) Tree-level upper bound on the mass of the lightest Higgs scalar as a function of $\tan\beta$ in the MSSM (solid line), NMSSM (lower dotted line), and E_6SSM (upper dotted line).

the evolution of the Yukawa couplings for any $q \lesssim M_\text{X}$ can be avoided if $\lambda(M_\text{t}) \lesssim \lambda_{\max}$. In the E_6SSM, the restrictions on the low energy values of $\lambda(M_\text{t})$ are weaker than in the NMSSM (Fig. 4a). The presence of exotic matter changes the evolution of the SM gauge couplings. Indeed, at the intermediate scales $q \gg M_\text{S}$, the values of these couplings are bigger in the E_6SSM than in the NMSSM. The growth of the SM gauge couplings and the extra $\mathrm{U}(1)_N$ gauge coupling reduce the values of the Yukawa couplings at intermediate scales, preventing the appearance of the Landau pole in the RG flow of these couplings. Therefore, within the E_6SSM, the values of $\lambda_{\max}$ are larger than in the NMSSM. The upper bound on $\lambda(M_\text{t})$ grows with increasing $\tan\beta$, since $h_\text{t}(M_\text{t})$ decreases. At large $\tan\beta$, this bound approaches the saturation limit. In the NMSSM and E_6SSM, the maximal possible values of $\lambda(M_\text{t})$ are 0.71 and 0.84, respectively (Fig. 4a).

In Fig. 4b the tree-level upper bound on the mass of the lightest Higgs scalar in the E_6SSM is compared to the corresponding bounds in the MSSM and NMSSM. At moderate values of $\tan\beta$, the theoretical restriction on the lightest Higgs boson mass in the E_6SSM and NMSSM exceeds the corresponding bound in the MSSM. Since in the E_6SSM λ is allowed to be larger than in the NMSSM, the tree-level theoretical restriction on m_{h_1} in the E_6SSM is also larger at moderate values of $\tan\beta$ than the one in the NMSSM. For $\tan\beta = 1.2-3.4$, the tree-level upper bound on the mass of the lightest Higgs boson in the E_6SSM is larger than 115 GeV [176]. Therefore, in this model, the contribution of loop corrections to $m_{\text{h}_1}^2$ is not needed to be as big as in the MSSM and NMSSM in order to get the SM-like Higgs boson with a mass of around 125 GeV. In the corresponding part of the parameter space, the coupling λ varies from 0.65 to 0.8. Assuming that $s_1 \simeq s_2 \geqslant 8.5$ TeV and using Eqn (63), one can estimate the value of Δ_{EW}, i.e.,

$$\Delta_{\mathrm{EW}} \sim \frac{\lambda^2 s_1^2}{M_Z^2} \sim 10^4 \,,$$

that characterizes the fine tuning which is needed to stabilize the EW scale in this case.

The upper bounds on m_{h_1} in the NMSSM and E$_6$SSM diminish when $\tan\beta$ rises, and at large $\tan\beta \gg 3$, the theoretical restriction on the mass of the lightest Higgs boson in the NMSSM approaches the corresponding limit in the MSSM. Nevertheless, even at very large values of $\tan\beta \sim 10$, the tree-level upper limit on m_{h_1} in the E$_6$SSM is still 6–7 GeV larger than the ones in the MSSM and NMSSM because of the extra $\mathrm{U}(1)_N$ D-term contribution to the Higgs potential (103)–(106) [176 – 180].

6. Limits on the superparticle spectrum in the simplest scenarios

Let us now consider the restrictions on the sparticle spectrum in the MSSM and E$_6$SSM caused by direct detection searches for dark matter and the Higgs mass measurement. Here, we explore scenarios in which the lightest neutralino χ_1^0 accounts for all or some of the observed cold dark matter relic density. Within the MSSM, the desired thermal dark matter density can be obtained in a few distinct regions of the parameter space (for a recent review, see [312]):

(i) if the mass of the lightest neutralino $m_{\chi_1^0}$ is nearly the same as that of some sfermion (co-annihilation) [313 – 315];

(ii) when $2m_{\chi_1^0}$ is close to the masses of the Z-boson [316], the SM-like Higgs boson [317], or one of the heavy Higgs states [318];

(iii) if χ_1^0 has a large higgsino or wino component [319–321].

In order to reduce the number of free parameters, we restrict our consideration in this section to the constrained SUSY models which impose extra unification constraints on the soft SUSY breaking parameters [322]. In particular, all soft scalar masses are set to be equal to m_0^2 at the scale M_{X}, i.e., $m_i^2(M_{\mathrm{X}}) = m_0^2$. Gaugino masses $M_i(M_{\mathrm{X}})$ are equal to an overall gaugino mass $M_{1/2}$ at the GUT scale, and all trilinear and bilinear scalar couplings coincide at this scale as well, i.e., $M_i(M_{\mathrm{X}}) = M_{1/2}$, $A_i(M_{\mathrm{X}}) = A_0$, and $B_i(M_{\mathrm{X}}) = B_0$.

Within the constrained MSSM, the lightest neutralino may have a mass which is close to either the lightest stau mass $m_{\tilde{\tau}_1}$ or the lightest stop mass $m_{\tilde{t}_1}$. Most scenarios with $m_{\chi_1^0} \approx m_{\tilde{\tau}_1}$ are characterized by $m_0 < 2$ TeV and $M_{1/2} < 1.5$ TeV [323 – 325]. Therefore, they are strongly constrained by LHC searches for squarks and gluinos. Moreover, the stringent limit on $M_{1/2}$ implies that in most cases $m_{\tilde{\tau}_1} - m_{\chi_1^0} \lesssim 5$ GeV [326]. This means that the realization of such scenarios requires an additional tuning of fundamental parameters. Moreover, in these scenarios, the mass of the lightest Higgs boson tends to be somewhat lower than 125 GeV. As a result, it is rather problematic to find phenomenologically acceptable solutions with $m_{\chi_1^0} \approx m_{\tilde{\tau}_1}$.

In case (ii), $m_{\chi_1^0} \simeq 40-70$ GeV or $m_{\chi_1^0} \simeq m_{\mathrm{A}}/2$. When $m_{\chi_1^0} \simeq 40-65$ GeV, the lightest neutralino is predominantly bino and $M_1 \simeq m_{\chi_1^0}$. Since in the constrained SUSY models $M_2 \simeq 2M_1$ and $M_3 \simeq 6.5M_1$ at low energies, the masses of the lightest chargino $\chi_1^{\pm}$ and next-to-lightest neutralino χ_2^0 states have to be relatively close to 100 GeV, whereas the gluino is lighter than 500 GeV in this case. Because of this, the scenarios with $m_{\chi_1^0} \simeq 40-70$ GeV are basically ruled out in these models.

Thus, in the constrained MSSM, cases (i) and (ii) mentioned above are reduced to the scenarios with $m_{\chi_1^0} \simeq m_{\tilde{t}_1}$ and $m_{\chi_1^0} \simeq m_{\mathrm{A}}/2$, which are associated with $\tan\beta \simeq 5-12$ and $\tan\beta \simeq 40-50$, respectively [325, 327]. They can only be achieved in narrow slices of the parameter space and require some extra tuning of the initial parameters to engineer the desired coincidence of masses. Therefore, here, we restrict our consideration to case (iii), which can be realized without any additional tuning. The low-energy relation $M_2 \simeq 2M_1$ implies that, in the constrained SUSY models, the lightest neutralino is predominantly the superposition of the bino and higgsino.

To calculate the particle spectrum within the MSSM and E$_6$SSM, FlexibleSUSY [328], SARAH [329–333], and SOFTSUSY [334, 335] were used. For the computation of the mass of the lightest Higgs boson, SUSYHD [336] was used. The values of the soft scalar masses $m_i^2(M_{\mathrm{S}})$ and trilinear scalar couplings $A_i(M_{\mathrm{S}})$ at the sparticle mass scale M_{S} are related to m_0^2, A_0, and $M_{1/2}$ by

$$\begin{aligned} m_i^2(M_{\mathrm{S}}) &= a_i(M_{\mathrm{S}}) m_0^2 + b_i(M_{\mathrm{S}}) M_{1/2}^2 \\ &\quad + c_i(M_{\mathrm{S}}) M_{1/2} A_0 + d_i(M_{\mathrm{S}}) A_0^2 \,, \\ A_i(M_{\mathrm{S}}) &= e_i(M_{\mathrm{S}}) M_{1/2} + f_i(M_{\mathrm{S}}) A_0 \,, \end{aligned} \tag{111}$$

where M_{S} is set to be equal to $\sqrt{m_{\tilde{t}_1} m_{\tilde{t}_2}}$. The values of $M_i(M_{\mathrm{S}})$ are determined by $M_{1/2}$. In the MSSM,

$$\begin{aligned} &M_1(M_{\mathrm{S}}) \approx 0.4 M_{1/2} \,, \qquad M_2(M_{\mathrm{S}}) \approx 0.8 M_{1/2} \,, \\ &M_3(M_{\mathrm{S}}) \approx 2.7 M_{1/2} \,, \end{aligned} \tag{112}$$

whereas, in the framework of the E$_6$SSM,

$$\begin{aligned} &M_1(M_{\mathrm{S}}) \approx M_1'(M_{\mathrm{S}}) \approx 0.2 M_{1/2} \,, \\ &M_2(M_{\mathrm{S}}) \approx 0.3 M_{1/2} \,, \qquad M_3(M_{\mathrm{S}}) \approx 0.7 M_{1/2} \,. \end{aligned} \tag{113}$$

Here, we shall assume that in the E$_6$SSM $\tilde{f}_{i\alpha} \sim f_{i\alpha} \lesssim 10^{-7}$. In this case, the lightest exotic states are basically fermion components of the superfields S_i with masses which are much smaller than 10^{-3} eV. These states form hot dark matter but make only a very minor contribution to the dark matter density. As in the MSSM, in this part of the E$_6$SSM parameter space, the lightest ordinary neutralino may account for all or some of the observed cold dark matter density since R-parity is conserved. From Eqns (112), (113), it follows that the mass of the lightest neutralino tends to be considerably lower than M_{S}.

To simplify the analysis, some E$_6$SSM parameters were fixed, i.e.,

$$\begin{aligned} &\lambda_{\alpha\beta} = \lambda_0 \delta_{\alpha\beta} \,, \quad \mu_\phi(M_{\mathrm{X}}) = 0 \,, \quad \mu_L(M_{\mathrm{X}}) = 10 \text{ TeV} \,, \\ &\kappa_{ij} = \kappa_0 \delta_{ij} \,, \quad \sigma(M_{\mathrm{X}}) = 2 \times 10^{-2} \,, \quad \kappa(M_{\mathrm{X}}) = 10^{-2} \,, \end{aligned} \tag{114}$$

and the Z$'$ boson mass was chosen to be very large, $M_{Z'} \approx 240$ TeV $\gg M_{\mathrm{S}}$, which corresponds to $s = (s_1^2 + s_2^2)^{1/2} \simeq 650$ TeV. Such large VEVs of S and $\overline{S}$ can be obtained for $\Lambda_F \gg M_S^2$. In this limit, $s_1 \approx s_2$, i.e., $\tan\theta = s_2/s_1$ is close to unity. The phenomenologically acceptable dark matter density is then achieved for very small $|\lambda| \ll \sigma$. Moreover, it is assumed that the couplings $\tilde{\sigma}$, g^D_{ij}, and $h^E_{i\alpha}$ are negligibly small, while $\lambda_0 \ll \sigma$ and $\kappa_0 \ll \sigma$.

The structure of the neutralino spectrum in the E_6SSM is simplified when $M_{Z'} \gg M_S$. The neutralino sector is formed by the superpartners of neutral gauge bosons ($\tilde{W}_3$, $\tilde{B}$, and $\tilde{B}'$) associated with the $SU(2)_W$, $U(1)_Y$, and $U(1)_N$ interactions as well as by the fermion components of the superfields H^0_d, H^0_u, S, $\overline{S}$, and ϕ, i.e., $\tilde{H}^0_d$, $\tilde{H}^0_u$, $\tilde{S}$, $\tilde{\overline{S}}$, and $\tilde{\phi}$. After the breakdown of gauge symmetry, all these fermion states mix. In the basis

$$\tilde{\psi}^0_j = (\tilde{H}^0_d, \tilde{H}^0_u, \tilde{W}_3, \tilde{B}, \tilde{B}', \tilde{S}\cos\theta - \tilde{\overline{S}}\sin\theta, \tilde{S}\sin\theta + \tilde{\overline{S}}\cos\theta, \tilde{\phi}), \tag{115}$$

the neutralino mass matrix can be written as

$$M_{\tilde{\chi}^0} = \begin{pmatrix} A & C^{\mathrm{T}} \\ C & B \end{pmatrix}, \tag{116}$$

where

$$A = \begin{pmatrix} 0 & -\mu_{\mathrm{eff}} & \dfrac{g_2 v}{2}\cos\beta & -\dfrac{g' v}{2}\cos\beta \\ -\mu_{\mathrm{eff}} & 0 & -\dfrac{g_2 v}{2}\sin\beta & \dfrac{g' v}{2}\sin\beta \\ \dfrac{g_2 v}{2}\cos\beta & -\dfrac{g_2 v}{2}\sin\beta & M_2 & 0 \\ -\dfrac{g' v}{2}\cos\beta & \dfrac{g' v}{2}\sin\beta & 0 & M_1 \end{pmatrix}, \tag{117}$$

$$B = \begin{pmatrix} M'_1 & g'_1\tilde{Q}_S s & 0 & 0 \\ g'_1\tilde{Q}_S s & \dfrac{\sigma\varphi}{\sqrt{2}}\sin(2\theta) & -\dfrac{\sigma\varphi}{\sqrt{2}}\cos(2\theta) & 0 \\ 0 & -\dfrac{\sigma\varphi}{\sqrt{2}}\cos(2\theta) & -\dfrac{\sigma\varphi}{\sqrt{2}}\sin(2\theta) & -\dfrac{\sigma s}{\sqrt{2}} \\ 0 & 0 & -\dfrac{\sigma s}{\sqrt{2}} & \sqrt{2}\kappa\varphi + \mu_\phi \end{pmatrix}, \tag{118}$$

$$C = \begin{pmatrix} \tilde{Q}_{H_d} g'_1 v\cos\beta & \tilde{Q}_{H_u} g'_1 v\sin\beta & 0 & 0 \\ -\dfrac{\lambda v}{\sqrt{2}}\sin\beta\cos\theta & -\dfrac{\lambda v}{\sqrt{2}}\cos\beta\cos\theta & 0 & 0 \\ -\dfrac{\lambda v}{\sqrt{2}}\sin\beta\sin\theta & -\dfrac{\lambda v}{\sqrt{2}}\cos\beta\sin\theta & 0 & 0 \\ 0 & 0 & 0 & 0 \end{pmatrix}. \tag{119}$$

In Eqns (117), (118), $\mu_{\mathrm{eff}} = \lambda s\cos\theta/\sqrt{2}$, whereas M_1, M_2, and M'_1 are gaugino masses for $\tilde{B}$, $\tilde{W}_3$, and $\tilde{B}'$, respectively. In matrix (119), the Abelian gaugino mass mixing M_{11} between $\tilde{B}$ and $\tilde{B}'$ is ignored. The submatrix A contains the neutralino mass matrix of the MSSM, where the parameter μ is replaced by μ_{eff}.

The submatrix B represents the mixing of extra neutralino states in the E_6SSM. If $M_{Z'} \gg M_S$, an inspection of Eqn (118) shows that two such neutralinos, those that are a mixture of $\tilde{B}'$ and $\tilde{S}\cos\theta - \tilde{\overline{S}}\sin\theta$, have their masses set by the large value of $M_{Z'}$. In this limit, two such neutralinos are the heaviest states in the neutralino spectrum. The remaining extra neutralino states are mixture of $\tilde{S}\sin\theta + \tilde{\overline{S}}\cos\theta$ and $\tilde{\phi}$. Their masses are expected to be of the order of M_S because they are defined by either $\sigma\varphi/\sqrt{2}$ or $\sigma s/\sqrt{2}$. Since $|\lambda| \ll \sigma$ and $M_1, M_2 \ll M_S$, all extra neutralino states in the E_6SSM are considerably heavier than the ones which are linear superpositions of $\tilde{H}^0_d$, $\tilde{H}^0_u$, $\tilde{W}_3$, and $\tilde{B}$.

Due to the lack of significant mixing between the heaviest states in the neutralino spectrum and the four lightest ones within the E_6SSM, the heaviest neutralinos can be ignored in the first approximation as far as determining the dark matter density goes. Thus, as in the MSSM, the masses of the lightest neutralino states in the E_6SSM are set by M_1, M_2, and μ_{eff}. Equations (112), (113) indicate that the lightest state in the neutralino spectrum is predominantly a mixture of the higgsino and gaugino associated with the $U(1)_Y$ interaction. Because its mass and couplings are defined by $M_{1/2}$ and μ, in our numerical analysis, it is worth fixing the value of $\mu(M_S)$ in the MSSM and E_6SSM. Then, using the minimization conditions, which determine the physical minimum of the Higgs effective potential in the MSSM and E_6SSM, one can compute m_0^2 and other parameters of these models for each set of $M_{1/2}$, A_0, and $\tan\beta$.

The relic density was calculated numerically with micrOMEGAS [337–340]. In the SUSY models under consideration, the values of $|\mu(M_S)| \gg 1$ TeV usually result in an unacceptably large dark matter density. Therefore, here, only scenarios with $|\mu(M_S)| \leqslant 1$ TeV are explored. In the case of the E_6SSM with $s \simeq 650$ TeV and $\tan\theta \simeq 1$, this leads to an upper bound $|\lambda(M_X)| \lesssim 2.4 \times 10^{-3}$. The results presented in Figs 5, 6 and Figs 7, 8 were obtained for $\mu(M_S) = \mu_{\mathrm{eff}}(M_S) = 417$ GeV, $\lambda_0(M_X) = \kappa_0(M_X) = 10^{-3}$ and $\mu(M_S) = \mu_{\mathrm{eff}}(M_S) = 1046$ GeV, $\lambda_0(M_X) = \kappa_0(M_X) = 3 \times 10^{-3}$, respectively. Only scenarios with the dark matter density $\Omega_{\mathrm{CDM}}h^2 \leqslant 0.120$ are considered.

In order to get the lightest Higgs boson with mass $m_{h_1} \simeq 125$ GeV, we restrict our consideration to $\tan\beta \gg 1$. Here, we set $\tan\beta \simeq 10$. The parameters $M_{1/2}$ and A_0 are varied from 0 to 20 TeV and from -20 TeV to 20 TeV, respectively. For each set of parameters $M_{1/2}$, A_0, and $\tan\beta$, the lightest Higgs mass can be computed. Here, all scenarios with $m_{h_1} \geqslant 122$ GeV and $m_{h_1} \leqslant 128$ GeV are considered. In all scenarios, soft scalar masses are required to satisfy constraints $m_i^2(M_S) > 0$. Negative values of $m_i^2(M_S)$ are allowed only for fields which acquire VEVs.

For $\mu(M_S) = \mu_{\mathrm{eff}}(M_S) = 417$ GeV, the allowed parts of the parameter space in the $(M_{1/2}, m_0)$ plane, in which all the constraints mentioned above are fulfilled, are shown in Figs 5, 6. The lightest Higgs state with mass, which is close to 125 GeV, can be obtained in this case only when $\ln(M_S^2/m_t^2)$ is sufficiently large. If $m_0^2 \gg M_{1/2}^2$, this corresponds to the lower bound $m_0 \gtrsim 5-6$ TeV. Another lower bound on m_0 arises when $m_0 \sim M_{1/2}$. For fixed values of $\tan\beta$ and $\mu(M_S) = \mu_{\mathrm{eff}}(M_S)$,

$$m_0^2 = \xi_1 M_{1/2}^2 + \xi_2 M_{1/2} A_0 + \xi_3 A_0^2 + \xi_0\,, \tag{120}$$

where ξ_0, ξ_1, ξ_2, and ξ_3 are some numbers and $\xi_1, \xi_3 > 0$. The right-hand side of Eqn (120) attains its minimal value for $A_0 = -(\xi_2/2\xi_3)M_{1/2}$, so that

$$m_0^2 \geqslant \xi_4 M_{1/2}^2 + \xi_0\,, \qquad \xi_4 = \xi_1 - \frac{\xi_2^2}{4\xi_3}\,,$$

where $\xi_4 > 0$. When $M_{1/2} \gg \mu(M_S) = \mu_{\mathrm{eff}}(M_S)$, the value of m_0 must be larger than $\sqrt{\xi_4}M_{1/2}$ (see Figs 5–8).

As follows from Figs 5–8, in the E_6SSM, there is also an upper bound on m_0. For fixed $M_{1/2}$, the value of m_0 grows

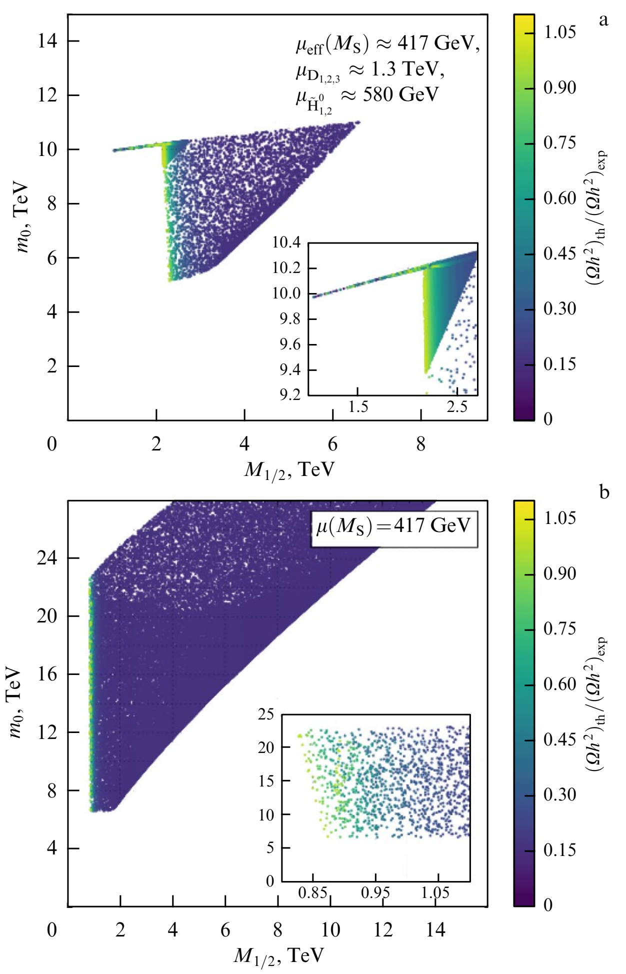

Figure 5. Contour plots in the $(M_{1/2}, m_0)$ plane of the dark matter density in the E_6SSM (a) and in the MSSM (b) for $\mu(M_{\rm S}) = \mu_{\rm eff}(M_{\rm S}) = 417$ GeV, $\tan\beta \simeq 10$, and $|A_0| \leqslant 20$ TeV. Mass of the lightest Higgs state varies from 122 to 128 GeV. In the case of the E_6SSM, $M_{Z'} \approx 240$ TeV, $s = (s_1^2 + s_2^2)^{1/2} \simeq 650$ TeV, and $\lambda_0(M_{\rm X}) = \kappa_0(M_{\rm X}) = 10^{-3}$. At large values of $M_{1/2}$, when the lightest neutralino is predominantly the higgsino, dark matter density is about 15% of its observed value (see also [347]).

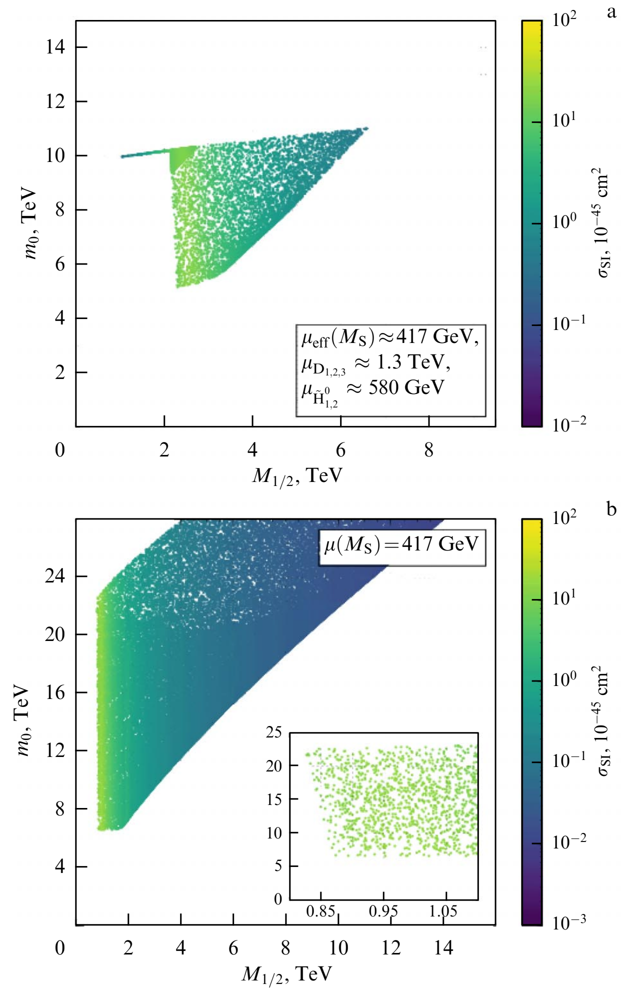

Figure 6. Contour plots in the $(M_{1/2}, m_0)$ plane of $\sigma_{\rm SI}$ in the E_6SSM (a) and in the MSSM (b) for $\mu(M_{\rm S}) = \mu_{\rm eff}(M_{\rm S}) = 417$ GeV, $\tan\beta \simeq 10$, and $|A_0| \leqslant 20$ TeV. Mass of the lightest Higgs state varies from 122 to 128 GeV. In the case of the E_6SSM, $M_{Z'} \approx 240$ TeV, $s = (s_1^2 + s_2^2)^{1/2} \simeq 650$ TeV, and $\lambda_0(M_{\rm X}) = \kappa_0(M_{\rm X}) = 10^{-3}$. At large values of $M_{1/2}$, when the lightest neutralino is predominantly the higgsino, dark matter density is about 15% of its observed value (see also [347]).

with increasing $|A_0|$. However, large values of $|A_0|$ give rise to large mixing in the CP-even and CP-odd Higgs sectors of the E_6SSM. As a consequence, at some value of A_0, either the mass squared of the lightest Higgs pseudoscalar $m^2_{A_1}$ or the mass squared of the lightest Higgs scalar $m^2_{h_1}$ becomes negative. Because of this, it is rather problematic to find any phenomenologically acceptable scenario within the E_6SSM for relatively large values of $|A_0|$ and m_0.

The results presented in Figs 5, 6 indicate that, for fixed $\mu(M_{\rm S})$ (or $\mu_{\rm eff}(M_{\rm S})$), a lower bound on $M_{1/2}$ exists that corresponds to $M_1(M_{\rm S}) \simeq \mu(M_{\rm S})$ (or $M_1(M_{\rm S}) \simeq \mu_{\rm eff}(M_{\rm S})$). Indeed, the lightest neutralino gives rise to an unacceptably large dark matter density when $M_1(M_{\rm S}) \lesssim \mu(M_{\rm S})$ (or $M_1(M_{\rm S}) \lesssim \mu_{\rm eff}(M_{\rm S})$). If $M_1(M_{\rm S}) \gtrsim \mu(M_{\rm S})$ (or $M_1(M_{\rm S}) \gtrsim \mu_{\rm eff}(M_{\rm S})$), then the lightest neutralino χ_1^0 is predominantly a higgsino in the SUSY models under consideration. As a consequence, the annihilation cross section for $\chi_1^0\chi_1^0 \to$ SM particles increases substantially, so that χ_1^0 can account for all or some fraction of the measured dark matter density if $\mu(M_{\rm S}), \mu_{\rm eff}(M_{\rm S}) \lesssim 1$ TeV. Figure 5 demonstrates that for $\mu(M_{\rm S})$, $\mu_{\rm eff}(M_{\rm S}) \ll 1$ TeV the measured value of the dark matter density can be obtained only in a narrow region of the parameter space near $M_1(M_{\rm S}) \simeq \mu(M_{\rm S})$ (or $M_1(M_{\rm S}) \simeq \mu_{\rm eff}(M_{\rm S})$). For $\mu(M_{\rm S}) = \mu_{\rm eff}(M_{\rm S}) = 417$ GeV, the lower bound on $M_{1/2}$ implies that $M_{1/2} \gtrsim 0.85$ TeV in the MSSM and $M_{1/2} \gtrsim 2.1-2.2$ TeV in the E_6SSM. Although the lower bounds on $M_{1/2}$ in the MSSM and E_6SSM differ significantly, they correspond to approximately the same lower bound on the gluino mass $M_{\tilde{g}} \gtrsim 2.1-2.2$ TeV. With increasing $M_{1/2}$ (or $M_1(M_{\rm S})$), the dark matter density decreases. For $\mu(M_{\rm S}) = \mu_{\rm eff}(M_{\rm S}) = 417$ GeV and $M_1(M_{\rm S}) \gg 417$ GeV, the dark matter density induced by χ_1^0 constitutes only 15% of its observed value.

The values of $M_{1/2}$ are even more strongly constrained by null results from direct detection experiments that set limits on the dark matter–nucleus scattering cross section. The lightest neutralino–nucleon scattering cross section involves two parts. The first spin-independent (SI) part of χ_1^0-nucleon cross section $\sigma_{\rm SI}$ makes a contribution to the dark matter–nucleus scattering cross section, which is proportional to A^2, where A is a number of nucleons in nucleus. The second spin-dependent (SD) part $\sigma_{\rm SD}$ does not lead to such an enhanced contribution to the corresponding cross section. We further focus on $\sigma_{\rm SI}$. The first spin-independent part is dominated by t-channel exchange of the lightest CP-even Higgs boson h_1. In the leading approximation, the SI part of the χ_1^0-nucleon cross

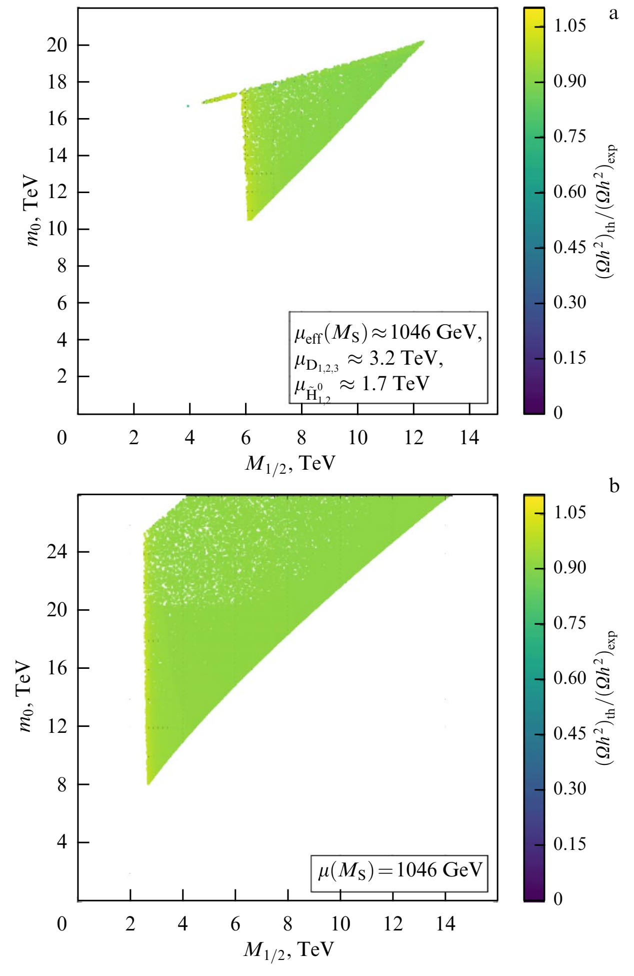

Figure 7. Contour plots in the $(M_{1/2}, m_0)$ plane of the dark matter density in the E$_6$SSM (a) and in the MSSM (b) for $\mu(M_{\rm S}) = \mu_{\rm eff}(M_{\rm S}) = 1046$ GeV, $\tan\beta \simeq 10$, and $|A_0| \leqslant 20$ TeV. Mass of the lightest Higgs state varies from 122 to 128 GeV. In the case of the E$_6$SSM, $M_{Z'} \approx 240$ TeV, $s = (s_1^2 + s_2^2)^{1/2} \simeq 650$ TeV, and $\lambda_0(M_{\rm X}) = \kappa_0(M_{\rm X}) = 3 \times 10^{-3}$ (see also [347]).

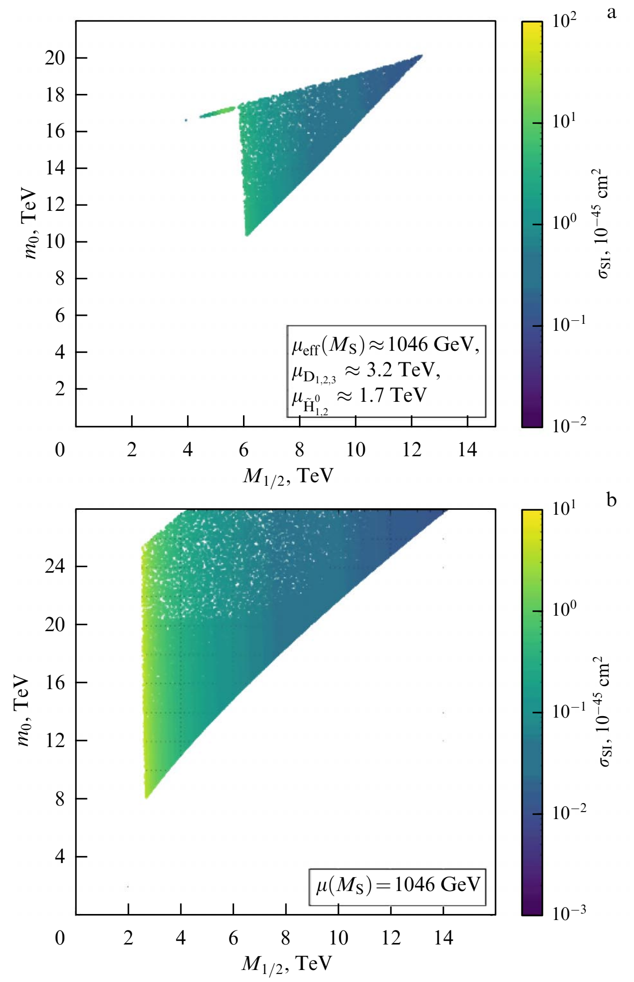

Figure 8. Contour plots in the $(M_{1/2}, m_0)$ plane of $\sigma_{\rm SI}$ in the E$_6$SSM (a) and in the MSSM (b) for $\mu(M_{\rm S}) = \mu_{\rm eff}(M_{\rm S}) = 1046$ GeV, $\tan\beta \simeq 10$, and $|A_0| \leqslant 20$ TeV. Mass of the lightest Higgs state varies from 122 to 128 GeV. In the case of the E$_6$SSM, $M_{Z'} \approx 240$ TeV, $s = (s_1^2 + s_2^2)^{1/2} \simeq 650$ TeV, and $\lambda_0(M_{\rm X}) = \kappa_0(M_{\rm X}) = 3 \times 10^{-3}$ (see also [347]).

section takes the form

$$\sigma_{\rm SI} \simeq \frac{4 m_{\rm r}^2 m_{\rm N}^2}{\pi v^2 m_{\rm h_1}^4} \, |g_{\rm h_1 \chi_1 \chi_1} F^{\rm N}|^2 \,, \qquad m_{\rm r} = \frac{m_{\chi_1^0} m_{\rm N}}{m_{\chi_1^0} + m_{\rm N}} \,,$$
$$F^{\rm N} = \sum_{q={\rm u,d,s}} f_{Tq}^{\rm N} + \frac{2}{27} \sum_{Q={\rm c,b,t}} f_{TQ}^{\rm N} \,, \tag{121}$$

where $m_{\rm N}$ and $m_{\chi_1^0}$ are the masses of the nucleon and lightest neutralino,

$$m_{\rm N} f_{Tq}^{\rm N} = \langle N | m_q \bar{q} q | N \rangle \,, \qquad f_{TQ}^{\rm N} = 1 - \sum_{q={\rm u,d,s}} f_{Tq}^{\rm N} \,,$$

while $f_{T\rm u}^{\rm N} \simeq 0.0153$, $f_{T\rm d}^{\rm N} \simeq 0.0191$, and $f_{T\rm s}^{\rm N} \simeq 0.0447$ [341]. In the MSSM and E$_6$SSM, $m_{\chi_1^0} \gg m_N$ and $m_{\rm r} \approx m_{\rm N}$. The size of the cross section (121) is set by the coupling $g_{\rm h_1 \chi_1 \chi_1}$ that determines the strength of the interaction of the lightest neutralino with the lightest Higgs boson. When $M_{\rm S} \gg M_{\rm Z}$, this coupling is given by

$$g_{\rm h_1 \chi_1 \chi_1} \approx \frac{1}{2} \left(g' R_{14} - g_2 R_{13} \right) \left[R_{11} (V)_{11} - R_{12} (V)_{12} \right] , \tag{122}$$

where the matrices V and R are defined as

$$\chi_i^0 = R_{ij} \tilde{\psi}_j \,, \qquad h_i = V_{ij} S'_j \,. \tag{123}$$

In Eqn (123), χ_i^0 are neutralino eigenstates, h_i are CP-even Higgs eigenstates, $\tilde{\psi}_j$ are components of the basis in the neutralino sector, and S'_j are components of the basis in the CP-even Higgs sector. In the case of the MSSM, $\tilde{\psi}_j = (\tilde{H}_{\rm d}^0, \tilde{H}_{\rm u}^0, \tilde{W}_3, \tilde{B})$ and $S'_j = (\sqrt{2}\,{\rm Re}\, H_{\rm d}^0, \sqrt{2}\,{\rm Re}\, H_{\rm u}^0)$. In the E$_6$SSM, the basis in the neutralino sector is given by Eqn (115), whereas

$$S'_j = \left(\sqrt{2}\,{\rm Re}\, H_{\rm d}^0, \sqrt{2}\,{\rm Re}\, H_{\rm u}^0, \sqrt{2}\,{\rm Re}\, S, \sqrt{2}\,{\rm Re}\, \overline{S}, \sqrt{2}\,{\rm Re}\, \phi \right) .$$

The cross section (121) attains its maximal value of $\sim 10^{-45} - 10^{-44}$ cm^2 for $|M_1(M_{\rm S})| \simeq |\mu(M_{\rm S})|$ (or $|M_1(M_{\rm S})| \simeq |\mu_{\rm eff}(M_{\rm S})|$), when $|R_{11} R_{14}| \sim |R_{12} R_{14}| \sim 1$. The 90% exclusion limits set by the experiments LUX (Large Underground Xenon experiment) [342], XENON1T [343], PandaX-4T [344], and LUX–ZEPLIN (LZ) [345] rule out such large cross sections $\sigma_{\rm SI}$. For $\Omega h^2 \approx 0.118 - 0.119$ and the lightest neutralino masses, which vary from 200 GeV to 1000 GeV, the experimental limits on $\sigma_{\rm SI}$, which are set by LZ, are of the order of 0.5×10^{-46}–3×10^{-46} cm^2 [345]. With increasing $M_1(M_S)$ and $M_{1/2}$, the cross section σ_{SI} diminishes because $|R_{14}|$ decreases (see Fig. 6). Additionally, the reduction in Ωh^2 for larger values of $M_{1/2}$ implies a reduction in the local number density of WIMPs and thereby weakens the limits from direct detection, i.e.,

$$\sigma_{SI} < \frac{0.119}{(\Omega h^2)_{th}}\, \sigma_{SI}^{exp}(m_{\tilde{\chi}_1^0})\,, \tag{124}$$

where σ_{SI} and $(\Omega h^2)_{th}$ are computed values of these quantities for each set of the parameters of either MSSM or E$_6$SSM, while $\sigma_{SI}^{exp}(m_{\tilde{\chi}_1^0})$ is the experimental limit on the cross section σ_{SI} at the given mass $m_{\tilde{\chi}_1^0}$. Any set of parameters of either MSSM or E$_6$SSM that does not satisfy condition (124) is basically ruled out [346, 347]. Simple estimates show that the lower bound on $M_{1/2}$ computed using condition (124) increases from 0.85 TeV to 2 TeV in the MSSM and from 2.1 TeV to 5 TeV in the E$_6$SSM. This corresponds to the lower bound on gluino mass $M_{\tilde{g}} \gtrsim 5.2$ TeV in the MSSM and E$_6$SSM.

The results of the numerical analysis presented in Figs 5a and 6a indicate that there is a small part of the E$_6$SSM parameter space in which a reasonable value of the dark matter density can be obtained even if $M_1(M_S) \ll \mu_{eff}(M_S)$ [347]. In this part of the parameter space, the mass of the lightest *CP*-odd Higgs boson $m_{A_1} \approx 2m_{\chi_1^0}$, which leads to the enhancement of the annihilation cross section for $\chi_1^0\chi_1^0 \to$ SM particles, reducing $\Omega_{CDM}h^2$. The cross section σ_{SI} is relatively small in this region of the parameter space, and condition (124) is satisfied. The lightest *CP*-odd Higgs state with mass $m_{A_1} \approx 2m_{\chi_1^0}$ appears only for certain values of A_0. Unfortunately, for $\mu_{eff}(M_S) = 417$ GeV, almost all such scenarios with $M_{1/2} \lesssim 2$ TeV have already been ruled out by the LHC experiments. In the framework of the MSSM, the corresponding scenarios with $\tan\beta \gtrsim 50$ were considered in Ref. [348].

For $\mu(M_S) = \mu_{eff}(M_S) = 1046$ GeV, the allowed parts of the parameter space in the $(M_{1/2}, m_0)$ plane are shown in Figs 7 and 8. They correspond to the substantially heavier spectrum of sparticles and the larger mass of the lightest Higgs boson as compared with the scenarios with $\mu(M_S) = \mu_{eff}(M_S) = 417$ GeV. As discussed earlier, the scenarios with sufficiently small $M_{1/2}$ associated with $M_1(M_S) \lesssim \mu(M_S)$ (or $M_1(M_S) \lesssim \mu_{eff}(M_S)$) give rise to unacceptably large dark matter density, so they are ruled out. In almost all scenarios from the allowed parts of the parameter space, which are presented in Fig. 7, the dark matter density is about 90% of its observed value. The lightest neutralino is predominantly the higgsino in all these cases. The absolute values of the matrix elements R_{14} and R_{13} are rather small, so the cross section σ_{SI} is smaller than the one associated with the scenarios with $\mu(M_S) = \mu_{eff}(M_S) = 417$ GeV. The results of the numerical analysis presented in Fig. 8 indicate that the cross section σ_{SI} diminishes when $M_{1/2}$ rises. The experimental upper limit on σ_{SI} weakens upon increasing the lightest neutralino mass $m_{\chi_1^0}$. Nevertheless, it still allows us to get the stringent lower bound on $M_{1/2}$. For $\mu(M_S) = \mu_{eff}(M_S) = 1046$ GeV, the experimental limit on σ_{SI} implies that $M_{1/2} \gtrsim 3.9$ TeV in the MSSM and $M_{1/2} \gtrsim 9.5$ TeV in the E$_6$SSM. This corresponds to $M_{\tilde{g}} \gtrsim$ 10 TeV in the MSSM and E$_6$SSM.

As before in the E$_6$SSM with $\mu_{eff}(M_S) = 1046$ GeV, one can find scenarios with $m_{A_1} \approx 2m_{\chi_1^0}$ which lead to the phenomenologically acceptable dark matter density and relatively small cross section σ_{SI}, even when $M_1(M_S) \lesssim \mu_{eff}(M_S)$ (see Figs 7a and 8a). However, all of them require a substantial degree of tuning and in all such scenarios the values of m_0 and $M_{1/2}$ are too large, so the observation of any sparticle at the LHC seems to be rather problematic. Exotic states are also too heavy in this case because $\kappa_0(M_X) = \lambda_0(M_X) = 3 \times 10^{-3}$. This choice of $\lambda_0(M_X)$ and $\kappa_0(M_X)$ corresponds to the masses of exotic quarks $\mu_{D_i} \approx 3.2$ TeV and the masses of the inert higgsino $\mu_{\tilde{H}^\pm_\alpha} \approx 1.7$ TeV. At the same time, it is worth noting that in the limit $\lambda_0(M_X), \kappa_0(M_X) \ll \sigma(M_X)$ the allowed region of the E$_6$SSM parameter space does not change much when $\lambda_0(M_X)$ and $\kappa_0(M_X)$ vary.

In the simplest scenarios under consideration, the annihilation cross section for $\chi_1^0\chi_1^0 \to$ SM particles becomes too small, and the dark matter density is unacceptably large when $\mu(M_S) \gg 1$ TeV or $\mu_{eff}(M_S) \gg 1$ TeV. Within the constrained MSSM, the allowed range of $\mu(M_S)$ enlarges in the limit when $m_{\chi_1^0} \approx m_A/2$. In this case, the mass of the lightest neutralino and $\mu(M_S)$ may be considerably larger than 2 TeV, because the annihilation cross section of $\chi_1^0\chi_1^0$ increases [327]. The sparticle spectrum becomes heavier as well. A relatively light sparticle spectrum arises in the constrained MSSM if $m_{\chi_1^0} \simeq m_{\tilde{t}_1}$. The corresponding solutions imply that m_0 varies from 2 TeV to 4.5 TeV. As a consequence, the masses of almost all scalars are larger than 2–3 TeV. The lightest neutralino is predominantly bino in this case. The dark matter density that it forms tends to be significantly smaller than its observed value, while σ_{SI} may be much lower than the corresponding experimental limits [325, 327].

In the near future, the experiments XENONnT [349], LUX–ZEPLIN (LZ) [350], DarkSide-20k [351], and DARWIN [352] may set even more stringent constraints on the cross section σ_{SI}. Furthermore, since neutralinos can annihilate, their annihilation products, which include neutrinos, gamma rays, positrons, and antiprotons, can be detected. In the context of annihilation of neutralinos with TeV scale masses, the detection of signals associated with very high energy gamma rays ($E \gtrsim 100$ GeV) plays a major role. The Cherenkov Telescope Array (CTA) [353] is going to be sensitive to such signals. It is expected that this experiment will be able to detect gamma rays which originate from the annihilation of neutralinos with masses $m_{\chi_1^0} \gtrsim 1$ TeV in the region around the Galactic center [353–355].

7. Searching for supersymmetric signals at the Large Hadron Collider

Searches for possible manifestations of SUSY models remain one of the main goals of the LHC experiments (see reviews [356–358]). Since in collider experiments the superpartners of SM particles can only be created in pairs and each of them decays into a final state, which involves at least one LSP, the typical SUSY search signature contains leptons and/or jets with high-p_T, which are produced in the decay chains of heavy sparticles, and significant missing momentum originating from the two LSPs produced at the end of the decay chain, which escape experimental detection. The absence of any observation of such phenomena at the LHC place stringent bounds on the parameters of SUSY models.

ATLAS (A Toroidal Large Hadron Collider (LHC) ApparatuS) and CMS (Compact Muon Solenoid) have adopted simplified models as the primary framework to provide interpretations of their searches. In these models, the production of a limited set of SUSY particles as well as their decay modes are examined. These models leave open the possibility of varying masses and other parameters freely. Since none of the searches performed so far have shown significant excess above the SM background prediction, the interpretation of the LHC results are exclusion limits on the SUSY parameter space. In practice, simplified model limits are often used as an approximation of the constraints that can be placed on sparticle masses for more complex SUSY spectra. Although simplified models are very convenient for the interpretation of individual SUSY production and decay topologies, care must be taken when applying the obtained limits to more complex SUSY scenarios.

When gluinos are lighter than squarks ($M_{\tilde{g}} \lesssim m_{\tilde{q}}$), they decay through $\tilde{g} \to q\tilde{q}^* \to q\bar{q} + \tilde{\chi}_1^0$. Therefore, gluino pair production should result in an appreciable enhancement of the cross section for $pp \to q\bar{q}q\bar{q} + E_T^{\text{miss}} + X$, where X refers, hereafter, to any number of light quark/gluon jets. Experimental limits on the gluino mass are strongly affected by the assumption of the lightest neutralino mass $m_{\tilde{\chi}_1^0}$. For massless neutralino $\tilde{\chi}_1^0$, the LHC experiments excluded gluino masses below 2.2–2.3 TeV [359–362]. For $m_{\tilde{\chi}_1^0} \gtrsim 1.2$ TeV, no limit on $M_{\tilde{g}}$ can be placed. If $m_{\tilde{\chi}_1^0} \lesssim 1$ TeV and $M_{\tilde{g}} \simeq m_{\tilde{q}}$, the mass exclusion is about 3 TeV [362]. The LHC experiments also search for the production of third generation squarks. Assuming that the bottom squark decays predominantly into $b\tilde{\chi}_1^0$ while the top squark decays either via $\tilde{t} \to t\tilde{\chi}_1^0$ or via $\tilde{t} \to b\tilde{\chi}_1^{\pm}$, $\tilde{\chi}_1^{\pm} \to W^{\pm}\tilde{\chi}_1^0$, ATLAS and CMS set lower mass limits of 1200–1300 GeV for massless neutralinos $\tilde{\chi}_1^0$ [359, 361, 363–365]. However, no limit can be placed for $m_{\tilde{\chi}_1^0} \geqslant 800$ GeV.

LEP (Large Electron–Positron collider) experiments set lower limits on the lightest chargino mass $m_{\tilde{\chi}_1^{\pm}}$. Depending on the mass of the lightest neutralino and other parameters, these limits vary from 92 to 103 GeV. At the LHC, charginos have been searched for via production of $\tilde{\chi}_1^{\pm}\tilde{\chi}_2^0$ and $\chi_1^{\pm}\chi_1^{\mp}$ in which the masses of $\chi_1^{\pm}$ and $\tilde{\chi}_2^0$ ($m_{\tilde{\chi}_2^0}$) are somewhat larger than $m_{\tilde{\chi}_1^0}$. The results of the search for $\tilde{\chi}_1^{\pm}\tilde{\chi}_2^0$ production is normally presented for $m_{\tilde{\chi}_1^{\pm}} = m_{\tilde{\chi}_2^0}$. The decay modes of $\tilde{\chi}_1^{\pm}$ and $\tilde{\chi}_2^0$ involving multilepton final states provide the best discrimination against the large multijet background. If the decays of $\tilde{\chi}_1^{\pm}$ and $\tilde{\chi}_2^0$ are predominantly mediated by light sleptons ($\tilde{e}$ and $\tilde{\mu}$), then ATLAS and CMS ruled out $m_{\tilde{\chi}_1^{\pm}} \approx m_{\tilde{\chi}_2^0}$, which are below 1100–1400 GeV for massless LSPs [366–368], but no limits can be set for $m_{\tilde{\chi}_1^0} \geqslant 1$ TeV. When the decays of $\tilde{\chi}_1^{\pm}$ and $\tilde{\chi}_2^0$ lead to tau leptons in the final state, the bound on $m_{\tilde{\chi}_1^{\pm}} \approx m_{\tilde{\chi}_2^0}$ reduces to 760–1000 GeV for $m_{\tilde{\chi}_1^0} \leqslant 400$ GeV [366, 369]. If all sparticles and additional Higgs bosons are heavy, it is assumed that $\tilde{\chi}_1^{\pm} \to W^{\pm}\tilde{\chi}_1^0$, whereas $\tilde{\chi}_2^0$ decays either via $\tilde{\chi}_2^0 \to Z\tilde{\chi}_1^0$ or via $\tilde{\chi}_2^0 \to h_1\tilde{\chi}_1^0$. In this case, ATLAS and CMS limits on the lightest chargino mass reach 900–1060 GeV for massless LSPs [366–368, 370–373]. These limits vanish for LSP masses above 400 GeV.

Multilepton analyses have also been used to set bounds on the $\tilde{\chi}_2^0\tilde{\chi}_3^0$ production for $m_{\tilde{\chi}_2^0} = m_{\tilde{\chi}_3^0} \geqslant m_{\tilde{\chi}_1^0}$. In the limit when the neutralino $\tilde{\chi}_2^0$ and $\tilde{\chi}_3^0$ decay through light sleptons, ATLAS sets a lower limit on the masses of these neutralino states, which is about 680 GeV for $m_{\tilde{\chi}_1^0} \leqslant 400$ GeV [374].

When the mass splitting between $\tilde{\chi}_1^{\pm}$ and $\tilde{\chi}_1^0$ is small, the chargino decay products are very soft and may escape detection. Therefore, the results of the search for charginos and neutralinos in such a compressed mass spectrum depend on $\Delta m = m_{\tilde{\chi}_1^{\pm}} - m_{\tilde{\chi}_1^0}$. ATLAS excluded chargino states with masses below 190–240 GeV for $\Delta m = 10$ GeV [375], while CMS ruled out charginos with masses below 112 GeV for $\Delta m = 1$ GeV [376]. In scenarios with compressed mass spectra, charginos may be long-lived. If their lifetime is longer than the time needed to pass through the detector, these states appear as charged stable massive particles. LHC experiments exclude such charginos with masses below 1090 GeV [377].

If the squark masses are much higher then the TeV scale, gluinos may hadronize to long-lived strongly interacting particles known as R-hadrons. ATLAS and CMS exclude such semi-stable gluinos with masses below 2 TeV [377, 378]. Top squarks can also be long-lived and hadronize to R-hadrons. This happens, for example, in the scenario where the lightest top squark is the next-to-lightest SUSY particle (NLSP) and has a mass which is very close to the mass of the LSP. ATLAS sets a lower limit of 1340 GeV on such top squarks [377].

Pair production of sleptons at the LHC is not only strongly suppressed with respect to pair production of squarks, but the corresponding cross section is also two orders of magnitude smaller then the one of pair production of charginos and neutralinos. LHC experiments searched for pair production of selectrons and smuons, assuming that each slepton decays into a lepton and the lightest neutralino $\tilde{\chi}_1^0$. ATLAS and CMS exclude such sleptons with masses below 700 GeV for $m_{\tilde{\chi}_1^0} \leqslant 400$ GeV [367, 379]. ATLAS and CMS also set a somewhat weaker lower limit on the mass of the superpartner of τ-lepton, which is around 390 GeV for the massless LSP, but no limit can be set for $m_{\tilde{\chi}_1^0} \geqslant 150$ GeV [380, 381]. When the masses of selectrons and smuons are just 5–10 GeV larger than $m_{\tilde{\chi}_1^0}$, ATLAS rules out such sleptons if their masses are lower than 230–250 GeV [375]. Sleptons may also appear to be stable charged massive particles if they have masses which are very close to that of the LSP. LHC experiments exclude such stable superpartners of the τ-lepton with masses below 430 GeV [377].

The LHC experiments have also searched for additional Higgs bosons predicted by SUSY models. Within the MSSM, the SM-like Higgs particle with a mass of around 125 GeV can be obtained only when $\tan\beta \gg 1$. In this case, the most stringent lower bound on the masses of additional Higgs states comes from searches for heavy neutral Higgs bosons decaying into $\tau^+\tau^-$ [382]. The corresponding experimental limit grows rapidly with increasing $\tan\beta$. For $\tan\beta \simeq 8$, ATLAS rules out $m_A \simeq m_{h_2} \simeq M_{H^{\pm}} \lesssim 1$ TeV, whereas, for $\tan\beta \simeq 21$, ATLAS excludes additional heavy Higgs states with masses $m_A \simeq m_{h_2} \simeq M_{H^{\pm}}$ below 1.5 TeV [382]. The lower experimental bound on the masses of extra Higgs particles mentioned here becomes substantially weaker when $\tan\beta \lesssim 6$. Nevertheless, it is quite difficult to find scenarios with a 125-GeV Higgs scalar for such values of $\tan\beta$ in the MSSM.

In the NMSSM, scenarios with an SM-like Higgs boson mass near 125 GeV can be found even for moderate values of $\tan\beta$, i.e., $2 \leqslant \tan\beta \leqslant 6$, if $|\lambda|$ is bigger than 0.55–0.6 at low energies. When $|\lambda| \gtrsim 0.6$, the validity of perturbation theory up to the scale M_X requires the low energy values of $|\kappa|$ to be relatively small, so that $|\kappa|^2 \ll |\lambda|^2$. As discussed in Section 5.2, in this part of the NMSSM parameter space, the heaviest *CP*-odd, heaviest *CP*-even, and charged Higgs states (A_2, h_3, and $H^{\pm}$) are mostly formed by the components of the Higgs doublets. They are almost degenerate, i.e., $m_{A_2} \simeq m_{h_3} \simeq M_{H^{\pm}} \simeq m_A$. Two other Higgs scalars and one pseudoscalar tend to be substantially lighter. One of these

Higgs scalars has to be a 125-GeV SM-like Higgs boson h. Another *CP*-even and the lightest *CP*-odd Higgs states (H_S and A_S) are singlet dominated. This structure of the NMSSM Higgs spectrum leads to a rich phenomenology associated with the decays of the heaviest *CP*-even and *CP*-odd Higgs bosons (see for example [383]) such as

$$h_3 \to hh\,, \quad h_3 \to hH_S\,, \quad h_3 \to H_SH_S\,, \quad A_2 \to A_Sh\,,$$
$$A_2 \to A_SH_S\,, \quad h_3 \to A_SZ\,, \quad A_2 \to Zh\,, \quad A_2 \to ZH_S\,.$$

LHC searches for heavy resonances decaying into Zh [384], ZZ [385], and hh [386] constrain the NMSSM parameter space if $2 \leqslant \tan\beta \leqslant 4$. For $\tan\beta \geqslant 4$, the most stringent experimental limit on m_A is again due to searches for heavy neutral Higgs states decaying into $\tau^+\tau^-$ [382]. All these constraints indicate that it is rather problematic to find phenomenologically viable scenarios with $m_A \lesssim 400$ GeV and moderate values of $\tan\beta$ $(2 \leqslant \tan\beta \leqslant 6)$. Moreover, from the search for the heavy Higgs boson h_3 decaying into hH_S in the $\tau\bar{\tau}b\bar{b}$ final state, it follows that a considerable part of the NMSSM parameter space is ruled out if m_A changes within the interval from 400 to 600 GeV [387].

In the case of the E_6SSM, one can obtain the 125-GeV Higgs boson for $\tan\beta \gtrsim 1.15$. When $\tan\beta$ varies from 1.15 to 1.8, the most stringent experimental limit on the masses of extra heavy Higgs states, which are composed of the components of Higgs doublets, comes from the search for the charged Higgs bosons decaying into a top quark and a bottom quark [388]. For such low values of $\tan\beta$, ATLAS excludes $M_{H^\pm}$ below 600–750 GeV [388]. On the other hand, because in this part of the E_6SSM parameter space $|\lambda|$ has to be larger than g_1' at low energies, all Higgs particles except the lightest Higgs boson lie beyond the multi-TeV range and therefore cannot be detected in the LHC experiments [198].

The search for decays of Z' bosons, which are associated with the linear superposition of $U(1)_\chi$ and $U(1)_\psi$ (3) into e^+e^- and $\mu^+\mu^-$ by the LHC experiments, sets lower limits on the masses of such states. Depending on θ_{E_6} these bounds vary from 4.5 TeV to 4.8 TeV [310, 311]. The LHC experiments have also been searching for pair production of scalar leptoquarks, which arise within E_6 inspired $U(1)$ extensions of the MSSM. Scalar leptoquarks that couple to the first (second, third) generation of SM fermions are referred as first- (second-, third-) generation leptoquarks. Since these states belong to the color–triplet representation of $SU(3)_C$, their pair production cross section at the LHC can be determined solely as a function of the mass of the scalar leptoquark. Then, the results of the corresponding analysis are determined by the branching fraction β_{LQ} of leptoquark decays into a final state that contains a charged lepton. When β_{LQ} changes from 0.5 to 1, the lower bound on the mass of the first-generation (second-generation) leptoquark increases from 1.4 TeV to 1.8 TeV (1.7 TeV) [389]. Experimental limits on the mass of the third-generation leptoquark are somewhat weaker. For $\beta_{LQ} = 0$ and $\beta_{LQ} = 1$, ATLAS and CMS rule out such states with masses below 1.2 TeV and 1.43 TeV, respectively [361, 390].

In the E_6SSM, all exotic states except the three lightest exotic fermions can be very heavy. Using the method proposed in [391 – 394], it was shown that the masses of fermions, which are predominantly linear superpositions of the fermion components of SM singlet superfields S_i, do not exceed 60–65 GeV [395 – 398]. The simplest phenomenologically viable scenario implies that the two lightest exotic fermions are substantially lighter than 1 eV. In this scenario, these lightest exotic particles form hot dark matter in the Universe but make only a very minor contribution to the dark matter density. At the same time, one exotic fermion $\tilde{H}_2^0$ can have a mass of the order of a few GeV and gives rise to nonstandard Higgs decays. In this case, the lightest ordinary neutralino may account for all or some of the observed cold dark matter density.

The LHC lower bounds on the masses of leptoquarks mentioned above are not directly applicable in the case of the E_6SSM. Since Z_2^E symmetry is conserved, every interaction vertex contains an even number of exotic states. As a consequence, each exotic particle must eventually decay into a final state that contains at least one lightest exotic fermion, which results in the missing energy and transverse momentum in the final state. The Z_2^E symmetry conservation also implies that in collider experiments exotic particles can only be created in pairs.

In this context, let us consider the production and sequential decays of the lightest exotic quarks at the LHC first. Because D and $\overline{D}$ states are odd under the Z_2^E symmetry, they can only be pair produced via strong interactions. The lifetime and decay modes of the lightest exotic quarks are determined by the operators $g_{ij}^D(Q_iL_4)\overline{D}_j$ and $h_{i\alpha}^E e_i^c(H_\alpha^d L_4)$ in the E_6SSM superpotential (27). These operators ensure that the lightest exotic quarks D_1 decay into

$$D_1 \to u_i(d_i) + \ell_j(\nu_j) + E_T^{\text{miss}} + X\,,$$

where ℓ_j (ν_j) is a charged lepton (neutrino). Here, X may contain extra charged leptons and/or jets that can originate from the decays of intermediate states. Since the lightest exotic quarks are pair produced, these states may lead to some enhancement of the cross sections of $pp \to jj\ell^+\ell^- + E_T^{\text{miss}} + X$ and $pp \to jj + E_T^{\text{miss}} + X$ if they are relatively light.

In general, exotic squarks are expected to be substantially heavier than exotic quarks, because their masses are determined by the soft SUSY breaking terms. Nevertheless, the lightest scalar leptoquark associated with the heavy exotic quark may be relatively light. Indeed, the large mass of the heavy exotic quark gives rise to large mixing in the exotic squark sector of the E_6SSM that may result in large mass splitting between the appropriate mass eigenstates. As a consequence, the lightest exotic squark $\tilde{D}_1$ can be even lighter than the lightest exotic quark. If this is the case, then the decays of the lightest scalar leptoquark are induced by the same operators which give rise to decays of the lightest exotic quarks in the limit when all exotic squarks are heavy. Therefore, the decay patterns of the lightest exotic color states are rather similar in both cases. Due to the Z_2^E symmetry conservation, E_T^{miss} should always contain a contribution associated with the lightest exotic fermion. However, since the lightest exotic squark is an *R*-parity even state, whereas the lightest exotic state is an *R*-parity odd particle, the final state in the decay of $\tilde{D}_1$ should also involve the lightest ordinary neutralino to ensure that *R*-parity is conserved.

If all states which are odd under the Z_2^E symmetry couple to the third generation fermions and sfermions mainly, then the presence of the relatively light D_1 or $\tilde{D}_1$ should give rise to an enhancement of the cross sections of $pp \to t\bar{t}\tau^+\tau^- + E_T^{\text{miss}} + X$ and $pp \to b\bar{b} + E_T^{\text{miss}} + X$. ATLAS and CMS have not set any limits on the masses of such states. Nevertheless, the decays of the relatively light superpartner of the b-quark $\tilde{b}_1$ would also lead to some enhancement of the cross section of $pp \to b\bar{b} + E_T^{miss} + X$. Therefore, one can expect that the experimental bounds on the masses of $\tilde{D}_1$ and $\tilde{b}_1$ should be approximately the same if $\tilde{D}_1$ decays predominantly into $b + \nu + E_T^{miss}$. In other words, $\tilde{D}_1$ tends to be heavier than 1.2–1.3 TeV.

Assuming that in the E_6SSM $\tilde{f}_{3\alpha} = f_{3\alpha} = 0$, let us consider the decays of the lightest Higgs boson $h_1 \to \tilde{H}_2^0\tilde{H}_2^0$. In this limit, the part of the Lagrangian that describes the interactions of two lightest exotic fermions ($\tilde{H}_1^0$ and $\tilde{H}_2^0$) with the Z boson and the SM-like Higgs particle can be presented in the following form:

$$\mathcal{L}_{Zh} = \sum_{\alpha,\beta} \frac{M_Z}{2v} Z_\mu \big(\tilde{H}_\alpha^{0T}\gamma_\mu\gamma_5\tilde{H}_\beta^0\big) R_{Z\alpha\beta} + \sum_{\alpha,\beta} (-1)^{\theta_\alpha+\theta_\beta} X_{\alpha\beta}^{h_1} \big(\psi_\alpha^{0T}(-i\gamma_5)^{\theta_\alpha+\theta_\beta}\psi_\beta^0\big) h_1 \,, \tag{125}$$

where $\alpha, \beta = 1, 2$. In Eqn (125), $\psi_\alpha^0 = (-i\gamma_5)^{\theta_\alpha}\tilde{H}_\alpha^0$ is the set of inert neutralino eigenstates with positive masses $\mu_{\tilde{H}_\alpha^0}$, while $\theta_\alpha = 0(1)$ if the eigenvalue of the mass matrix corresponding to $\tilde{H}_\alpha^0$ is positive (negative). Although $\tilde{H}_1^0$ and $\tilde{H}_2^0$ are substantially lighter than 100 GeV, their couplings to the Z boson and other SM particles are negligibly small [399]. Therefore, any possible signal which $\tilde{H}_1^0$ and $\tilde{H}_2^0$ could give rise to in previous and present collider experiments would be extremely suppressed, and such states could remain undetected.

The couplings of the SM-like Higgs boson h_1 to $\tilde{H}_1^0$ and $\tilde{H}_2^0$ are determined by the masses of the lightest exotic states [395]. Since $\tilde{H}_1^0$ is extremely light, it does not affect the Higgs phenomenology. The absolute value of the coupling of h_1 to another lightest exotic fermion $|X_{22}^h| \simeq |\mu_{\tilde{H}_2^0}|/v$ [395]. This coupling gives rise to decays of h_1 into $\tilde{H}_2^0$ pairs with the partial width given by

$$\Gamma(h_1 \to \tilde{H}_2^0\tilde{H}_2^0) = \frac{|X_{22}^h|^2 m_{h_1}}{4\pi}\left(1 - 4\,\frac{|\mu_{\tilde{H}_2^0}|^2}{m_{h_1}^2}\right)^{3/2}. \tag{126}$$

The partial decay width (126) depends rather strongly on $|\mu_{\tilde{H}_2^0}|$. To avoid the suppression of the branching ratios for the lightest Higgs decays into SM particles, we restrict our consideration here to the GeV-scale masses of $\tilde{H}_2^0$.

The results of the numerical analysis are presented in Table 5. In order to get the lightest Higgs boson with mass $m_{h_1} \simeq 125$ GeV, the E_6SSM parameters are chosen so that $m_Q \simeq m_U \simeq M_S \simeq 4$ TeV, $X_t \simeq -\sqrt{6}M_S$, $\lambda(M_S) \simeq 0.6$, $\tan\beta \simeq 1.5$, and $s \simeq 12$ TeV ($M_{Z'} \simeq 4500$ GeV). In all benchmark scenarios presented in Table 5, the structure of the Higgs spectrum is very hierarchical, and the partial widths of the decays of h_1 into SM particles are basically the same as in the SM, in which the Higgs boson with a mass of 125 GeV decays predominantly into $b\bar{b}$. The corresponding branching ratio is about 60%. The branching ratios associated with the Higgs decays into $\gamma\gamma$, ZZ, and WW are about 0.2%, 2%, and 20%, respectively [300]. The total decay width of this Higgs boson is about 4 MeV.

The benchmark scenarios A, B, C, and D presented in Table 5 demonstrate that the branching ratio of the exotic decays of h_1 changes from 0.2% to 20% when $\mu_{\tilde{H}_2^0}$ varies from 0.3 GeV to 2.7 GeV [399–402]. For smaller (larger) values of $\mu_{\tilde{H}_2^0}$, the branching ratio of these decays is even smaller (larger). On the other hand, the couplings of $\tilde{H}_1^0$ and $\tilde{H}_2^0$ to the Z boson are so small that these exotic fermions could not be observed before. In particular, their contribution to the Z-boson width tend to be negligibly small. After being produced, $\tilde{H}_2^0$ sequentially decay into $\tilde{H}_1^0$ and a fermion–antifermion pair via virtual Z. Nevertheless, since $|R_{Z12}|$ is quite small, in the scenarios A, C, and D, $\tilde{H}_2^0$ tends to live longer than 10^{-8} s and typically decays outside the detectors. As a consequence, in these cases, the decay channel $h_1 \to \tilde{H}_2^0\tilde{H}_2^0$ gives rise to an invisible branching ratio of the SM-like Higgs boson [399]. In the case of benchmark scenario B, $|R_{Z12}|$ is larger so that $\tau_{\tilde{H}_2^0} \sim 10^{-11}$ s and some of the decay products of $\tilde{H}_2^0$ might be observed at the LHC.

Table 5. Masses and couplings of the lightest exotic fermions ($\tilde{H}_1^0$ and $\tilde{H}_2^0$) as well as the branching ratios of the lightest Higgs boson h_1 associated with scenarios A, B, C, and D.

	A	B	C	D
λ_{22}	−0.03	−0.012	−0.06	0
λ_{21}	0	0	0	0.02
λ_{12}	0	0	0	0.02
λ_{11}	0.03	0.012	0.06	0
f_{22}	−0.1	−0.1	−0.1	0.6
f_{21}	−0.1	−0.1	−0.1	0.00245
f_{12}	0.00001	0.00001	0.00001	0.00245
f_{11}	0.1	0.1	0.1	0.00001
$\tilde{f}_{22}$	0.1	0.1	0.1	0.6
$\tilde{f}_{21}$	0.1	0.1	0.1	0.002
$\tilde{f}_{12}$	0.000011	0.000011	0.000011	0.002
$\tilde{f}_{11}$	0.1	0.1	0.1	0.00001
$\lvert\mu_{\tilde{H}_1^0}\rvert$, GeV	2.7×10^{-11}	6.5×10^{-11}	1.4×10^{-11}	0.31×10^{-9}
$\lvert\mu_{\tilde{H}_2^0}\rvert$, GeV	1.09	2.67	0.55	0.319
$\lvert R_{Z11}\rvert$	0.0036	0.0212	0.00090	1.5×10^{-7}
$\lvert R_{Z12}\rvert$	0.0046	0.0271	0.00116	1.7×10^{-4}
$\lvert R_{Z22}\rvert$	0.0018	0.0103	0.00045	0.106
$\mathrm{Br}(h_1 \to \tilde{H}_2^0\tilde{H}_2^0)$	4.7%	21.9%	1.23%	0.22%
$\mathrm{Br}(h_1 \to b\bar{b})$	56.6%	46.4%	58.7%	59.3%

Because R_{Z12} is relatively small, $\tilde{H}_2^0$ may decay during or after Big Bang Nucleosynthesis (BBN), destroying the agreement between the predicted and observed light element abundances. To preserve the success of the BBN, $\tilde{H}_2^0$ should decay before BBN, i.e., its lifetime $\tau_{\tilde{H}_2^0}$ should not be longer than 1 s. This requirement constrains $|R_{Z12}|$. Indeed, for $\mu_{\tilde{H}_2^0} \simeq 1$ GeV, the absolute value of the coupling R_{Z12} has to be larger than 1×10^{-6} [403]. The constraint on $|R_{Z12}|$ becomes more stringent with decreasing $\mu_{\tilde{H}_2^0}$ because $\tau_{\tilde{H}_2^0} \sim 1/(|R_{Z12}|^2\mu_{\tilde{H}_2^0}^5)$. The results of our analysis indicate that it is somewhat problematic to ensure that $\tau_{\tilde{H}_2^0} \lesssim 1$ s if $\mu_{\tilde{H}_2^0} \lesssim 100$ MeV [399, 402].

ATLAS and CMS set an upper limit on the branching ratio of the invisible Higgs decay of about 10–20% [404]. It is expected that High-Luminosity (HL) LHC as well as future e^+e^- colliders (ILC, CLIC, etc.) will allow measuring the Higgs mass and its branching ratios much more precisely. HL LHC should also be beneficial in the search for the production of the chargino, the neutralino, and long-lived sparticles.

8. Conclusions

Despite the fact that no sparticle has been discovered at the LHC so far, active investigations of SUSY extensions of the SM continue. The muon $g-2$ from the Fermi National Accelerator Laboratory (Fermilab) measurement [405] combined with the Brookhaven National Laboratory (BNL) result [406] has a value which is 4.2σ above the SM prediction [407]. Just during 2021, more than twenty articles were released in which the corresponding deviation was discussed in the context of the MSSM and its extensions [408–430]. In 2022, there have been already several studies on SUSY contributions to the W-boson mass [431–436] inspired by the CDF II W-mass measurement, which shows a 7σ deviation from the SM prediction [437]. Within the SUSY extensions of the SM, the deviations mentioned above can be explained if some sparticles have masses below 1 TeV. However, the muon $g-2$ and W-boson mass measurements may not be a real hint of new physics. For instance, if the lattice simulation result of the hadronic contribution to muon $g-2$ is taken, then the 4.2σ deviation can be reduced to 1.5σ [438]. Therefore, in this review paper, we focus on more reliable measurements of the cold dark matter density and the SM-like Higgs boson mass.

One of the main motivations to consider models with softly broken SUSY is associated with the possible unification of forces and incorporation of gravitational interactions into this unification scheme. Indeed, supersymmetry is a necessary ingredient in GUTs. The breakdown of E_6 (or E_8) gauge symmetry at the GUT scale M_X may lead to either the MSSM/NMSSM or $U(1)_N$ extension of the MSSM (E_6SSM) at low energies. In the MSSM and NMSSM, an approximate gauge coupling unification takes place around the scale $M_X \simeq 2 \times 10^{16}$ GeV. Within the E_6SSM, the exact unification of the gauge couplings near $M_X \simeq 3 \times 10^{16}$ GeV can be attained for any value of $\alpha_3(M_Z)$ which is in agreement with current data.

In GUTs, an enormous fine tuning is generally required to prevent the EW scale from becoming of the same order as M_X. This so-called hierarchy problem can be significantly alleviated if the low-energy limit of such high scale theories is described by extensions of the SM with softly broken SUSY. However, since superpartners of the SM particles have not yet been observed, the sparticle mass scale lies well above the TeV scale. As a consequence, a substantial tuning, $\sim 10^{-3}-10^{-2}$, is needed to stabilize the EW scale in this case. At the same time, a much larger degree of tuning is required to keep the total vacuum energy density around the observed value of the cosmological constant. It is not clear if these two problems can be considered separately. In string theory, there can be a small subset of vacua in which the sparticle mass scale is below 1 TeV. However, a much larger number of such vacua is needed to ensure the existence of the vacuum with the cosmological constant as small as observed. Nevertheless, the total number of vacua in string theory is large enough to allow for the ground state with the measured value of the cosmological constant and the 125-GeV Higgs boson. Although most sparticles tend to have masses beyond LHC search limits in this case [62, 63], the soft SUSY breaking parameters can still be consistent with generating the EW scale. Thus, the solution to the problems mentioned above may not involve natural cancellations but follow from the anthropic principle [50].

At tree-level, the lightest Higgs boson mass m_{h_1} in the MSSM does not exceed the mass of the Z-boson M_Z. The inclusion of one-loop and two-loop corrections permits us to increase the upper bound on m_{h_1} to 130–135 GeV. The theoretical restriction on m_{h_1} is saturated when the sparticle mass scale M_S is much bigger than M_Z and $\tan\beta \gg 1$. In order to reproduce the observed value of the SM-like Higgs mass in the MSSM, the contribution of loop corrections to $m_{h_1}^2$ has to be nearly as large as M_Z^2. Such a large loop contribution can be obtained if M_S is considerably larger than 1 TeV. As was noted above, the emergence of such a mass gap between M_S and m_{h_1} gives rise to fine-tuning which is of the order of $10^{-3}-10^{-2}$. The fine-tuning of the MSSM can be partially ameliorated within the NMSSM in which the upper bound on m_{h_1} attains its maximal value for $\tan\beta \sim 1$. The tree-level theoretical restriction on the SM-like Higgs boson mass in the NMSSM can be 10 GeV larger than in the MSSM. Therefore, the mass gap between M_S and m_{h_1} in the NMSSM may be somewhat smaller than the one in the MSSM. In the NMSSM, one or two Higgs states can be lighter than the SM-like Higgs boson, which may lead to some interesting phenomenological implications.

Within the E_6SSM, the tree-level mass of the lightest Higgs scalar can be larger than 115 GeV if $\tan\beta \simeq 1.2-3.4$. Because of this, one can obtain the SM-like Higgs state with a mass of around 125 GeV even when the contribution of loop corrections to $m_{h_1}^2$ is much smaller than M_Z^2. However, in the corresponding part of the E_6SSM parameter space, the stabilization of the EW scale requires a tuning at least of the order of 10^{-4}, which is higher than in the MSSM and NMSSM. The lightest exotic fermions may give rise to nonstandard decays of the lightest Higgs boson in the E_6SSM. The branching ratio of such decays can be as large as 10–20%.

The measurements of the SM-like Higgs boson mass and the cold dark matter density set stringent limits on the parameter space of the constrained SUSY models. In our analysis, only scenarios with the relic dark matter density $\Omega_{CDM}h^2 \leqslant 0.120$ were taken into consideration. The phenomenologically acceptable density of dark matter can be obtained in the MSSM if the mass of the lightest neutralino $m_{\chi_1^0}$ is nearly the same as the mass of one of the sfermions or if $2m_{\chi_1^0}$ is close to the mass of heavy Higgs bosons m_A. Nevertheless, such scenarios require some additional tuning of the initial parameters to engineer the desired coincidence of masses. Therefore, we restrict our consideration to the part of the MSSM and E_6SSM parameter space where the lightest neutralino has a large higgsino component. In this case, the appropriate dark matter density can be obtained if $m_{\chi_1^0} \lesssim 1-1.1$ TeV. Such phenomenologically viable scenarios with $\Omega_{CDM}h^2 \leqslant 0.120$ and $m_{h_1} \simeq 125$ GeV imply that all scalars are heavier than 5–6 TeV [327, 347]. The direct detection experiments XENON1T [343], PandaX-4T [344], and LZ [345] set lower limits on $M_{1/2}$ in this case. As a consequence, in the allowed part of the parameter space, the lightest neutralino is basically a higgsino, whereas a gluino is heavier than 5 TeV if $m_{\chi_1^0} \gtrsim 400$ GeV. The constraints mentioned above are considerably more stringent than the limits on the masses of sparticles set by the LHC experiments.

The relatively light sparticle spectrum in the constrained MSSM can be obtained when $m_{\chi_1^0}$ is close to the mass of the lightest stop. Since m_0 vary from 2 TeV to 4.5 TeV, almost all scalars are heavier than 2–3 TeV in this case [327]. In the corresponding part of the parameter space, the dark matter density formed by the lightest neutralino, which is predominantly a bino, tends to be lower than its observed value, whereas the lightest neutralino–nucleon scattering cross section may be extremely small. The sparticle spectrum in such scenarios includes the lightest stop with a mass below 1 TeV that can be discovered at HL LHC in the near future, while HE–LHC [439] or FCC [440, 441] may open a new era in elementary particle physics.

Acknowledgments
The author acknowledges fruitful discussions with P Athron, E E Boos, M N Dubinin, S V Demidov, S A Duplij, A V Gladyshev, D S Gorbunov, D I Kazakov, S F King, M V Libanov, D J Miller, S Moretti, M Mühlleitner, V A Rubakov, M Sher, X Tata, S V Troitsky, and P V Zinin.

The reported study was funded by the Russian Foundation for Basic Research, project number 20-12-50111 .

References

1. Aad G et al. (ATLAS Collab.) *Phys. Lett. B* **716** 1 (2012); arXiv:1207.7214
2. Chatrchyan S et al. (CMS Collab.) *Phys. Lett. B* **716** 30 (2012); arXiv:1207.7235
3. de Florian D et al. (LHC Higgs Cross Section Working Group) (Eds), Handbook of LHC Higgs Cross Sections: 4. Deciphering the Nature of the Higgs Sector (CERN Yellow Reports: Monographs, Vol. 2, CERN-2017-002-M) (Geneva: CERN, 2017) https://doi.org/10.23731/CYRM-2017-002; arXiv:1610.07922
4. Coleman S R, Mandula J *Phys. Rev.* **159** 1251 (1967)
5. Georgi H, Glashow S L *Phys. Rev. Lett.* **32** 438 (1974)
6. Minkowski P *Phys. Lett. B* **67** 421 (1977)
7. Mohapatra R N, Senjanović G *Phys. Rev. Lett.* **44** 912 (1980)
8. Hewett J L, Rizzo T G *Phys. Rep.* **183** 193 (1989)
9. Langacker P *Rev. Mod. Phys.* **81** 1199 (2009); arXiv:0801.1345
10. Nilles H P *Phys. Rep.* **110** 1 (1984)
11. Haber H E, Kane G L *Phys. Rep.* **117** 75 (1985)
12. Vysotskii M I *Sov. Phys. Usp.* **28** 667 (1985); *Usp. Fiz. Nauk* **146** 591 (1985)
13. Lahanas A B, Nanopoulos D V *Phys. Rep.* **145** 1 (1987)
14. Ade P A R et al. (Planck Collab.) *Astron. Astrophys.* **594** A13 (2016); arXiv:1502.01589
15. Li T *Phys. Lett. B* **520** 377 (2001); hep-th/0107136
16. Kawamura Y *Prog. Theor. Phys.* **105** 691 (2001); hep-ph/0012352
17. Susskind L *Phys. Rev. D* **20** 2619 (1979)
18. 't Hooft G, in *Recent Developments in Gauge Theories* (NATO Science Ser. B, Vol. 59, Eds G 't Hooft) (New York: Springer, 1980) p. 135, https://doi.org/10.1007/978-1-4684-7571-5_9
19. Veltman M *Acta Phys. Polon. B* **12** 437 (1981)
20. Gol'fand Yu A, Likhtman E P *JETP Lett.* **13** 323 (1971); *Pis'ma Zh. Eksp. Teor. Fiz.* **13** 452 (1971)
21. Likhtman E P *Phys. Usp.* **44** 973 (2001); *Usp. Fiz. Nauk* **171** 1025 (2001)
22. Volkov D V, Akulov V P *JETP Lett.* **16** 438 (1972); *Pis'ma Zh. Eksp. Teor. Fiz.* **16** 621 (1972)
23. Wess J, Zumino B *Phys. Lett. B* **49** 52 (1974)
24. Nath P, Arnowitt R *Phys. Lett. B* **56** 177 (1975)
25. Freedman D Z, van Nieuwenhuizen P, Ferrara S *Phys. Rev. D* **13** 3214 (1976)
26. Deser S, Zumino B *Phys. Lett. B* **62** 335 (1976)
27. Green M B, Schwarz J H, Witten E *Superstring Theory* (Cambridge: Cambridge Univ. Press, 1987)
28. del Aguila F et al. *Nucl. Phys. B* **272** 413 (1986)
29. Deser S, Zumino B *Phys. Rev. Lett.* **38** 1433 (1977)
30. Gremmer E et al. *Phys. Lett. B* **79** 231 (1978)
31. Gremmer E et al. *Nucl. Phys. B* **147** 105 (1979)
32. Barbieri R, Ferrara S, Savoy C A *Phys. Lett. B* **119** 343 (1982)
33. Nilles H P, Srednicki M, Wyler D *Phys. Lett. B* **120** 346 (1983)
34. Hall L, Lykken J, Weinberg S *Phys. Rev. D* **27** 2359 (1983)
35. Soni S K, Weldon H A *Phys. Lett. B* **126** 215 (1983)
36. Giudice G F, Rattazzi R *Phys. Rep.* **322** 419 (1999); hep-ph/9801271
37. Gorbunov D S, Dubovskii S L, Troitskii S V *Phys. Usp.* **42** 623 (1999); *Usp. Fiz. Nauk* **169** 705 (1999)
38. Gherghetta T, Pomarol A *Nucl. Phys. B* **586** 141 (2000); hep-ph/0003129
39. Gherghetta T, Pomarol A *Nucl. Phys. B* **602** 3 (2001); hep-ph/0012378
40. Witten E *Nucl. Phys. B* **188** 513 (1981)
41. Sakai N *Z. Phys. C* **11** 153 (1981)
42. Dimopoulos S, Georgi H *Nucl. Phys. B* **193** 150 (1981)
43. Kaul R K, Majumdar P *Nucl. Phys. B* **199** 36 (1982)
44. van Beekveld M, Caron S, Ruiz de Austri R *J. High Energy Phys.* **2020** (01) 147 (2020); arXiv:1906.10706
45. Baer H et al. *Eur. Phys. J. Spec. Top.* **229** 3085 (2020); arXiv:2002.03013
46. Nilles H P *Int. J. Mod. Phys. A* **05** 4199 (1990)
47. Bousso R, Polchinski J *J. High Energy Phys.* **2000** (06) 006 (2000); hep-th/0004134
48. Susskind L, hep-th/0302219
49. Bousso R, Polchinski J *Sci. Am.* **291** (3) 78 (2004) https://doi.org/10.1038/scientificamerican0904-78
50. Weinberg S *Phys. Rev. Lett.* **59** 2607 (1987)
51. Ashok S K, Douglas M R *J. High Energy Phys.* **2004** (01) 060 (2004); hep-th/0307049
52. Agrawal V et al. *Phys. Rev. Lett.* **80** 1822 (1998); hep-ph/9801253
53. Agrawal V et al. *Phys. Rev. D* **57** 5480 (1998); hep-ph/9707380
54. Hogan C J *Rev. Mod. Phys.* **72** 1149 (2000); astro-ph/9909295
55. Rees M J, in *Fred Hoyle's Universe. Proc. of a Conf. Celebrating Fred Hoyle's Extraordinary Contributions to Science 25–26 June 2002 Cardiff Univ., United Kingdom* (Eds C Wickramasinghe, G Burbidge, J Narlikar) (Dordrecht: Kluwer Acad. Publ., 2003) p. 95, https://doi.org/10.1007/978-94-017-1605-5_13; *Astrophys. Space Sci.* **285** 375 (2003); astro-ph/0401424
56. Douglas M R *J. High Energy Phys.* **2003** (05) 046 (2003); hep-th/0303194
57. Giryavets A, Kachru S, Tripathy P K *J. High Energy Phys.* **2004** (08) 002 (2004); hep-th/0404243
58. Conlon J P, Quevedo F *J. High Energy Phys.* **2004** (10) 039 (2004); hep-th/0409215
59. Denef F, Douglas M R *J. High Energy Phys.* **2004** (05) 072 (2004); hep-th/0404116
60. Douglas M R *C.R. Phys.* **5** 965 (2004); hep-th/0409207
61. Susskind L, in *From Fields to Strings: Circumnavigating Theoretical Physics. Ian Kogan Memorial Collection* (Eds M Shifman, A Vainshtein, J Wheater) (Singapore: World Scientific, 2005) p. 1745, https://doi.org/10.1142/9789812775344_0040; hep-th/0405189
62. Baer H et al. *J. High Energy Phys.* **2018** (03) 2 (2018); arXiv:1712.01399
63. Baer H, Barger V, Salam S *Phys. Rev. Res.* **1** 023001 (2019); arXiv:1906.07741
64. Arkani-Hamed N, Dimopoulos S *J. High Energy Phys.* **2005** (06) 073 (2005); hep-th/0405159
65. Giudice G F, Romanino A *Nucl. Phys. B* **699** 65 (2004); *Nucl. Phys. B* **706** 65 (2005) Erratum; hep-ph/0406088
66. Arkani-Hamed N et al. *Nucl. Phys. B* **709** 3 (2005); hep-ph/0409232
67. Pierce A *Phys. Rev. D* **70** 075006 (2004); hep-ph/0406144
68. Masiero A, Profumo S, Ullio P *Nucl. Phys. B* **712** 86 (2005); hep-ph/0412058
69. Antoniadis I, Dimopoulos S *Nucl. Phys. B* **715** 120 (2005); hep-th/0411032
70. Körs B, Nath P *Nucl. Phys. B* **711** 112 (2005); hep-th/0411201
71. Babu K S, Enkhbat Ts, Mukhopadhyaya B *Nucl. Phys. B* **720** 47 (2005); hep-ph/0501079
72. Demidov S V, Gorbunov D S *J. High Energy Phys.* **2007** (02) 055 (2007); hep-ph/0612368
73. Demidov S V, Gorbunov D S, Kirpichnikov D V *J. High Energy Phys.* **2016** (11) 148 (2016); *J. High Energy Phys.* **2017** (08) 080 (2017) Erratum; arXiv:1608.01985
74. Demidov S V, Gorbunov D S, Kirpichnikov D V *Phys. Lett. B* **779** 191 (2018); arXiv:1712.00087
75. Krippendorf S et al. *Phys. Lett. B* **712** 87 (2012); arXiv:1201.4857
76. Badziak M et al. *J. High Energy Phys.* **2013** (03) 94 (2013); arXiv:1212.0854
77. Nilles H P *Adv. High Energy Phys.* **2015** 412487 (2015)

78. Baer H et al. *J. High Energy Phys.* **2017** (06) 101 (2017); arXiv:1705.01578
79. Choi K et al. *J. High Energy Phys.* **2004** (11) 076 (2004); hep-th/0411066
80. Choi K et al. *Nucl. Phys. B* **718** 113 (2005); hep-th/0503216
81. Conlon J P, Quevedo F, Suruliz K *J. High Energy Phys.* **2005** (08) 007 (2005); hep-th/0505076
82. Pierce A, Thaler J *J. High Energy Phys.* **2006** (09) 017 (2006); hep-ph/0604192
83. Kaufman B L, Nelson B D, Gaillard M K *Phys. Rev. D* **88** 025003 (2013); arXiv:1303.6575
84. Choi K et al. *J. High Energy Phys.* **2011** (02) 47 (2011); arXiv:1011.0999
85. Aparicio L, Quevedo F, Valandro R *J. High Energy Phys.* **2016** (03) 36 (2016); arXiv:1511.08105
86. Acharya B S, Kane G, Kumar P *Int. J. Mod. Phys. A* **27** 1230012 (2012); arXiv:1204.2795
87. Kumar P, in *Perspectives on String Phenomenology* (Advanced Series on Directions in High Energy Physics, Vol. 22, Eds B Acharya, G L Kane, P Kumar) (Singapore: World Scientific, 2015) p. 277, https://doi.org/10.1142/9789814602686_0010
88. Wess J, Zumino B *Nucl. Phys. B* **78** 1 (1974)
89. Girardello L, Grisaru M T *Nucl. Phys. B* **194** 65 (1982)
90. Salam A, Strathdee J *Phys. Rev. D* **11** 1521 (1975)
91. Grisaru M T, Siegel W, Roček M *Nucl. Phys. B* **159** 429 (1979)
92. Fayet P *Phys. Lett. B* **84** 416 (1979)
93. Nilles H P, Srednicki M, Wyler D *Phys. Lett. B* **120** 346 (1983)
94. Frère J-M, Jones D R T, Raby S *Nucl. Phys. B* **222** 11 (1983)
95. Derendinger J-P, Savoy C A *Nucl. Phys. B* **237** 307 (1984)
96. Vysotskii M I, Ter-Martirosian K A *Sov. Phys. JETP* **63** 489 (1986); *Zh. Eksp. Teor. Fiz.* **90** 838 (1986)
97. Ellis J R et al. *Phys. Rev. D* **39** 844 (1989)
98. Drees M *Int. J. Mod. Phys. A* **04** 3635 (1989)
99. Durand L, Lopez J L *Phys. Lett. B* **217** 463 (1989)
100. Ellwanger U, Rausch de Traubenberg M, Savoy C A *Nucl. Phys. B* **492** 21 (1997)
101. Ellwanger U *Phys. Lett. B* **303** 271 (1993)
102. Pandita P *Z. Phys. C* **59** 575 (1993)
103. Elliott T, King S F, White P L *Phys. Rev. D* **49** 2435 (1994)
104. King S F, White P L *Phys. Rev. D* **52** 4183 (1995)
105. Franke F *Int. J. Mod. Phys. A* **12** 479 (1997)
106. Ellwanger U, Hugonie C, Teixeira A M *Phys. Rep.* **496** 1 (2010); arXiv:0910.1785
107. Ellwanger U *Eur. Phys. J. C* **71** 1782 (2011); arXiv:1108.0157
108. Maniatis M *Int. J. Mod. Phys. A* **25** 3505 (2010); arXiv:0906.0777
109. Peccei R D, Quinn H R *Phys. Rev. Lett.* **38** 1440 (1977)
110. Peccei R D, Quinn H R *Phys. Rev. D* **16** 1791 (1977)
111. Wilczek F *Phys. Rev. Lett.* **40** 279 (1978)
112. Dicus D A et al. *Phys. Rev. D* **18** 1829 (1978)
113. Grifols J A, Massó E *Phys. Lett. B* **173** 237 (1986)
114. Ellis J, Olive K A *Phys. Lett. B* **193** 525 (1987)
115. Raffelt G, Seckel D *Phys. Rev. Lett.* **60** 1793 (1988)
116. Grifols J A, Massó E, Peris S *Mod. Phys. Lett. A* **04** 311 (1989)
117. Raffelt G G *Phys. Rep.* **198** 1 (1990)
118. Raffelt G, Weiss A *Phys. Rev. D* **51** 1495 (1995); hep-ph/9410205
119. Zel'dovich Ya B, Kobzarev I Yu, Okun' L B *Sov. Phys. JETP* **40** 1 (1975); *Zh. Eksp. Teor. Fiz.* **67** 3 (1974)
120. Vilenkin A *Phys. Rep.* **121** 263 (1985)
121. Abel S A, Sarkar S, White P L *Nucl. Phys. B* **454** 663 (1995)
122. Panagiotakopoulos C, Tamvakis K *Phys. Lett. B* **446** 224 (1999); hep-ph/9809475
123. Panagiotakopoulos C, Tamvakis K *Phys. Lett. B* **469** 145 (1999); hep-ph/9908351
124. Dedes A et al. *Phys. Rev. D* **63** 055009 (2001); hep-ph/0009125
125. Panagiotakopoulos C, Pilaftsis A *Phys. Rev. D* **63** 055003 (2001); hep-ph/0008268
126. Menon A, Morrissey D E, Wagner C E M *Phys. Rev. D* **70** 035005 (2004); hep-ph/0404184
127. Balázs C et al. *J. High Energy Phys.* **2007** (06) 066 (2007); arXiv:0705.0431
128. Nevzorov R B, Ter-Martirosyan K A, Trusov M A *Phys. Atom. Nucl.* **65** 285 (2002); *Yad. Fiz.* **65** 311 (2002); hep-ph/0105178
129. Nevzorov R B, Trusov M A *Phys. Atom. Nucl.* **65** 335 (2002); *Yad. Fiz.* **65** 359 (2002); hep-ph/0301179
130. King S F, White P L *Phys. Rev. D* **53** 4049 (1996); hep-ph/9508346
131. Nevzorov R B, Trusov M A *J. Exp. Theor. Phys.* **91** 1079 (2000); *Zh. Eksp. Teor. Fiz.* **118** 1251 (2000); hep-ph/0106351
132. Ross G G, Schmidt-Hoberg K, Staub F *J. High Energy Phys.* **2012** (08) 74 (2012); arXiv:1205.1509
133. Ross G G, Schmidt-Hoberg K *Nucl. Phys. B* **862** 710 (2012); arXiv:1108.1284
134. Gunion J F et al. *The Higgs Hunter's Guide* (Boca Raton, FL: CRC Press, 2000); hep-ph/9302272, Erratum
135. Binétruy P et al. *Nucl. Phys. B* **273** 501 (1986)
136. Ellis J R et al. *Mod. Phys. Lett. A* **01** 57 (1986)
137. Ibánez L E, Mas J *Nucl. Phys. B* **286** 107 (1987)
138. Gunion J F, Roszkowski L, Haber H E *Phys. Lett. B* **189** 409 (1987)
139. Haber H E, Sher M *Phys. Rev. D* **35** 2206 (1987)
140. Ellis J R et al. *Nucl. Phys. B* **283** 93 (1987)
141. Drees M *Phys. Rev. D* **35** 2910 (1987)
142. Gunion J F, Roszkowski L, Haber H E *Phys. Lett. B* **189** 409 (1987)
143. Baer H et al. *Phys. Rev. D* **36** 1363 (1987)
144. Gunion J F, Roszkowski L, Haber H E *Phys. Rev. D* **38** 105 (1988)
145. Accomando E et al. *Phys. Rev. D* **83** 075012 (2011); arXiv:1010.6058
146. Kang J, Langacker P, Nelson B D *Phys. Rev. D* **77** 035003 (2008); arXiv:0708.2701
147. Langacker P, Wang J *Phys. Rev. D* **58** 115010 (1998)
148. Cvetič M, Langacker P *Phys. Rev. D* **54** 3570 (1996)
149. Cvetič M, Langacker P *Mod. Phys. Lett. A* **11** 1247 (1996)
150. Cvetič M et al. *Phys. Rev. D* **56** 2861 (1997); *Phys. Rev. D* **58** 119905 (1998) Erratum
151. Suematsu D, Yamagishi Y *Int. J. Mod. Phys. A* **10** 4521 (1995)
152. Keith E, Ma E *Phys. Rev. D* **56** 7155 (1997)
153. Daikoku Y, Suematsu D *Phys. Rev. D* **62** 095006 (2000)
154. Kang J H, Langacker P, Li T *Phys. Rev. D* **71** 015012 (2005)
155. Ma E *Phys. Lett. B* **380** 286 (1996)
156. Stech B, Tavartkiladze Z *Phys. Rev. D* **77** 076009 (2008); arXiv:0802.0894
157. King S F, Luo R, Miller D J, Nevzorov R *J. High Energy Phys.* **2008** (12) 042 (2008); arXiv:0806.0330
158. Hambye T et al. *Phys. Lett. B* **512** 373 (2001)
159. Ma E, Raidal M *J. Phys. G* **28** 95 (2002)
160. Kang J et al. *Phys. Rev. Lett.* **94** 061801 (2005)
161. Grifols J A, Méndez A, Solà J *Phys. Rev. Lett.* **57** 2348 (1986)
162. Morris D A *Phys. Rev. D* **37** 2012 (1988)
163. Suematsu D *Mod. Phys. Lett. A* **12** 1709 (1997)
164. Gutiérrez-Rodríguez A, Hernández-Ruíz M A, Pérez M A *Int. J. Mod. Phys. A* **22** 3493 (2007); hep-ph/0611235
165. Suematsu D *Phys. Lett. B* **416** 108 (1998)
166. Ham S W et al. *J. High Energy Phys.* **2008** (12) 017 (2008); arXiv:0810.4194
167. Suematsu D *Phys. Rev. D* **57** 1738 (1998)
168. Keith E, Ma E *Phys. Rev. D* **54** 3587 (1996)
169. Hesselbach S, Franke F, Fraas H *Eur. Phys. J. C* **23** 149 (2002)
170. Barger V, Langacker P, Lee H-S *Phys. Lett. B* **630** 85 (2005)
171. Choi S Y et al. *Nucl. Phys. B* **778** 85 (2007)
172. Barger V et al. *Phys. Rev. D* **75** 115002 (2007)
173. Gherghetta T, Kaeding T A, Kane G L *Phys. Rev. D* **57** 3178 (1998); hep-ph/9701343
174. Barger V, Langacker P, Shaughnessy G *New J. Phys.* **9** 333 (2007)
175. Barger V et al. *Phys. Rev. D* **73** 115010 (2006)
176. King S F, Moretti S, Nevzorov R *Phys. Rev. D* **73** 035009 (2006); hep-ph/0510419
177. King S F, Moretti S, Nevzorov R *Phys. Lett. B* **634** 278 (2006); hep-ph/0511256
178. King S F, Moretti S, Nevzorov R, in *High Energy Physics, ICHEP'06. Proc. of the 33rd Intern. Conf. on High Energy Physics, Moscow, Russia, July 26 – August 2, 2006* (Eds A Sissakian, G Kozlov, E Kolganova) (Singapore: World Scientific, 2007) p. 1125, https://doi.org/10.1142/9789812790873_0242; eConf. C060726 (2006); *AIP Conf. Proc.* **881** 138 (2007); hep-ph/0610002
179. King S F, Moretti S, Nevzorov R, in *Particle Physics at the Year of 250th Anniversary of Moscow University. Proc. of the 12th Lomonosov Conf. on Elementary Particle Physics, Moscow, Russia, 25–31 August 2005* (Ed. A I Studenikin) (Singapore: World Scientific,

2006) p. 371, https://doi.org/10.1142/9789812772657_0065; hep-ph/0601269
180. Athron P et al., in *Proc. of the 2011 Meeting of the Division of Particles and Fields of the American Physical Society, Providence, Rhode Island, USA, 9–13 August 2011* (Ed. T Speer); eConf C110809 (2011); arXiv:1109.6373
181. Nevzorov R *Phys. Rev. D* **87** 015029 (2013); arXiv:1205.5967
182. King S F, Nevzorov R *J. High Energy Phys.* **2016** (03) 139 (2016); arXiv:1601.07242
183. Nevzorov R *Symmetry* **14** 2090 (2022); arXiv:2209.00505
184. King S F, Moretti S, Nevzorov R *Phys. Lett. B* **650** 57 (2007); hep-ph/0701064
185. Athron P et al., in *Proc. of the 17th Intern. Conf. on Supersymmetry and the Unification of Fundamental Interactions* (*SUSY09*)*, Boston, USA, 2009* (Eds P Nath, G Alverson, B Nelson); *AIP Conf. Proc.* **1200** 466 (2010); arXiv:0909.4530
186. Howl R, King S F *J. High Energy Phys.* **2008** (01) 030 (2008); arXiv:0708.1451
187. Athron P et al. *Nucl. Phys. B Proc. Suppl.* **200–202** 120 (2010)
188. Athron P et al. *Phys. Lett. B* **681** 448 (2009); arXiv:0901.1192
189. Athron P et al. *Phys. Rev. D* **80** 035009 (2009); arXiv:0904.2169
190. Athron P et al. *Phys. Rev. D* **84** 055006 (2011); arXiv:1102.4363
191. Athron P et al. *Phys. Rev. D* **86** 095003 (2012); arXiv:1206.5028
192. Athron P et al., in *Proc. of the 34th Intern. Conf. in High Energy Physics* (*ICHEP08*)*, Philadelphia, USA, 2008*; eConf C080730; arXiv:0810.0617
193. Rich J, Lloyd Owen D, Spiro M *Phys. Rep.* **151** 239 (1987)
194. Smith P F *Contemp. Phys.* **29** 159 (1988)
195. Hemmick T K et al. *Phys. Rev. D* **41** 2074 (1990)
196. Wolfram S *Phys. Lett. B* **82** 65 (1979)
197. Dover C B, Gaisser T K, Steigman G *Phys. Rev. Lett.* **42** 1117 (1979)
198. King S F, Moretti S, Nevzorov R *Symmetry* **12** 557 (2020); arXiv:2002.02788
199. Athron P, Mühlleitner M, Nevzorov R, Williams A G *J. High Energy Phys.* **2015** (01) 153 (2015); arXiv:1410.6288
200. Athron P, Muhlleitner M, Nevzorov R, Williams A G, in *Particle Physics at the Year of Light. Proc. of the Seventeenth Lomonosov Conf. on Elementary Particle Physics, Moscow, Russia, 20–26 August 2015* (Ed. A I Studenikin) (Singapore: World Scientific, 2017) p. 487, https://doi.org/10.1142/9789813224568_0079; arXiv:1602.04453
201. Nevzorov R *Phys. Lett. B* **779** 223 (2018); arXiv:1710.11533
202. Nevzorov R *Int. J. Mod. Phys. A* **33** 1844007 (2018); arXiv:1805.08260
203. Giudice G F, Masiero A *Phys. Lett. B* **206** 480 (1988)
204. Casas J A, Muñoz C *Phys. Lett. B* **306** 288 (1993)
205. Hall L J, Nomura Y *Phys. Rev. D* **64** 055003 (2001); hep-ph/0103125
206. Kobakhidze A B *Phys. Lett. B* **514** 131 (2001); hep-ph/0102323
207. Nomura Y *Phys. Rev. D* **65** 085036 (2002); hep-ph/0108170
208. Hall L J, Nomura Y *Phys. Rev. D* **65** 125012 (2002); hep-ph/0111068
209. Dermíšek R, Mafi A *Phys. Rev. D* **65** 055002 (2002); hep-ph/0108139
210. Hebecker A, March-Russell J *Phys. Lett. B* **539** 119 (2002); hep-ph/0204037
211. Hall L J, Nomura Y *Phys. Rev. D* **66** 075004 (2002); hep-ph/0205067
212. Kim H D, Raby S *J. High Energy Phys.* **2003** (01) 056 (2003); hep-ph/0212348
213. Shafi Q, Tavartkiladze Z *Nucl. Phys. B* **665** 469 (2003); hep-ph/0303150
214. Dorsner I *Phys. Rev. D* **69** 056003 (2004); hep-ph/0310175
215. Buchmüller W et al. *J. High Energy Phys.* **2004** (09) 004 (2004); hep-ph/0407070
216. Ellis J R, Gaillard M K, Nanopoulos D V *Phys. Lett. B* **88** 320 (1979)
217. Jones D R T *Nucl. Phys. B* **87** 127 (1975)
218. Inoue K et al. *Prog. Theor. Phys.* **67** 1889 (1982); *Prog. Theor. Phys.* **68** 927 (1982)
219. Jones D R T, Mezincescu L *Phys. Lett. B* **136** 242 (1984)
220. West P *Phys. Lett. B* **137** 371 (1984)
221. Parkes A, West P *Phys. Lett. B* **138** 99 (1984)
222. Jones D R T, Mezincescu L *Phys. Lett. B* **138** 293 (1984)
223. Machacek M E, Vaughn M T *Nucl. Phys. B* **236** 221 (1984)
224. Martin S P, Vaughn M T *Phys. Rev. D* **50** 2282 (1994)
225. Chankowski P H et al. *Phys. Lett. B* **358** 264 (1995)
226. Antoniadis I, Kounnas C, Tamvakis K *Phys. Lett. B* **119** 377 (1982)
227. Antoniadis I, Kounnas C, Lacaze R *Nucl. Phys. B* **211** 216 (1983)
228. Carena M, Pokorski S, Wagner C E M *Nucl. Phys. B* **406** 59 (1993)
229. Hempfling R *Phys. Lett. B* **351** 206 (1995); hep-ph/9502201
230. Langacker P, Polonsky N *Phys. Rev. D* **52** 3081 (1995)
231. Langacker P, Polonsky N *Phys. Rev. D* **47** 4028 (1993)
232. Ross G G, Roberts R G *Nucl. Phys. B* **377** 571 (1992)
233. Barger V D, Berger M S, Ohmann P *Phys. Rev. D* **47** 1093 (1993)
234. Langacker P, Polonsky N *Phys. Rev. D* **49** 1454 (1994)
235. de Boer W, Sander C *Phys. Lett. B* **585** 276 (2004)
236. de Boer W et al. *Phys. Lett. B* **636** 13 (2006)
237. Bagger J, Matchev K, Pierce D *Phys. Lett. B* **348** 443 (1995)
238. Holdom B *Phys. Lett. B* **166** 196 (1986)
239. Babu K S, Kolda C, March-Russell J *Phys. Rev. D* **54** 4635 (1996)
240. Langacker P, Wang J *Phys. Rev. D* **58** 115010 (1998)
241. Rizzo T G *Phys. Rev. D* **59** 015020 (1999)
242. Suematsu D *Phys. Rev. D* **59** 055017 (1999)
243. Ellis J et al. *Mod. Phys. Lett. A* **01** 57 (1986)
244. Barbieri R, Giudice G F *Nucl. Phys. B* **306** 63 (1988)
245. Baer H et al. *Phys. Rev. Lett.* **109** 161802 (2012)
246. Ellis J, Ridolfi G, Zwirner F *Phys. Lett. B* **262** 477 (1991)
247. Gladyshev A V et al. *Nucl. Phys. B* **498** 3 (1997)
248. Carena M, Quirós M, Wagner C E M *Nucl. Phys. B* **461** 407 (1996)
249. Brignole A *Phys. Lett. B* **281** 284 (1992)
250. Dabelstein A *Z. Phys. C* **67** 495 (1995)
251. Drees M, Nojiri M M *Phys. Rev. D* **45** 2482 (1992)
252. Sasaki K, Carena M, Wagner C E M *Nucl. Phys. B* **381** 66 (1992)
253. Haber H E, Hempfling R *Phys. Rev. D* **48** 4280 (1993)
254. Carena M et al. *Phys. Lett. B* **355** 209 (1995)
255. Gladyshev A V, Kazakov D I *Mod. Phys. Lett. A* **10** 3129 (1995)
256. Chankowski P H, Pokorski S, Rosiek J *Phys. Lett. B* **274** 191 (1992)
257. Yamada A *Z. Phys. C* **61** 247 (1994)
258. Chankowski P H, Pokorski S, Rosiek J *Nucl. Phys. B* **423** 437 (1994)
259. Pierce D M et al. *Nucl. Phys. B* **491** 3 (1997)
260. Brignole A et al. *Phys. Lett. B* **271** 123 (1991)
261. Díaz M A, Haber H E *Phys. Rev. D* **45** 4246 (1992)
262. Brignole A *Phys. Lett. B* **277** 313 (1992)
263. Kovalenko P A, Nevzorov R B, Ter-Martirosian K A *Phys. Atom. Nucl.* **61** 812 (1998); *Yad. Fiz.* **61** 898 (1998)
264. Okada Y, Yamaguchi M, Yanagida T *Prog. Theor. Phys.* **85** (1) 1 (1991)
265. Ellis J, Ridolfi G, Zwirner F *Phys. Lett. B* **257** 83 (1991)
266. Barbieri R, Frigeni M *Phys. Lett. B* **258** 395 (1991)
267. Pierce D M, Papadopoulos A, Johnson S B *Phys. Rev. Lett.* **68** 3678 (1992)
268. Barbieri R, Frigeni M, Caravaglios F *Phys. Lett. B* **258** 167 (1991)
269. Okada Y, Yamaguchi M, Yanagida T *Phys. Lett. B* **262** 54 (1991)
270. Haber H E, Hempfling R, Hoang A H *Z. Phys. C* **75** 539 (1997)
271. Haber H E, Hempfling R *Phys. Rev. Lett.* **66** 1815 (1991)
272. Hempfling R, Hoang A H *Phys. Lett. B* **331** 99 (1994)
273. Zhang R-J *Phys. Lett. B* **447** 89 (1999)
274. Espinosa J R, Zhang R-J *J. High Energy Phys.* **2000** (03) 026 (2000)
275. Espinosa J R, Quirós M *Phys. Lett. B* **266** 389 (1991)
276. Kodaira J, Yasui Y, Sasaki K *Phys. Rev. D* **50** 7035 (1994)
277. Casas J A et al. *Nucl. Phys. B* **436** 3 (1995)
278. Heinemeyer S, Hollik W, Weiglein G *Phys. Rev. D* **58** 091701 (1998)
279. Heinemeyer S, Hollik W, Weiglein G *Phys. Lett. B* **440** 296 (1998)
280. Heinemeyer S, Hollik W, Weiglein G *Phys. Lett. B* **455** 179 (1999)
281. Heinemeyer S, Hollik W, Weiglein G *Eur. Phys. J. C* **9** 343 (1999)
282. Carena M et al. *Nucl. Phys. B* **580** 29 (2000)
283. Inoue K et al. *Prog. Theor. Phys.* **67** 1889 (1982)
284. Flores R, Sher M *Ann. Physics* **148** 95 (1983)
285. Li S P, Sher M *Phys. Lett. B* **140** 339 (1984)
286. Vysotskii M I, Nevzorov R B *Phys. Usp.* **44** 919 (2001); *Usp. Fiz. Nauk* **171** 939 (2001)
287. Slavich P et al. *Eur. Phys. J. C* **81** 450 (2021); arXiv:2012.15629
288. Ham S W, Oh S K, Song H S *Phys. Rev. D* **61** 055010 (2000)
289. Elliott T, King S F, White P L *Phys. Lett. B* **314** 56 (1993)
290. Ellwanger U *Phys. Lett. B* **303** 271 (1993)
291. Elliott T, King S F, White P L *Phys. Rev. D* **49** 2435 (1994)
292. King S F, White P L *Phys. Rev. D* **52** 4183 (1995)
293. Ham S W, Oh S K, Kim B R *Phys. Lett. B* **414** 305 (1997)
294. Pandita P N *Phys. Lett. B* **318** 338 (1993)
295. Ellwanger U, Lindner M *Phys. Lett. B* **301** 365 (1993)

296. Pandita P N *Z. Phys. C* **59** 575 (1993)
297. Ham S W, Oh S K, Kim B R *J. Phys. G* **22** 1575 (1996)
298. Durand L, Lopez J L *Phys. Lett. B* **217** 463 (1989)
299. Drees M *Int. J. Mod. Phys. A* **4** 3635 (1989)
300. King S F, Mühlleitner M, Nevzorov R *Nucl. Phys. B* **860** 207 (2012); arXiv:1201.2671
301. King S F, Mühlleitner M, Nevzorov R, Walz K *Nucl. Phys. B* **870** 323 (2013); arXiv:1211.5074
302. Miller D J, Nevzorov R, Zerwas P M *Nucl. Phys. B* **681** 3 (2004); hep-ph/0304049
303. Nevzorov R, Miller D J, in *Proc. of the 7th Workshop "What Comes beyond the Standard Model?", Bled, Slovenia, 2004* (Eds N M Borstnik et al.) (Ljubljana: DMFA–ZALOZNISTVO, 2004) p. 107; hep-ph/0411275
304. Miller D J, Moretti S, Nevzorov R, in *Proc. of the 18th Intern. Workshop on High Energy Physics and Quantum Field Theory, QFTHEP 2004, St. Petersburg, Russia, 17–23 June 2004* (Eds M N Dubinin, V I Savrin) (Moscow: Moscow State Univ., 2004) p. 212; hep-ph/0501139
305. Nevzorov R, in *Proc. of the 19th Intern. Workshop on High Energy Physics and Quantum Field Theory, QFTHEP 2010, Golitsyno, Moscow Region, Russia, 2010* (Ed. N Nikitin); *PoS QFTHEP* **2010** 015 (2010); arXiv:1103.2141
306. Nevzorov R B, Trusov M A *Phys. Atom. Nucl.* **64** 1299 (2001); *Yad. Fiz.* **64** 1375 (2001); hep-ph/0110363
307. Nevzorov R *Phys. Rev. D* **89** 055010 (2014); arXiv:1309.4738
308. Nevzorov R *PoS EPS-HEP* **2015** 381 (2015); arXiv:1510.05387
309. Kolda C, Martin S P *Phys. Rev. D* **53** 3871 (1996); hep-ph/9503445
310. Sirunyan A M et al. (CMS Collab.) *J. High Energy Phys.* **2021** (07) 208 (2021); arXiv:2103.02708
311. Aad G et al. (ATLAS Collab.) *Phys. Lett. B* **796** 68 (2019); arXiv:1903.06248
312. Kowalska K, Sessolo E M *Adv. High Energy Phys.* **2018** 6828560 (2018); arXiv:1802.04097
313. Griest K, Seckel D *Phys. Rev. D* **43** 3191 (1991)
314. Ellis J, Falk T, Olive K A *Phys. Lett. B* **444** 367 (1998); hep-ph/9810360
315. Ellis J R et al. *Astropart. Phys.* **13** 181 (2000); *Astropart. Phys.* **15** 413 (2001) Erratum; hep-ph/9905481
316. Griest K *Phys. Rev. D* **38** 2357 (1988); *Phys. Rev. D* **39** 3802 (1989) Erratum
317. Ellis J R, Roszkowski L, Lalak Z *Phys. Lett. B* **245** 545 (1990)
318. Drees M, Nojiri M M *Phys. Rev. D* **47** 376 (1993); hep-ph/9207234
319. Chan K L, Chattopadhyay U, Nath P *Phys. Rev. D* **58** 096004 (1998); hep-ph/9710473
320. Feng J L, Matchev K T, Moroi T *Phys. Rev. D* **61** 075005 (2000); hep-ph/9909334
321. Feng J L, Matchev K T, Wilczek F *Phys. Lett. B* **482** 388 (2000); hep-ph/0004043
322. Kane G L et al. *Phys. Rev. D* **49** 6173 (1994); hep-ph/9312272
323. Buchmueller O et al. *Eur. Phys. J. C* **74** 3212 (2014); arXiv:1408.4060
324. Bagnaschi E A et al. *Eur. Phys. J. C* **75** 500 (2015); arXiv:1508.01173
325. Han C et al. *Phys. Lett. B* **769** 470 (2017); arXiv:1612.02296
326. Citron M et al. *Phys. Rev. D* **87** 036012 (2013); arXiv:1212.2886
327. Athron P et al. (GAMBIT Collab.) *Eur. Phys. J. C* **77** 824 (2017); arXiv:1705.07935
328. Athron P et al. *Comput. Phys. Commun.* **190** 139 (2015); arXiv:1406.2319
329. Staub F, Porod W, Herrmann B *J. High Energy Phys.* **2010** (10) 40 (2010); arXiv:1007.4049
330. Staub F *Comput. Phys. Commun.* **181** 1077 (2010); arXiv:0909.2863
331. Staub F *Comput. Phys. Commun.* **182** 808 (2011); arXiv:1002.0840
332. Staub F *Comput. Phys. Commun.* **184** 1792 (2013); arXiv:1207.0906
333. Staub F *Comput. Phys. Commun.* **185** 1773 (2014); arXiv:1309.7223
334. Allanach B C *Comput. Phys. Commun.* **143** 305 (2002); hep-ph/0104145
335. Allanach B C et al. *Comput. Phys. Commun.* **185** 2322 (2014); arXiv:1311.7659
336. Vega J P, Villadoro G *J. High Energy Phys.* **1507** 159 (2015); arXiv:1504.05200
337. Bélanger G et al. *Comput. Phys. Commun.* **149** 103 (2002); hep-ph/0112278
338. Bélanger G et al. *Comput. Phys. Commun.* **174** 577 (2006); hep-ph/0405253
339. Bélanger G et al. *Comput. Phys. Commun.* **180** 747 (2009); arXiv:0803.2360
340. Bélanger G et al. *Comput. Phys. Commun.* **182** 842 (2011); arXiv:1004.1092
341. Bélanger G et al. *Comput. Phys. Commun.* **185** 960 (2014); arXiv:1305.0237
342. Akerib D S et al. (LUX Collab.) *Phys. Rev. Lett.* **118** 021303 (2017); arXiv:1608.07648
343. Aprile E et al. (XENON Collab.) *Phys. Rev. Lett.* **121** 111302 (2018); arXiv:1805.12562
344. Meng Y et al. (PandaX-4T Collab.) *Phys. Rev. Lett.* **127** 261802 (2021); arXiv:2107.13438
345. Aalbers J et al. (LUX-ZEPLIN Collab.) *Phys. Rev. Lett.* (2023) to be published, accepted 7 June 2023; arXiv:2207.03764
346. Athron P, Harries D, Nevzorov R, Williams A G *Phys. Lett. B* **760** 19 (2016); arXiv:1512.07040
347. Athron P, Harries D, Nevzorov R, Williams A G *J. High Energy Phys.* **2016** (12) 128 (2016); arXiv:1610.03374
348. Roszkowski L, Ruiz de Austri R, Nihei T *J. High Energy Phys.* **2001** (08) 024 (2001); hep-ph/0106334
349. Aprile E et al. (XENON Collab.) *JCAP* **2020** (11) 031 (2020); arXiv:2007.08796
350. Akerib D S et al. (LUX-ZEPLIN Collab.) *Phys. Rev. D* **101** 052002 (2020); arXiv:1802.06039
351. Aalseth C E et al. (DarkSide-20k Collab.) *Eur. Phys. J. Plus* **133** 131 (2018); arXiv:1707.08145
352. Aalbers J et al. (DARWIN Collab.) *JCAP* **2016** (11) 017 (2016); arXiv:1606.07001
353. Acharyya A et al. (CTA Collab.) *JCAP* **2021** (01) 057 (2021); arXiv:2007.16129
354. Hryczuk A et al. *J. High Energy Phys.* **2019** (10) 043 (2019); arXiv:1905.00315
355. Rinchiuso L et al. *Phys. Rev. D* **103** 023011 (2021); arXiv:2008.00692
356. Krasnikov N V, Matveev V A *Phys. Usp.* **47** 643 (2004); *Usp. Fiz. Nauk* **174** 697 (2004)
357. Kazakov D I *Phys. Usp.* **62** 364 (2019); *Usp. Fiz. Nauk* **189** 387 (2019)
358. Bednyakov V A, Khramov E V *Phys. Usp.* **65** 997 (2022); *Usp. Fiz. Nauk* **192** 1065 (2022)
359. Sirunyan A M et al. (CMS Collab.) *J. High Energy Phys.* **2019** (10) 244 (2019); arXiv:1908.04722
360. Aad G et al. (ATLAS Collab.) *Eur. Phys. J. C* **81** 600 (2021); *Eur. Phys. J. C* **81** 956 (2021) Erratum; arXiv:2101.01629
361. Sirunyan A M et al. (CMS Collab.) *Eur. Phys. J. C* **80** 3 (2020); arXiv:1909.03460
362. Aad G et al. (ATLAS Collab.) *J. High Energy Phys.* **2021** (02) 143 (2021); arXiv:2010.14293
363. Aad G et al. (ATLAS Collab.) *J. High Energy Phys.* **2021** (05) 093 (2021); arXiv:2101.12527
364. Aad G et al. (ATLAS Collab.) *Eur. Phys. J. C* **80** 737 (2020); arXiv:2004.14060
365. Sirunyan A M et al. (CMS Collab.) *Phys. Rev. D* **104** 052001 (2021); arXiv:2103.01290
366. Tumasyan A et al. (CMS Collab.) *J. High Energy Phys.* **2022** 147 (2022); arXiv:2106.14246
367. Aad G et al. (ATLAS Collab.) *Eur. Phys. J. C* **80** 123 (2020); arXiv:1908.08215
368. Aaboud M et al. (ATLAS Collab.) *Eur. Phys. J. C* **78** 995 (2018); arXiv:1803.02762
369. Aaboud M et al. (ATLAS Collab.) *Eur. Phys. J. C* **78** 154 (2018); arXiv:1708.07875
370. Aad G et al. (ATLAS Collab.) *Eur. Phys. J. C* **80** 691 (2020); arXiv:1909.09226
371. Aad G et al. (ATLAS Collab.) *Eur. Phys. J. C* **81** 1118 (2021); arXiv:2106.01676
372. Tumasyan A et al. (CMS Collab.) *J. High Energy Phys.* **2021** (10) 045 (2021); arXiv:2107.12553
373. Aad G et al. (ATLAS Collab.) *Phys. Rev. D* **104** 112010 (2021); arXiv:2108.07586
374. Aad G et al. (ATLAS Collab.) *Phys. Rev. D* **93** 052002 (2016); arXiv:1509.07152

375. Aad G et al. (ATLAS Collab.) *Phys. Rev. D* **101** 052005 (2020); arXiv:1911.12606
376. Sirunyan A M et al. (CMS Collab.) *J. High Energy Phys.* **2019** (08) 150 (2019); arXiv:1905.13059
377. Aaboud M et al. (ATLAS Collab.) *Phys. Rev. D* **99** 092007 (2019); arXiv:1902.01636
378. Sirunyan A M et al. (CMS Collab.) *Phys. Rev. D* **104** 012015 (2021); arXiv:2012.01581
379. Sirunyan A M et al. (CMS Collab.) *J. High Energy Phys.* **2021** (04) 123 (2021); arXiv:2012.08600
380. Aad G et al. (ATLAS Collab.) *Phys. Rev. D* **101** 032009 (2020); arXiv:1911.06660
381. Sirunyan A M et al. (CMS Collab.) *Eur. Phys. J. C* **80** 189 (2020); arXiv:1907.13179
382. Aad G et al. (ATLAS Collab.) *Phys. Rev. Lett.* **125** 051801 (2020); arXiv:2002.12223
383. King S F, Mühlleitner M, Nevzorov R, Walz K *Phys. Rev. D* **90** 095014 (2014); arXiv:1408.1120
384. Aaboud M et al. (ATLAS Collab.) *J. High Energy Phys.* **2018** (03) 174 (2018); arXiv:1712.06518
385. Aaboud M et al. (ATLAS Collab.) *Eur. Phys. J. C* **78** 293 (2018); arXiv:1712.06386
386. Aad G et al. (ATLAS Collab.) *Phys. Lett. B* **800** 135103 (2020); arXiv:1906.02025
387. Tumasyan A et al. (CMS Collab.) *J. High Energy Phys.* **2021** (11) 057 (2021); arXiv:2106.10361
388. Aad G et al. (ATLAS Collab.) *J. High Energy Phys.* **2021** (06) 145 (2021); arXiv:2102.10076
389. Aad G et al. (ATLAS Collab.) *J. High Energy Phys.* **2020** (10) 112 (2020); arXiv:2006.05872
390. Aad G et al. (ATLAS Collab.) *J. High Energy Phys.* **2021** (06) 179 (2021); arXiv:2101.11582
391. Hesselbach S et al. *Phys. Lett. B* **662** 199 (2008); arXiv:0712.2001
392. Hesselbach S et al., in *Proc. of the 15th Intern. Conf. on Supersymmetry and the Unification of Fundamental Interactions, SUSY07, Karlsruhe, Germany, 2007* (Eds W de Boer, I Gebauer) (Karlsruhe: Univ. of Karlsruhe, 2008) p. 918; arXiv:0710.2550
393. Hesselbach S et al., in *Proc. of the 13th Lomonosov Conf. on Elementary Particle Physics, Moscow, Russia, August 23–29, 2007* (Ed. A I Studenikin) (Singapore: World Scientific, 2008) p. 370; arXiv:0712.2014
394. Hesselbach S et al., in *Proc. of the 34th Intern. Conf. in High Energy Physics (ICHEP08), Philadelphia, USA, 2008*, eConf C080730; arXiv:0810.0511
395. Hall J P et al. *Phys. Rev. D* **83** 075013 (2011); arXiv:1012.5114
396. Hall J P et al., in *Proc. of the 19th Intern. Workshop on High Energy Physics and Quantum Field Theory, QFTHEP 2010*), Golitsyno, Moscow Region, Russia, 2010 (Ed. N Nikitin); *PoS QFTHEP* **2010** 069 (2010); arXiv:1012.5365
397. Hall J P et al., in *Proc. of the 2011 Meeting of the Division of Particles and Fields of the American Physical Society, Providence, Rhode Island, USA, 9–13 August 2011* (Ed. T Speer); eConf C110809 (2011); arXiv:1109.4972
398. Hall J P et al. *AIP Conf. Proc.* **1560** 303 (2013)
399. Nevzorov R, Pakvasa S *Phys. Lett. B* **728** 210 (2014); arXiv:1308.1021
400. Nevzorov R, Pakvasa S *Nucl. Part. Phys. Proc.* **273–275** 690 (2016); arXiv:1411.0386
401. Nevzorov R *PoS EPSHEP* **2015** 381 (2015); arXiv:1510.05387
402. Nevzorov R *Phys. Atom. Nucl.* **83** 338 (2020)
403. King S F, Merle A *JCAP* **2012** (08) 016 (2012); arXiv:1205.0551
404. Sirunyan A M et al. (CMS Collab.) *Phys. Lett. B* **793** 520 (2019); arXiv:1809.05937
405. Abi B et al. (Muon g-2 Collab.) *Phys. Rev. Lett.* **126** 141801 (2021); arXiv:2104.03281
406. Bennett G W et al. (Muon g-2 Collab.) *Phys. Rev. D* **73** 072003 (2006); hep-ex/0602035
407. Aoyama T et al. *Phys. Rep.* **887** 1 (2020); arXiv:2006.04822
408. Athron P et al. *J. High Energy Phys.* **2021** (09) 080 (2021); arXiv:2104.03691
409. Baer H, Barger V, Serce H *Phys. Lett. B* **820** 136480 (2021); arXiv:2104.07597
410. Chakraborti M et al. *Eur. Phys. J. C* **82** 483 (2022); arXiv:2112.01389
411. Altmannshofer W et al. *J. High Energy Phys.* **2021** (07) 118 (2021); arXiv:2104.08293
412. Ahmed W et al. *Phys. Lett. B* **827** 136879 (2022); arXiv:2104.03491
413. Wang F et al. *Nucl. Phys. B* **970** 115486 (2021); arXiv:2104.03262
414. Chakraborti M, Roszkowski L, Trojanowski S *J. High Energy Phys.* **2021** (05) 252 (2021); arXiv:2104.04458
415. Aboubrahim A, Nath P, Syed R M *J. High Energy Phys.* **2021** (06) 002 (2021); arXiv:2104.10114
416. Li Z et al. *J. High Energy Phys.* **2021** (12) 219 (2021); arXiv:2106.04466
417. Abdughani M et al. *Sci. Bull.* **66** 2170 (2021); arXiv:2104.03274
418. Cao J et al. *J. High Energy Phys.* **2021** (09) 175 (2021); arXiv:2104.03284
419. Wang K, Zhu J *Chinese Phys. C* **47** 013107 (2023); arXiv:2112.14576
420. Li S, Xiao Y, Yang J M *Eur. Phys. J. C* **82** 276 (2022); arXiv:2107.04962
421. Cao J et al. *Phys. Rev. D* **104** 055009 (2021); arXiv:2102.11355
422. Ali M I et al. *Eur. Phys. J. C* **83** 60 (2023); arXiv:2112.09867
423. Han C, arXiv:2104.03292
424. Li S, Xiao Y, Yang J M *Nucl. Phys. B* **974** 115629 (2022); arXiv:2108.00359
425. Aboubrahim A, Klasen M, Nath P *Phys. Rev. D* **104** 035039 (2021); arXiv:2104.03839
426. Baum S et al. *J. High Energy Phys.* **2022** (01) 25 (2022); arXiv:2104.03302
427. Cox P, Han C, Yanagida T T *Phys. Rev. D* **104** 075035 (2021); arXiv:2104.03290
428. Iwamoto S, Yanagida T T, Yokozaki N *Phys. Lett. B* **823** 136768 (2021); arXiv:2104.03223
429. Zheng M-D, Zhang H-H *Phys. Rev. D* **104** 115023 (2021); arXiv:2105.06954
430. Wang F et al. *Universe* **8** (3) 178 (2022); arXiv:2201.00156
431. Zheng M-D, Chen F-Z, Zhang H-H, arXiv:2204.06541
432. Gu J et al. *Chinese Phys. C* **46** 123107 (2022); arXiv:2204.05296
433. Athron P et al. *Phys. Rev. D* **106** 095023 (2022); arXiv:2204.05285
434. Yang J-M, Zhang Y *Sci. Bull.* **67** 1430 (2022); arXiv:2204.04202
435. Tang T-P et al. *Sci. China Phys. Mech. Astron.* **66** 239512 (2023); arXiv:2204.04356
436. Du X K et al. *Nucl. Phys. B* **989** 116151 (2023); arXiv:2204.04286
437. Aaltonen T et al. (CDF Collab.) *Science* **376** 170 (2022)
438. Borsanyi S et al. *Nature* **593** 51 (2021); arXiv:2002.12347
439. Abada A et al. (FCC Collab.) *Eur. Phys. J. Spec. Top.* **228** 1109 (2019); CERN-ACC-2018-0059
440. Abada A et al. (FCC Collab.) *Eur. Phys. J. C* **79** 474 (2019); CERN-ACC-2018-0056
441. Abada A et al. (FCC Collab.) *Eur. Phys. J. Spec. Top.* **228** 755 (2019); CERN-ACC-2018-0058